

# Characteristics of deep moist convection and rainfall in cut-off lows over South Africa

By

Tshimbiluni Percy Muofhe

11632362

The dissertation is submitted in fulfillment of the requirements for the degree of Master of Environmental Sciences

Department of Geography & Geo-Information Sciences

School of Environmental Sciences

UNIVERSITY OF VENDA

Supervisor: Dr. H. Chikoore

Co-Supervisors: Dr. M.M Bopape (South African Weather Service)

: Dr. N.S. Nethengwe

March 2019

## Declaration

I, Tshimbiluni Percy Muofhe, declare that this dissertation hereby submitted to the University of Venda, for the degree of Master of Environmental Sciences in Geography has not been previously submitted by me for a degree at this or any other university; that it is my own work in design and in execution, and that all material contained herein has being duly acknowledged.

Signature.....

Date.....

## Acknowledgements

This dissertation was supervised by Dr. H, Chikoore, Dr. M.M Bopape and Dr. N.S Nethengwe and funded by the National Research Foundation (NRF).

Primary datasets for this study were obtained from the following agencies: -

South African Weather Service (SAWS),

National Oceanic and Atmospheric Administration (NOAA),

Physical Services Division (PSD),

National Centers for Environmental Prediction - National Centre for Atmospheric Research (NCEP-NCAR),

European Centre for Medium-Range Weather Forecasting (ECMWF), and

National Aeronautics and Space Administration (NASA).

Mr. G. Rambuwani, Mrs. P. Mulovhedzi, Mr. R. Rapolaki, and Mr. S. Mbatha patiently provided helpful insights about the accessing and displaying different datasets throughout the study.

## Abstract

Out of all rain-producing weather systems, cut-off lows (COLs) are linked with the occurrence of high impact rainfall and in some cases short-lived floods which can last for 24 hours over South Africa. This study examined the characteristics associated with the present occurrence of the severe COL systems over South Africa from 2011 to 2017. The accuracy of the 4.4 km Unified Model (UM) which is currently in use for simulating areas of deep moist convection in South Africa was evaluated. The UM simulated geopotential height at 500 hPa as well as the associated 24 hours precipitation which were compared against the daily fields of geopotential height and 6-hourly precipitation from the European Centre for Medium-Range Weather Forecasts (ECMWF). COL events were categorized and analyzed according to the associated surface circulation patterns at 850 hPa. The seasonal distribution and duration of the systems over northern ( $10^{\circ}\text{E}-33^{\circ}\text{E} // 22^{\circ}-32^{\circ}\text{S}$ ) and southern ( $10^{\circ}\text{E}-33^{\circ}\text{E} // 32^{\circ}-35^{\circ}\text{S}$ ) regions of the study area were also analyzed. Results show COL systems shifting with season towards the north eastern parts of the country, with an increased number of events during the austral winter season during the study period. Systems which lasted for long time were observed during the austral winter and spring seasons. The UM tends to simulate areas of heavy precipitation accurately with poor simulation during the initial stages of the systems. The UM provided a more realistic-looking closed geopotential height and rainfall fields for systems which are coupled with a cold front at the surface. Application of the knowledge about the evolution in the characteristics of COL events from this study can improve the operational forecasting of these weather systems over the country.

**Key words:** Cut-off lows, deep moist convection, circulation, synoptic patterns, simulation

## Table of Contents

Declaration .....	i
Acknowledgements .....	ii
Abstract .....	iii
List of Figures .....	vii
List of Tables .....	xi
Acronyms.....	xii
CHAPTER 1 .....	1
BACKGROUND AND INTRODUCTION.....	1
1.1 Background.....	1
1.2 Problem analysis and motivation .....	2
1.3 Research questions.....	4
1.4 Aim and objectives .....	4
1.5 Description of the study area .....	5
1.6 Dissertation structure .....	8
CHAPTER 2 .....	9
LITERATURE REVIEW .....	9
2.1 Introduction .....	9
2.2 Rainfall-producing systems over South Africa .....	9
2.2.1 Tropical-Temperate Troughs .....	10
2.2.2 Tropical cyclones .....	11
2.2.3 Continental tropical lows .....	12
2.2.4 Ridging anticyclones .....	12
2.2.5 Cut-off lows .....	12
2.3 Classification of cut-off lows.....	14
2.4 Atmospheric blocking .....	15
2.5 Cut-off lows and large-scale climate modes .....	17
2.5.1 Southern Annular Mode .....	17
2.5.2 El Niño-Southern Oscillation .....	18
2.6 Forecasting cut-off lows .....	19
2.6.1 Numerical Weather Prediction .....	19
2.6.2 Unified Model .....	20
2.6.3 Application of the 4.4 km Unified Model at SAWS .....	21
2.6.4 Importance of the model .....	22
2.7 Impacts of cut-off lows.....	22

2.8	Summary .....	23
CHAPTER 3 .....		24
DATA AND METHODS .....		24
3.1	Introduction .....	24
3.2	Long-term rainfall and temperature data .....	24
3.3	Satellite data .....	24
3.3.1	Climate Hazards Group InfraRed Precipitation with Station data .....	24
3.3.2	HIRS Out-going Longwave Radiation data .....	25
3.3.3	High cloud cover .....	26
3.3.4	Satellite imagery.....	27
3.4	Reanalysis and derived data.....	27
3.4.1	Geopotential height .....	28
3.4.2	Potential vorticity .....	29
3.4.3	Vertical vorticity (Omega).....	29
3.4.4	Temperature fields .....	30
3.4.5	Relative humidity .....	30
3.4.6	Vector winds.....	31
3.4.7	Convective Available Potential Energy .....	31
3.5	Methods of Analysis .....	33
3.5.1	Methods of Identification of Cut-off Lows .....	33
3.5.2	Analysis of Cut-off Lows characteristics .....	35
3.5.3	Trend analysis .....	35
3.5.4	Composite analysis .....	35
3.5.5	Self-Organizing Maps.....	36
3.5.6	Unified Model simulations .....	36
3.5.7	Visual inspection .....	36
3.5.8	Case study approach .....	37
3.6	Data display .....	37
3.6.1	The Grid Analysis and Display System .....	37
3.6.2	Royal Netherlands Meteorological Institute Climate Explorer.....	37
3.6.3	National Aeronautics and Space Administration Giovanni.....	38
3.7	Summary .....	38
Chapter 4.....		40
Evolution and meteorological structure of recent cut-off lows over South Africa .....		40
4.1	Introduction .....	40

4.2	Mean annual cycles of rainfall and Outgoing Longwave Radiation over South Africa	40
4.3	Long-term seasonal patterns of rainfall and OLR variabilities over South Africa.....	44
4.3.1	Austral Summer season.....	44
4.3.2	Austral autumn season .....	45
4.3.3	Winter (JJA) season.....	46
4.3.4	Austral spring season.....	47
4.4	Seasonal distribution and duration of identified Cut-off Lows systems.....	48
4.4.1	Seasonal distribution of identified Cut-off Lows systems.....	48
4.4.2	Seasonal distribution of Cut-off Lows over region A and B.....	49
4.4.3	Duration of the Cut-off Lows during different seasons in South Africa .....	50
4.4	Observed Cut-off Lows systems .....	52
4.5.1	Event of 13-15 July 2012 .....	52
4.5.2	Event of 12-15 May 2016.....	53
4.5.3	Associated weather and effects.....	54
4.5.4	Conceptual Model .....	54
4.6	Summary .....	55
Chapter 5.....		69
Unified Model Cut-off Low rainfall simulations .....		69
5.1	Introduction.....	69
5.2	Testing Unified Model simulating Cut-off Low events from 2016 to 2017.....	69
5.2.1	Event of 14-16 May 2016.....	69
5.2.2	Event of 26-27 July 2016 .....	74
5.2.3	Event of 10-11 October 2017.....	77
5.2.4	Event of 15-17 November 2017.....	80
5.3	Summary .....	84
Chapter 6.....		86
Conclusions and future work.....		86
6.1	Introduction .....	86
6.2	Discussion and synthesis of key findings.....	86
6.2.1	Recent Cut-off Lows in South Africa: seasonality and structure .....	86
6.2.2	Simulating rainfall in Cut-off Lows using the 4.4 km Unified Model .....	87
6.3	Implications and future work .....	88
6.4	Conclusion .....	88
References.....		90

## List of Figures

Figure 1. 1: South African topological map, with altitudes ranging from 300 m to 3473 m above mean sea level. (Source: Molekwa, 2013).....	5
Figure 1. 2: A map of South Africa (study area), showing its nine provinces. For Cut-off Lows (COLs) classification, South Africa is divided into two regions, A and B.....	7
Figure 1. 3: A study area map categorized into 4 regions, with a homogeneous annual rainfall cycle. ....	7
Figure 2. 1: The main mechanisms which play an important role in the formation of Tropical-temperate troughs (TTT) during austral summer: Angola low (AL), Kalahari heat low (HL), South Atlantic high (SAH), and south Indian Ocean high (SIH). (Source: Macron <i>et al.</i> , 2014).....	11
Figure 2. 2: A schematic representation of the development of a Cut-off Low (COL) in the upper troposphere in the South African region at 500 hPa, in association with the establishment of a blocking anticyclone at high latitudes, and a COL at low latitudes (Source: Molekwa, 2013). ....	13
Figure 2. 3: The positive phase of the Southern Annular Mode (SAM), with its influence in the distribution of pressure over southern Hemisphere (Source: Renwick and Thompson, 2006).....	17
Figure 3. 1: Distribution of Mean annual Outgoing Longwave Radiation (OLR) values in $W/m^2$ over poles, tropical, deserts and warm dry ocean regions during the period 1974-2006 from NOAA.....	26
Figure 4. 1: Long-term mean annual global precipitation climatology project (GPCP) rainfall (mm/month) and Out-going Longwave Radiation (OLR) ( $Wm^{-2}$ ) cycles over region 1. .	41
Figure 4. 2: Long-term mean annual global precipitation climatology project (GPCP) rainfall (mm/month) and Out-going Longwave Radiation (OLR) ( $Wm^{-2}$ ) cycles over region 2. .	42
Figure 4. 3: Long-term mean annual global precipitation climatology project (GPCP) rainfall (mm/month) and Out-going Longwave Radiation (OLR) ( $Wm^{-2}$ ) cycles over region 3. .	43

Figure 4. 4: Long-term mean annual global precipitation climatology project (GPCP) rainfall (mm/month) and Out-going Longwave Radiation (OLR) ( $Wm^{-2}$ ) cycles over region 4. .	44
Figure 4. 5: Long-term summer seasonal (a) global precipitation climatology project (GPCP) rainfall (mm/month) and Out-going Longwave Radiation (OLR) ( $Wm^{-2}$ ) distribution over South Africa. ....	45
Figure 4. 6: Long-term Autumn seasonal (a) global precipitation climatology project (GPCP) rainfall (mm/month) and (b) Out-going Longwave Radiation (OLR) ( $Wm^{-2}$ ) distribution over South Africa. ....	46
Figure 4. 7: Long-term seasonal Winter (a) global precipitation climatology project (GPCP) rainfall (mm/month) and (b) Out-going Longwave Radiation (OLR) ( $Wm^{-2}$ ) distribution over South Africa. ....	47
Figure 4. 8: Long-term Spring seasonal (a) global precipitation climatology project (GPCP) rainfall (mm/month) and (b) Out-going Longwave Radiation (OLR) ( $Wm^{-2}$ ) distribution over South Africa. ....	48
Figure 4. 9: Seasonal distribution in percentage of Cut-off Lows (COLs) with their synoptic near surface patterns from 2011 to 2017 .....	49
Figure 4. 10: The seasonal distribution of Cut-off Lows (COLs) in percentage over region A and B from 2011 to 2017 .....	50
Figure 4. 11: Seasonal distribution of Cut-off Lows (COLs) in percentages from 2011 to 2017 in three categories over South Africa .....	51
Figure 4. 12: Geopotential height (hPa) vs potential vorticity @ 500 (a), Geopotential height (hPa) vs Temperature ( $^{\circ}C$ ) @500hPa (b), Geopotential Height (hPa) vs Winds @ 850hPa (c) and Geopotential Height (hPa) vs Temperature ( $^{\circ}C$ ) @850hPa (d), <b>13 July 2012</b> .....	56
Figure 4. 13: Geopotential height (hPa) @ 500 (hPa) vs Relative humidity (a), High Cloud Cover (HCC) (d), Out-going Longwave Radiation (OLR) (c), Total rainfall (mm/day) (d), Vertical velocity (e) and Infrared image of COL at 18:00Z <i>copyright (2019) EUMETSAT</i> (f), <b>13 July 2012</b> .....	57
Figure 4. 14: Geopotential Height (hPa) vs Potential vorticity @ 500 (a), Geopotential Height (hPa) vs Temperature ( $^{\circ}C$ ) @500hPa (b), Geopotential height (hPa) vs Winds @ 850hPa (c) and Geopotential height (hPa) vs Temperature ( $^{\circ}C$ ) @850hPa (d), <b>14 July 2012</b> .....	58

Figure 4. 15: Geopotential Height (hPa) @ 500 (hPa) vs Relative humidity (a), High Cloud Cover (HCC) (d), OLR (c), Total rainfall (mm/day) (d) Vertical velocity (e) and Infrared image of COL at 10:00Z *copyright (2019) EUMETSAT* (f), **14 July 2012**..... 59

Figure 4. 16: Geopotential height (hPa) vs Potential vorticity @ 500 (a), Geopotential height (hPa) vs Temperature (°C) @500hPa (b), Geopotential height (hPa) vs Winds @ 850hPa (c) and Geopotential height (hPa) vs Temperature (°C) @850hPa (d), **15 July 2012**..... 60

Figure 4. 17: Geopotential Height (hPa) @ 500 (hPa) vs Relative humidity (a), High Cloud Cover (d), Out-going Longwave Radiation (OLR) (c), Total rainfall (mm/day) (d) Vertical velocity (e), **15 July 2012**..... 61

Figure 4. 18: Figure 1.26: Geopotential height (hPa) vs Potential vorticity @ 500 (a), Geopotential height (hPa) vs Temperature (°C) @500hPa (b), Geopotential height (hPa) vs Winds @ 850hPa (c) and Geopotential height (hPa) vs Temperature (°C) @850hPa (d), **12 May 2016**. .... 62

Figure 4. 19: Geopotential height (hPa) @ 500 (hPa) vs Relative humidity (a), High Cloud Cover (HCC) (d), OLR (c) and Total rainfall (mm/day) (d), Vertical velocity (e) 00:00Z Meteosat-10 Airmass Red Green Blue (RGB) snapshot, *copyright (2019) EUMETSAT* (f), **12 May2016**. .... 63

Figure 4. 20: Figure 1.26: Geopotential height (hPa) vs Potential vorticity @ 500 (a), Geopotential height (hPa) vs Temperature (°C) @500hPa (b), Geopotential height (hPa) vs Winds @ 850hPa (c) and Geopotential height (hPa) vs Temperature (°C) @850hPa (d), **13 May 2016**. .... 64

Figure 4. 21: Geopotential Height (hPa) @ 500 (hPa) vs Relative humidity (a), High Cloud Cover (d), OLR (c), Total rainfall (mm/day) (d), Vertical velocity (e) and Infrared image of cold front and COL at 12:00Z, *copyright (2019) EUMETSAT* (f), **13 May2016**..... 65

Figure 4. 22: Figure 1.26: Geopotential height (hPa) vs Potential vorticity @ 500 (a), Geopotential Height (hPa) vs Temperature (°C) @500hPa (b), Geopotential height (hPa) vs Winds @ 850hPa (c) and Geopotential height (hPa) vs Temperature (°C) @850hPa (d), **14 May 2016**. .... 66

Figure 4. 23: Geopotential Height (hPa) @ 500 (hPa) vs Relative humidity (a), High Cloud Cover (HCC) (d), Out-going Longwave Radiation (OLR) (c), Total rainfall (mm/day) (d), Vertical velocity (e) and Infrared image of a COL at 18:00Z, *copyright (2019) EUMETSAT* (f), **14 May2016** ..... 67

Figure 4. 24: The four stages indicating geopotential heights @ 500 hPa and typical cloud patterns, as observed during the occurrence of the COL systems (source: EUMETSAT 2012)..... 68

Figure 5. 1: 24hr. Total precipitation at (a) 00Z, (b) 12Z and (c)18Z runs of the 4.4 km Unified Model vs (d) observation on **14 May 2016**..... 71

Figure 5. 2: 4.4 km Unified Model run simulations vs observation 24 hours total precipitation at -32s to 23s//27e on **14 May 2016**. .... 72

Figure 5. 3: 24hr. Total precipitation at (a) 00Z, (b) 12Z and (c)18Z runs of the 4.4 km Unified Model vs (d) observation on **15 May 2016**..... 73

Figure 5. 4: 24hr. Total precipitation at (a) 00Z, (b) 12Z and (c)18Z runs of the 4.4 km Unified Model vs (d) observation on **16 May 2016**..... 74

Figure 5. 5: 24hr. Total precipitation at (a) 00Z, (b) 12Z and (c)18Z runs of the 4.4 km Unified Model vs (d) observation **25 July 2016**. .... 75

Figure 5. 6: 4.4 km Unified Model run simulations vs observation 24 hours total precipitation at -33s to 23s//28e on **26 July 2016**. .... 76

Figure 5. 7: 24hr. Total precipitation at (a) 00Z, (b) 12Z and (c)18Z runs of the 4.4 km Unified Model vs (d) observation **27 July 2016**. .... 77

Figure 5. 8: 24hr. Total precipitation at (a) 00Z, (b) 12Z and (c)18Z runs of the 4.4 km Unified Model vs (d) observation on **10 October 2017**..... 78

Figure 5. 9: 4.4 km Unified Model run simulations vs observation 24 hours total precipitation at -35s to 23s//30e on 10 October 2017. .... 79

Figure 5. 10: 24 hours Total precipitation at (a) 00Z, (b) 12Z and (c)18Z runs of the 4.4 km Unified Model vs (d) observation on **11 October 2017**. .... 80

Figure 5. 11: 24hr. Total precipitation at (a) 00Z, (b) 12Z and (c)18Z runs of the 4.4 km Unified Model vs (d) observation on **15 November 2017**. .... 81

Figure 5. 12: 4.4 km Unified Model run simulations vs observation 24 hours total precipitation at -40s to -18s//30e on **15 November 2017**. .... 82

Figure 5. 13: 24hr. Total precipitation at (a) 00Z, (b) 12Z and (c)18Z runs of the 4 km Unified Model vs (d) observation on **16 November 2017**..... 83

Figure 5. 14. 15: 24hr. Total precipitation at (a) 00Z, (b) 12Z and (c)18Z runs of the 4.4 km Unified Model vs (d) observation on **17 November 2017**. .... 84

## List of Tables

Table 3. 1: Primary characteristics associated with the occurrence of COL weather systems over South Africa. ....	32
Table 4. 1: Number of Cut-off Lows (COLs) over region A and B with their seasons of occurrence from 2011 to 2017 .....	50
Table 4. 2: Number of Cut-off Lows (COLs) associated with heavy rainfall from 2011 to 2017 in three duration categories.....	51

## Acronyms

AAO	Antarctic Oscillation
AGCM	Atmospheric General Circulation Model
CAPE	Convective Available Potential Energy
CCAM	Conformal Cubic Atmospheric Model
COL	Cut-off Low
CSIRO	Commonwealth Scientific and Industrial Research Organization
DJF	December January February
ECMWF	European Centre for Medium-Range Weather Forecasts
ENSO	El Niño Southern Oscillation
GCM	General Circulation Model
GPCP	Global Precipitation Climatology Project
GPM	Global Precipitation Measurement
HCC	High Cloud Cover
hPa	Hectopascal
ITCZ	Inter-Tropical Convergence Zone
JAXA	Japan Aerospace Exploration Agency
JFM	January-February-March
JJA	June-July-August
KNMI	Royal Netherlands Meteorological Institute
MAM	March-April-May
NASA	National Aeronautics and Space Administration
NCAR	National Center for Atmospheric Research

NCEP	National Centers for Environmental Prediction
NESDIS	National Environmental Satellite Data and Information Service
NOAA	National Oceanic and Atmospheric Administration
NWP	Numerical Weather Prediction
OLR	Outgoing Longwave Radiation
PV	Potential Vorticity
RCM	Regional Climate Model
RH	Relative Humidity
SAM	Southern Annular Model
SAST	South African Standard Time
SAWS	South Africa Weather Service
SLP	Sea Level Pressure
SOM	Self Organizing Maps
SON	September-October-November
SST	Sea Surface Temperature
TIROS	Television Infrared Observation Satellite
TOGA	Tropical Ocean Global Atmosphere
TRMM	Tropical Rainfall Measuring Mission
UKMO	United Kingdom Met Office
UM	Unified Model
WMO	World Meteorological Organization

# CHAPTER 1

## BACKGROUND AND INTRODUCTION

### 1.1 Background

Seasonal characteristics of weather over the subtropics are greatly influenced by anticyclonic circulation, which is caused by the descending limb of the Hadley cell (Taljaard, 1986). South Africa is one of the countries whose climate is influenced by the position and intensity of the Hadley cell circulation. This is due to its location underneath the anticyclonic circulation of the Hadley cell (Taljaard, 1959). The majority of the country experiences rainfall during the austral summer season as a result of the dominance of low-pressure systems over the interior (Harrison, 1984; Weldon and Reason, 2014). The replacement of the anticyclonic circulation by a heat-driven synoptic trough system in summer, promotes the southward flow of moist tropical air over South Africa (Taljaard, 1986). Some of the major rain-producing weather systems during the austral summer season include cloud bands associated with the ridging anticyclone, Inter-tropical Convergence Zone (ITCZ), Angola low and tropical cyclones.

During the austral winter, most of the interior is dry while the southwestern parts of the country become wet. This happens because of the cold fronts passing through the country, due to their equatorward move during this season. This is also influenced by the northward shifting of the Atlantic as well as the Indian Ocean high pressure systems. The small portion along the southern coastal region of the country, called Cape south coast, receives rainfall throughout the year (Hart *et al.*, 2012; Engelbrecht *et al.*, 2013; Weldon and Reason, 2014). Most of the rainfall activities over this area are experienced during transitional seasons, associated with COLs, ridging high pressure systems and tropical-temperate troughs, which occur during autumn and spring (Jury and Levey, 1993). The COLs are most frequent during the transitional seasons, while ridging highs peak during the austral summer (Singleton and Reason, 2007).

While characteristics of some weather systems that contribute to rainfall over the northern part, the southwestern area and Cape south coast part of the country have been studied extensively, others remain poorly understood. For example, rainfall associated with tropical-temperate troughs, and the land-falling tropical systems have been quantified (Hart *et al.*, 2010 and Malherbe *et al.*, 2012). Out of these weather systems, COLs play a major role in the distribution of the rainfall, not only on the Cape south coast region but also across many regions of the country

(Favre *et al.*, 2012). This is because they are associated with high intensity deep convection and vertical motion, which lead to high impact rainfall events. COLs can produce 24- hour rainfall totals which can exceed the climatological monthly rainfall total (e.g. Singleton and Reason, 2006,2007b). Knowledge about the characteristics of COLs can provide insights of the relevant circulation dynamics, which in turn can potentially be applied to improve the simulation of deep moist convection and rainfall in COLs over country. South Africa is characterized by a complex topography that can influence the atmospheric circulation and modify characteristics of the COL events (Fig. 1.1). In comparison to the number of COLs rainfall distribution studies over South Africa, more focus has been on the Cape south coast than other regions in the country.

Characteristics of rain-producing weather systems can be influenced by large-scale climate modes, such as the Southern Annular Mode (SAM) (Reason and Renault 2005 and Malherbe *et al.*, 2014) and the El Niño Southern Oscillation (ENSO) (Lindsay 1988 and Reason 2000). The change in location and intensity of rain-producing weather systems over the winter and summer rainfall regions of the country may be influenced by SAM and ENSO. These are evident particularly during wet and dry seasons. It has been suggested that COLs contribute in the interannual rainfall variability, as the occurrence of these systems is disrupted during the dry years (Jury and Levey, 1993). Over the Cape south coast, there is a link between anomalous rainfall years with the ENSO events. An increased number of COLs occurrence has been observed during the early phase of La Niña events (Weldon and Reason, 2014). Seasonal forecasting over South Africa has focused mostly on the summer rainfall region for the October to March period (e.g. Landman and Goddrad, 2005; Engelbrecht and Landman, 2015) with ENSO as the main predictor. This means the seasons in which COLs mainly occur has not been studied in detail because they usually occur during autumn/spring.

## 1.2 Problem analysis and motivation

COL events are slow-moving weather systems which typically persist over the same region for several days. As a result, these systems have a significant impact on the weather conditions that can be felt for couple of days (Gimeno *et al.* 2007). During austral spring and autumn seasons, the southern and eastern coastal regions of South Africa experience cold conditions and extreme rainfall, which often leads to flooding when COLs occur (Singleton and Reason, 2007b). As these systems originate in the upper troposphere, they are also associated with the exchange of ozone between the stratosphere and troposphere. The downwards movement from the stratosphere is

also linked with a significant number of reactive species into the troposphere (Singleton and Reason, 2007).

There are fewer studies that have been undertaken on COLs over Southern Hemisphere, in comparison to the Northern Hemisphere (e.g., Romero *et al.* 2000; Yu and Smull 2000). The effects of topography as well as the influence of mid-latitude storms on the COLs have been adequately investigated in different locations in the Northern Hemisphere (e.g., Neiman *et al.* 2004) but not in the South African context. However, there are important differences between the Northern and Southern Hemispheres, which suggests that simply transferring Northern Hemisphere findings about COLs to Southern Hemisphere, particularly in South Africa, is inappropriate.

COL events often occur over the Western Cape and Cape south regions of Eastern Cape in spring and autumn. Therefore, simulation of deep moist convection during the occurrence of COL events is more focused over these regions than other regions over the country (Favre *et al.*, 2012). Most studies have analyzed the characteristics of COLs occur that over southern parts of South Africa, during the March-April-May (MAM) season. It has been found that there is an evolution in the preferred season for COL events, from (MAM) to June-July-August (JJA), and location from southwestern (34°S) towards the northeast of the subtropical southern Africa for COLs occurrence since 1980s (Singleton and Reason, 2007b). Thus, COL systems may also play a significant role in the contribution of the average rainfall during austral winter seasons.

Singleton and Reason (2007) indicated that the weakening of SAM is often associated with the shifting of COL events from the southwest (34°S) towards the northeastern part of the country in the 1980s. These COL systems are associated with extreme rainfall, which can last for 24 hours (Singleton and Reason, 2006b) and in some cases resulting in flash floods over the northern part of the country. While it has been possible to analyze the frequency, duration and size of COLs over Cape south coast, there are challenges in predicting these characteristics over the northern part of South Africa (e.g., Romero *et al.*, 2000; Yu and Smull 2000).

Most of the studies which are conducted over South Africa cover a very short period. For example, Taljaard (1985) analyzed COLs over South Africa, covering only a study period of ten years. In addition, only the study of Taljaard was confined to COLs in the region bounded by latitudes 20° and 38°S and lines drawn approximately 5° longitude off the west and east coasts. Various characteristics of COLs, which include seasonality, frequency, geographical distribution, the duration and size could not be investigated in the ten-year data set of Taljaard (1985).

While it has been possible for analyzing the characteristics of COLs Singleton and Reason 2007 and Favre *et al.* 2012), they have been less successful in simulating the characteristics of COL events mostly in the northern part of the country (Doswell *et al.* 1996). This limitation in models can lead to end-users not taking future warnings seriously (Doswell *et al.* 1996).

Numerical weather and climate models are the primary tools used to forecast weather, predict on seasonal timescales, as well as provide future climate projections. The spatial resolution used by these models affects the skill with which they can simulate different atmospheric feature. When used with course spatial resolution, they do not accurately simulate the characteristics of small-scale features (MacKellar *et al.* 2014). It is therefore important that the skill of models in simulating these events over the region is studied so that we can better understand shortcoming in the models. Findings from such studies can help model developers identify areas to improve on as they develop or upgrade their models. The South African Weather Service (SAWS) uses the Unified Model (UM) which was developed by the UK Met Office (UKMO) as its main Numerical Weather Prediction (NWP) Model. SAWS has a mandate to provide weather, climate and air quality services to the country for purposes of saving lives and property over land, sea and the air. It is therefore important that the skill of the model used by SAWS in predicting systems that can lead to flooding is understood.

### 1.3 Research questions

- There has been observed drying over the southwestern Cape region in Western Cape Province during the austral autumn (MAM) (Reason and Jagadheesha 2005). Could this be a result of a recent seasonal shift of COLs?
- How do dynamic and thermodynamic variables evolve with the approach and passage of a heavy rainfall producing COL?
- How do surface pressure patterns influence the predictability of rainfall during the occurrence of COLs over South Africa?
- How accurate is the UM model used by SAWS in simulating deep moist convection and rainfall amounts during COL events?

### 1.4 Aim and objectives

The main aim of this study is to analyze the characteristics, deep moist convection and rainfall in COL events over South Africa.

Specific research objectives are to:

- Examine the recent (2011 to 2017) seasonal distribution of COLs over South Africa.
- Analyze physical and thermodynamic processes associated with deep convection in COLs.
- Investigate the characteristics of the COLs in relation to their associated surface pressure patterns.
- To test the accuracy of SAWS UM in simulating areas of deep moist convection and rainfall in COL events from 2016 to 2017.

## 1.5 Description of the study area

Over the east, the South African topography is characterized by an elevated plateau, with the highest being 2.5 km above mean sea level (Taljaard, 1994). From the north it is characterized by a steep escarpment, which runs from the Soutpansberg region in Limpopo Province, becoming Drakensberg over KwaZulu-Natal Province, and the northern parts of the Eastern Cape Province. Over Lesotho there are the Maluti Mountains, which rise to over 3 km above mean sea level (Fig. 1.1).

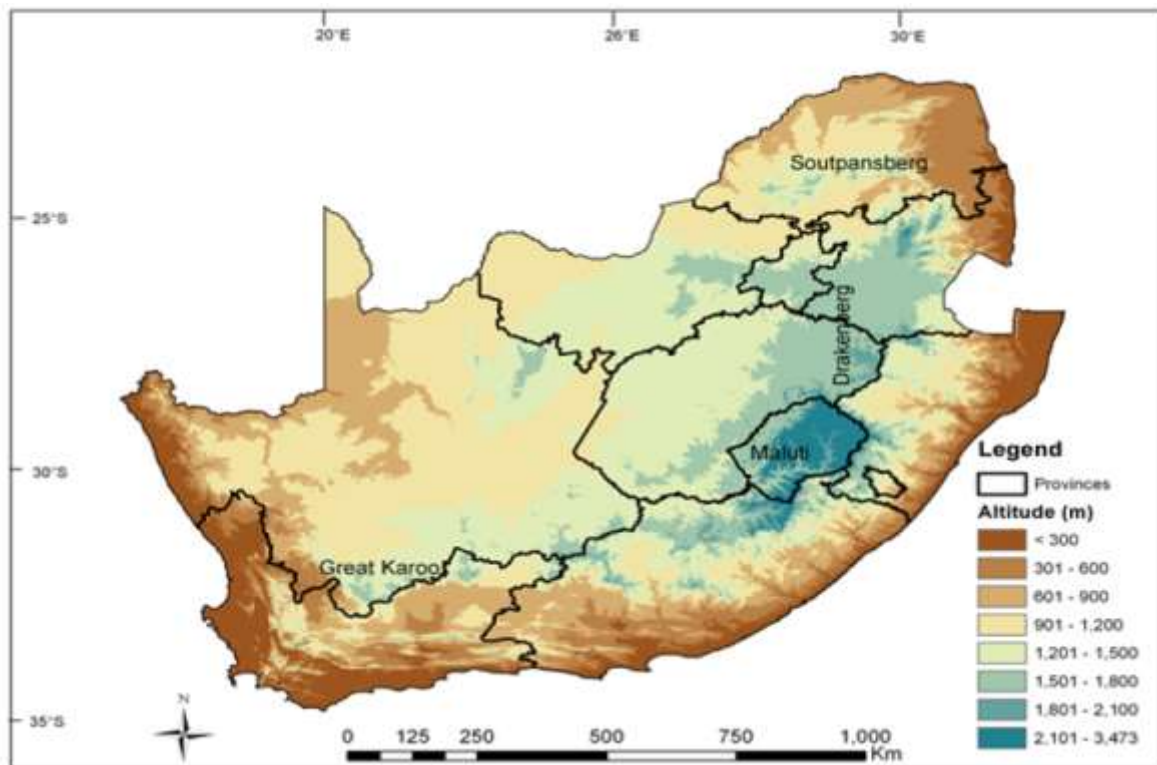


Figure 1. 1: South African topological map, with altitudes ranging from 300 m to 3473 m above mean sea level. (Source: Molekwa, 2013)

South Africa is located in southern Africa and shares borders with Namibia, Botswana, Zimbabwe, Mozambique, Lesotho and Swaziland. In the east and southeast, South Africa is bordered by the

south Indian Ocean, with the south Atlantic Ocean in the west and southwest. The country is made up of nine provinces; namely, Limpopo, North-West, Mpumalanga, Gauteng, Northern Cape, Western Cape, KwaZulu-Natal, Free State, and Eastern Cape Province (Fig. 1.2).

The study area is divided into two regions, referred to as Regions A and B (Fig. 1.2) which was done to analyze the geographical distribution of COL system over South Africa. The study area was divided based on the relatively homogeneous occurrence of COLs and their contribution to the overall rainfall over the country. Region A ( $10^{\circ}\text{E}-33^{\circ}\text{E} // 22^{\circ}\text{S}-32^{\circ}\text{S}$ ) tends to receive rainfall during the austral summer seasons, whilst region B ( $10^{\circ}\text{E}-33^{\circ}\text{E} // 32^{\circ}\text{S}-35^{\circ}\text{S}$ ) tend to receive more rainfall during the austral winter seasons, with a high occurrence of COL events. Thus, COL events play a most significant role in the overall rainfall over region B than A (Molekwa 2013). Singleton and Reason (2007) observed a shift in the preferred season and location of COLs in 1980s over South Africa.

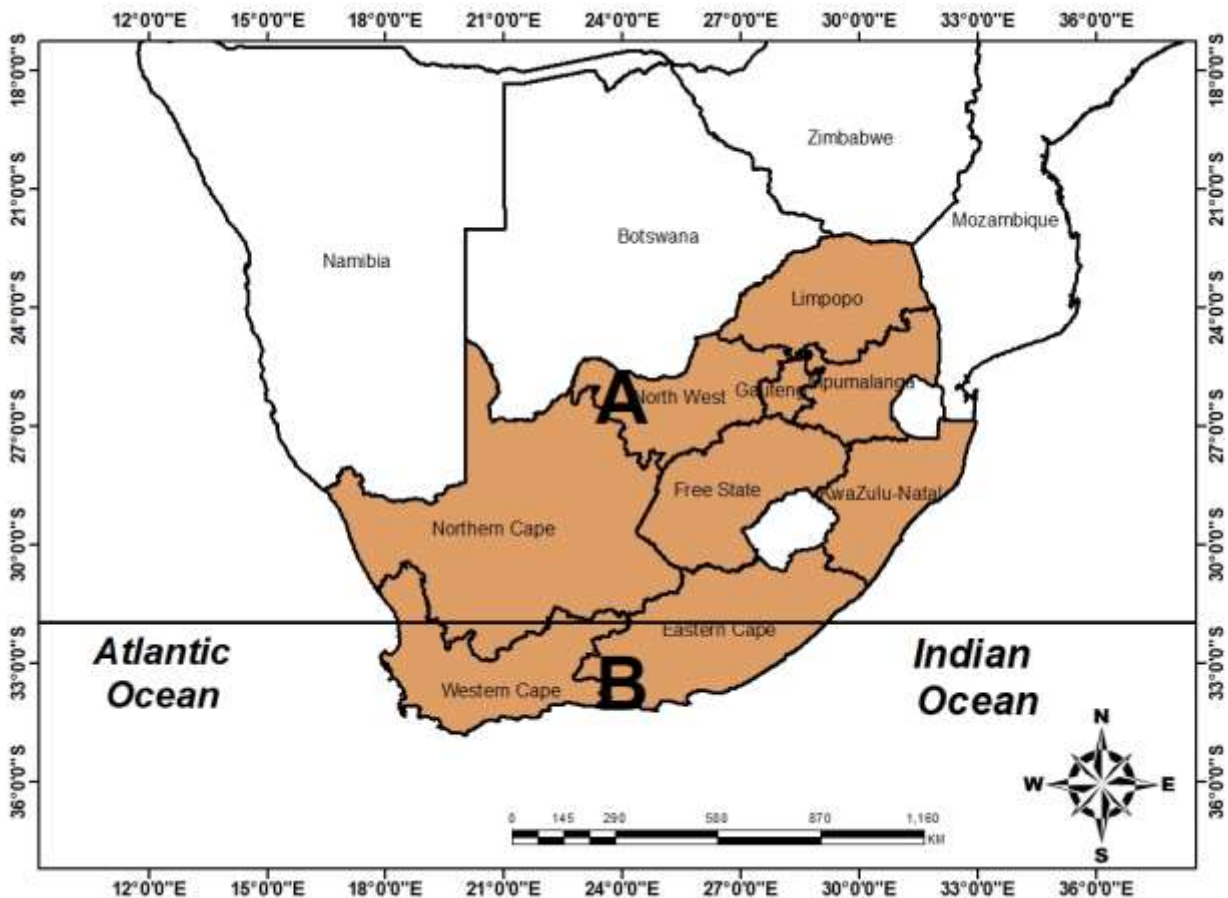


Figure 1. 2: A map of South Africa (study area), showing its nine provinces. For Cut-off Lows (COLs) classification, South Africa is divided into two regions, A and B

Based on the analysis on a cluster of South African rainfall by SAWS (South African Weather Bureau, 1972), and the mean annual cycle rainfall of eight climatic areas, indicated by Rouault and Richard (2003), the study further categorized the areas into four regions (Fig. 1.3). The areas were categorized according to homogenous months of maximum rainfall. Region 1 combines the central interior, KwaZulu-Natal and the north-eastern interior of the study area, which tend to receive maximum rainfall in January (Rouault and Richard, 2003). Region 2 consists of southern interior and some parts of western interior, with the highest rainfall during March. Region 3 is made up of the Cape south coast of the country, with its southern part receiving rainfall throughout the year. Region 4 combines the north and south western Cape of Northern and Western Cape respectively, with most rainfall during Winter.

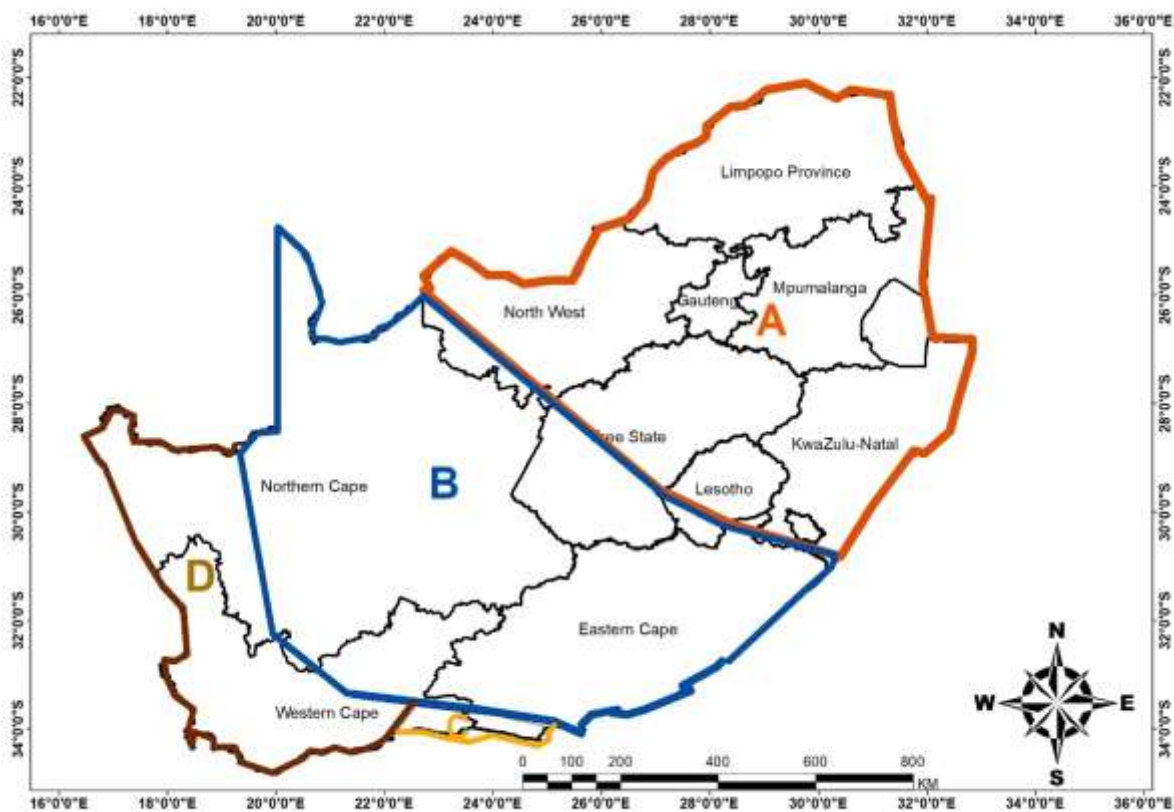


Figure 1. 3: A study area map categorized into 4 regions, with a homogeneous annual rainfall cycle.

## 1.6 Dissertation structure

This study consists of six chapters. Chapter 1 detailed the background, motivation, research questions, aim and objectives as well as the description of the research.

Chapter 2 reviews literature about COLs to identify the major gaps left by previous studies and to acquire important insights about different approaches which can be used to analyze the characteristics of COLs over South Africa.

Chapter 3 presents the datasets, methods and approaches for analyzing data used in the study.

Chapter 4 Identified the different COL events using closed geopotential height at 500 hPa clearly cut-off from main westerly flow further south, with a strong pool of negative potential vorticity. rainfall, temperature, convective available potential energy, outgoing long-wave radiation (OLR) and wind vector, associated with the identified COL events, were analyzed for a better understanding of the weather system over the country.

The accuracy of the 4.4 km UM to simulate rainfall and deep moist convection in COL is evaluated in chapter 5. The model was used to simulate rainfall and convection for COL events which were experienced between 2016 and 2017. The model outputs were further compared with the observation for the events to check the accuracy.

The key findings, recommendations and conclusions of this dissertation are offered in chapter 6. All chapters in this study begin with an introduction and conclude with a summary.

## CHAPTER 2

### LITERATURE REVIEW

#### 2.1 Introduction

Several studies have been carried out on characteristics of cut-off lows (COLs) over the South Africa (e.g. Fuenzalida *et al.* 2005; Ndarana and Waugh 2010; Reboita *et al.* 2010; Favre *et al.* 2011; Singleton and Reason, 2006a, 2007ab). Over the Cape south coast region, COLs are some of the rain-producing weather systems, which provide rainfall throughout the year (Hart *et al.*, 2012, Weldon and Reason., 2014, and Engelbrecht *et al.* 2015). In recent decades there have been several documented cases of heavy rainfall associated with COLs in the different parts of South Africa. In 1987, KwaZulu-Natal province experienced severe floods when a COL moved towards the eastern parts of Northern Cape and Northwest provinces, leading to an accumulation of the rainfall of more than 900mm in 3 days (Triegaardt *et al.*, 1988).

Some studies have analyzed the characteristics of COLs over the regions which often experience these weather systems. Taljaard (1985), for example, analyzed some of the characteristics of the COLs in the region bounded by latitudes 20° and 38°S and lines were drawn approximately 5° longitude off the west and east coasts of South Africa. Other studies have analyzed the rainfall and impacts which are usually experienced during the occurrence of COLs. Engelbrecht *et al.* (2016) also analyzed synoptic types, which are associated with heavy rainfall during the occurrence of COLs over the Cape south coast.

The aim of this chapter is to synthesize and discuss the existing literature on characteristics of COLs, which include seasonality, frequency, geographical distribution, duration size and their predictability over South Africa. Reviewing the literature helps to determine the state of the science, identify major gaps that still exist and provide important insights about approaches used to analyze characteristics of COLs over South Africa.

#### 2.2 Rainfall-producing systems over South Africa

Most regions of South Africa receive rainfall during the austral summer months (December, January and February (DJF), while limited areas in the west receive rainfall from May to September with most during the austral winter months (June, July and August (JJA)). According to Taljaard (1996), only a small portion of the country located over the southern coastal belt receives rainfall throughout the year. Over the eastern parts of the country, rainfall is associated

with moisture transported from the warm Indian Ocean (Reason and Molenga, 1999). Most of the summer extreme precipitation events over the eastern part of the country are usually the result of the tropical lows, extratropical lows (Hart *et al.* 2010,2013), mesoscale convective complexes (Blamey and Reason 2012, 2013). Weather systems such as Inter-tropical Convergence Zone (ITCZ), Angola low, Mascarene high, play an important role in the moisture advection from the tropics and Indian Ocean towards the eastern parts of the country (Molekwa 2013).

During the austral winter, the northward migration of ITCZ and semi-permanent South Atlantic anticyclone reduces the moisture source from the tropics, while the approach of frontal troughs over the southwest with cold fronts leads to wet conditions over the west of the country (Tyson and Preston-Whyte, 2000). The rest of the subcontinent experiences a dry season as an anticyclonic circulation becomes dominant with a continental anticyclonic situated over the land and the South Indian anticyclone moves west.

### 2.2.1 Tropical-Temperate Troughs

Tropical-temperate troughs (TTT) are estimated to produce about 40% of the average annual rainfall over South Africa during austral summer (DJF) (Hart *et al.*, 2013). TTTs are identified as extended cloud bands which connect a tropical convective system with a mid-latitude frontal system passing south of South Africa (Harrison 1984). TTTs often develop after a tropical disturbance at the low latitudes is coupled to a midlatitude trough over the Southern Ocean. The establishment of a summer low over Angola (Angola low) is fundamental (Fig.2.1). TTTs tend to move eastward, through southern Africa, Mozambique channel and towards Madagascar (Pohl *et al.*, 2009).

The formation of TTTs might associated with moisture convergence by strong easterly and westerly fluxes from Indian and Atlantic Oceans (Hart *et al.* 2010). The development of TTTs can be promoted by the low-level penetration of moisture flux from the eastern Atlantic Ocean (Hart *et al.*, 2010). Cloud formation due to the Angola heat low during austral summer may also play a significant role in the development of TTTs (Chikoore and Jury 2010).

The occurrence of TTTs is greatly influenced by the variability of El Niño–Southern Oscillation (ENSO) (Fauchereau *et al.* 2009; Pohl *et al.* 2009). Over southern Africa, a slightly number of TTTs tends to be experienced during La Niña condition. This is influenced by the sea surface temperature near the southern African coasts (Crimp *et al.*, 1998). The presence of above-normal warm temperatures over southwestern Indian Ocean (Agulhas) current which leads to high level of moisture fluxes, increases the occurrences of TTTs (Vigaud *et al.*, 2012). During El Niño events,

anticyclonic wind anomalies become established over the subcontinent such that TTTs are displaced to the warm ocean east of the Madagascar (Fauchereau *et al.* 2009).

The preferential location and persistence of TTTs have significant influence on intraseasonal rainfall distribution. In February 1988, TTT was associated with extremely heavy rainfall in the interior central regions of South Africa (Lindesay and Jury, 1991).

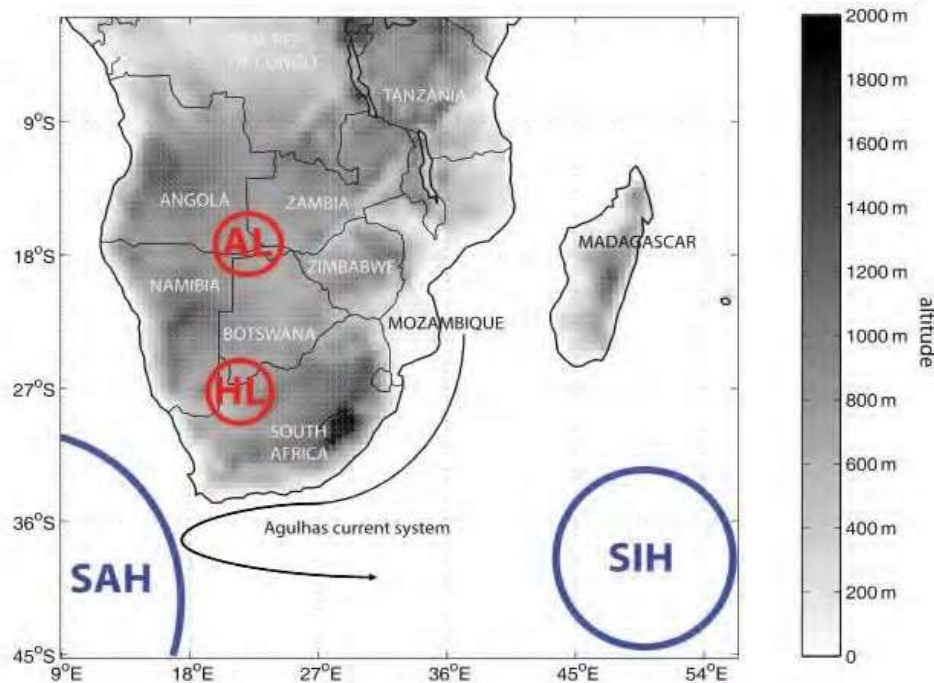


Figure 2. 1: The main mechanisms which play an important role in the formation of Tropical-temperate troughs (TTT) during austral summer: Angola low (AL), Kalahari heat low (HL), South Atlantic high (SAH), and south Indian Ocean high (SIH). (Source: Macron *et al.*, 2014).

### 2.2.2 Tropical cyclones

Tropical cyclones form over the southwest Indian Ocean during November to April. They seldom make landfall over the southern African main land. When they do, they are often associated with large amounts of rainfall over the northern eastern parts of South Africa, Zimbabwe and Mozambique. However, landfall in Madagascar is not common. These weather systems develop in the southwest Indian Ocean or in the Mozambique Channel and tend to propagate in a westwards direction. One of the most significant system in recent decade was tropical cyclone Eline which made landfall over southern Africa during February 2000, and caused devastating floods to areas in Mozambique, Zimbabwe and South Africa (Reason and Keibel, 2004). In March 2019, tropical cyclone Idai also caused significant loss of life and massive damage in

Mozambique, Malawi and Zimbabwe. Most of the tropical cyclones which make landfall tend to transit over the large southern African river basins and are often associated with devastating floods (Dyson and van Heerden, 2002).

### 2.2.3 Continental tropical lows

Continental tropical low-pressure systems are also referred to as V-shaped trough (Dyson and Van Heerden, 2002). The weather system is identified as a low-pressure system that extends from the surface to 400 hPa above which is by a high-pressure system in the upper troposphere. The low-pressure system is characterized by warm core from 500 hPa with relatively low temperatures over the surface at 700 hPa. These systems are linked with surface dew point temperatures of 18–20 °C with precipitable water of above 20mm. In February 1988 and 2000, a tropical continental low caused heavy rainfalls and floods over Free State Province and north-eastern parts of the country respectively (Dyson and Van Heerden, 2001). Tropical continental low-pressure systems are characterized by semi-stationary convective cells with little vertical wind shear.

### 2.2.4 Ridging anticyclones

Ridging anticyclones are characterized with the breaking of the Rossby wave at lower stratosphere. Anomalous stratospheric potential vorticity (PV) extending from 70 hPa towards the surface often leads to a cyclonic flow forming the ridging anticyclone to take a bean-like shape (Ndarana *et al.* 2018). At the surface, the positive anomaly produces internal anticyclonic flow causing the ridging end to break off (Ndarana *et al.* 2018). Ridging high pressure systems are some of the weather systems which play a significant role on the distribution of rainfall over the Cape south region as they contribute about 50% to the annual rainfall (Engelbrecht *et al.* 2015). Their contribution to the annual rainfall decreases from south coast to north with high rainfall during March and April. Surface convergence over the subcontinent is often caused by maritime onshore winds from a ridging anticyclone.

### 2.2.5 Cut-off lows

COLs are typically known for their tempestuous weather as well as high precipitation events (Favre *et al.*, 2012; Molekwa, 2013). They tend to form and develop over the mid-latitudes, on the equatorial-side of the polar or subtropical jet-stream and end up as closed cyclones over the middle and upper troposphere. This occurs when an upper air system separates from the main westerly flow of the mid-latitudes (Palmer, 1949).

Several definitions of COLs exist in the literature. Qi *et al* (2000) defined COLs as synoptic scale low-pressure systems, whose deep trough is at the 500 hPa and a closed circulation at the lower level. According to Tyson and Preston-White (2000), a COL is a feature that is explained by a cold-cored depression produced by a westerly trough. It usually starts over the upper westerlies as a trough and deepens to form a closed circulation which extends to the surface (Fig. 2.2). Taljaard (1985) defined COLs as a deep low-pressure system over the upper troposphere where it forms at 500 hPa.

Typically, they develop as a trough in the upper-air flow becoming a closed circulation which is then cut-off from its source region (westerlies flow) (Fig. 2.2) expanding downward but without reaching a surface. A surface low may develop if the low can become deep and extended towards the lower troposphere (Palmen and Newton, 1969). When the cyclone is totally closed in the middle and upper troposphere it is known as a “cold pool” characterized by strong instability, thunderstorms, strong winds and heavy precipitation (Porcu, *et al.* 2007). The low-pressure system begins to weaken as it becomes baro-tropic becoming characterized by less intense precipitation (Favre *et al.*, 2012).

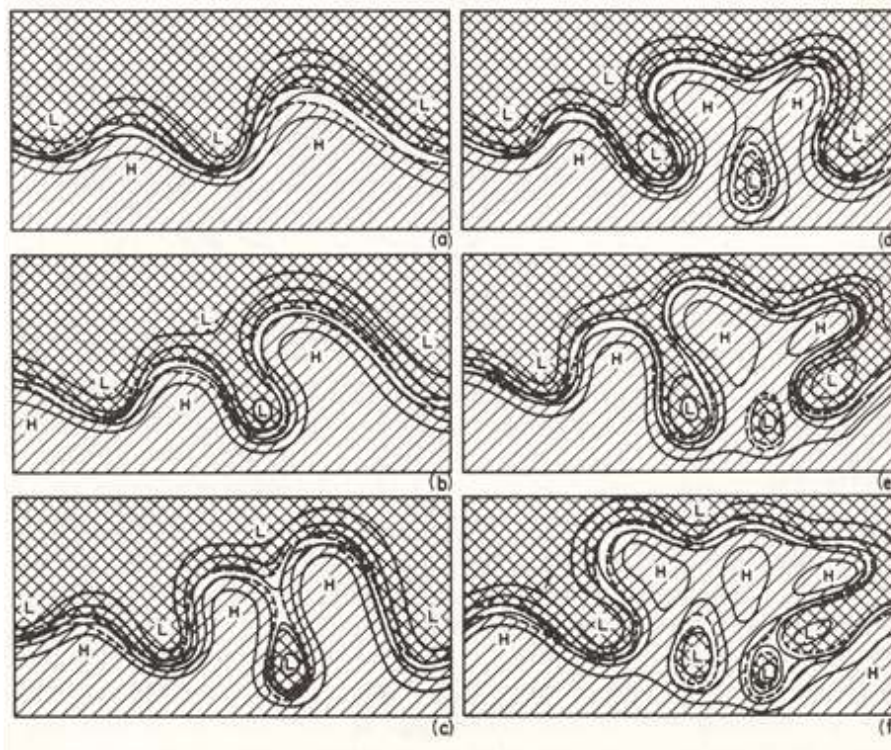


Figure 2. 2: A schematic representation of the development of a Cut-off Low (COL) in the upper troposphere in the South African region at 500 hPa, in association with the establishment of a blocking anticyclone at high latitudes, and a COL at low latitudes (Source: Molekwa, 2013).

## 2.3 Classification of cut-off lows

In South Africa, COLs are often accompanied by a ridge of surface high pressure system on the south of the system and near surface lower depression east of the systems aloft, promoting a rise in the baroclinic structure (Taljaard, 1985). Because of the nature of the jet streak, which results in their development, COLs can be classified into 'polar', 'subtropical' and 'polar vortex' (Price and Vaughan, 1992).

- Polar-type COLs develop because of equatorward extensions of a polar jet and they are typically located pole-wards of the jet (Molekwa, 2013; Singleton and Reason, 2007b).
- Subtropical COLs usually develop where there is an equatorial extension of a zonal polar or subtropical jet (Molekwa, 2013; Singleton and Reason, 2007b).
- Polar vortex-type COLs tend to form because of polar vortex and tend not to move away from the main vortex (Molekwa, 2013; Singleton and Reason, 2007b).

COLs are some of the weather systems which have a dynamic trajectory over South Africa. Furthermore, these systems can have a life-time longer or equal to two days and tend to propagate slowly eastward (Favre *et al.*, 2012). Usually COLs are characterized by a quasi-stationary movement, as it is associated with a blocking situation. The slow movement and persistence of COLs can produce heavy rainfall for two or three consecutive days over the same region, often leading to severe floods (Favre *et al.*, 2012). Most of the regions which are particularly subjected to a high accumulation of precipitation are coastal and mountain regions, due to orographic lifting (Singleton and Reason 2007b; Davolio *et al.*, 2008; and Muller *et al.*, 2008). COLs are cold cored systems such that they often bring bitter conditions and even snowfalls on higher ground in winter. This may lead to disrupt of transportation and electric networks.

COLs are well-noted over the sub-continent but there is limited evidence of occurrence over the Indian Ocean (Favre *et al.*, 2012). From several studies on characteristics of COLs over the entire Southern Hemisphere (e.g., Campetella and Possia, 2006; Risbey *et al.*, 2009 and Singleton and Reason, 2007b), it has been found that South Africa is one of the regions which are affected significantly dominated by the occurrence of COLs (Reboita *et al.*, 2010). A total of about 11 COLs per year has been estimated to occur over southern Africa (Singleton and Reason, 2007a). Despite being less frequent, they have been associated with extreme rainfall and temperatures, particularly in South Africa, where the daily amount of rainfall is associated with a COL and can

exceed 3 times the long-term monthly mean (e.g., Taljaard, 1985; Singleton and Reason, 2006 2007a).

## 2.4 Atmospheric blocking

Occasionally, the persistence and slow-moving character of COLs is due to the presence of atmospheric blocking due to a blocking high.

The first widely accepted definition of blocking was provided by Rex (1950a), which divided the basic westerly current into two categories. In his paper Rex (1950b) noted the influence of geographical characteristics and argued that most blockings tend to dominate the eastern ocean basins over Northern Hemisphere. Although most studies have focused on the Northern Hemisphere because of high density of observations, blocking also occurs over the Southern Hemisphere. Blocking episodes over the Southern Hemisphere tend to be less well-pronounced and do not last long because of the smaller continental areas and a more uniform zonal flow (Pook, 1994).

Owing to its persistence and intensity, blocking is associated with prolonged weather extremes, such as dry spells, flooding and anomalous temperatures over certain extra tropical regions (Pelly, 2001). As a result, this large-scale quasi-stationary extra tropical flow regime has attracted many synoptic and meteorological studies for decades. Atmospheric blocking is analyzed on the upper air circulation and is mostly used for forecasting. Blocking, which covers a large spatial area, is mostly associated with the occurrence of a high-pressure system because this system tends to move slower than low pressure (Tang and Lou, 2006). In some cases, a low-pressure system can also lead to atmospheric blocking.

Atmospheric blocking is commonly defined according to its temporal persistence. As a result, the concept of sector blocking may therefore also be extended to define various blocking episodes. Following the findings of Tibaldi and Molteni (1990), a minimum time-scale of 4 days is used to define an atmospheric blocking episode. Thus, an atmospheric blocking episode is said to occur when there is a sector blocking over a given sector lasting for at least 4 four consecutive days.

Occasionally, an atmospheric blocking high is characterized by three major patterns; namely, monopole-type blocking (or  $\Omega$ -type blocking), dipole-type blocking (McWilliams, 1980; Malguzzi and Malanotte-Rizzoli, 1984; Luo and Ji, 1991) as well as multipole-type blocking, which features COLs (Berggren *et al.* 1949; Luo, 2000; Pelly, 2001). The amplified ridges which tend to be observed over the North Pacific Ocean are not explicitly identified as blocks because they are

characterized by an irreversible deformation of potential vorticity contours which have the same structure as  $\Omega$ -blocks (Twitchett, 2012).

Dipole blocking pattern episodes, occasionally located over the mid-high latitudes and mainly over the ocean, were first identified by Rex (1950a, b). A breaking down over the prevailing tropospheric westerly flow at midlatitudes, which is occasionally linked with a separation of a jet and long-lasting ridging at mid-high latitudes, is denoted by the term “blocking” (Rex, 1950a, b; Illari, 1984). A dipole blocking pattern is the basic pattern which often occurs within background westerlies (Luo, 2005b). Weak background westerlies, as a major condition for the development of blocking high, were first observed by Shutts (1983).

Monopoly blocking often takes place over the North Pacific Ocean and is better analyzed at 250 hPa geopotential height. This type of blocking often takes place during the austral summer season but can also be identified at other times of the year (Luo and Ji, 1991)

COLs are different from blocking anticyclone highs in terms of potential vorticity (Hoskins *et al.* 1985). However, both features are formed in a similar way through advection, which leads to the total cut-off of upper-level isentropic potential vorticity which anomalies of the appropriate sign (Hoskins *et al.* 1985). Occasionally COLs tend to cover a smaller area and last for fewer days than blocking highs. Blocking highs tend to block the westerly flow and synoptic systems better than COLs. Nevertheless, some COLs can sufficiently cover a large area and last for more than three days, to meet the index of blocking episodes definition (Pelly 2001).

The development and decaying of blocking are not well understood and its prediction remains a major challenge for medium-range forecasters over the extra-tropics. A better understanding of weather characteristics associated with the early development of the blocking pattern increases the accuracy to forecast weather for several days in advance. Furthermore, the interaction of migratory, synoptic-scale transient eddies may play a major part for blocking information (Berggren *et al.*, 1949) and (Rex, 1950). The possibility for interaction to cause anticyclone blocking was successfully demonstrated by numerical simulations (Shutts, 1983; Metz, 1986).

The characteristics of rain-producing weather systems over the country have not been adequately quantified. This is because much attention has been on the summer rain-producing systems with regards to simulation of their seasonality, frequency, geographical distribution, duration and size. Furthermore, seasonal forecast skill for austral winter rain-producing systems is poorer than forecast skill for summer rain-producing systems. This study has objectively tested the skill of the

different convection schemes in the Unified Model (UM) in simulating deep moist convection and rainfall in COL events.

## 2.5 Cut-off lows and large-scale climate modes

Variability in the occurrence of rain-producing weather systems can be influenced by large-scale climate modes such as the Southern Annular Mode (SAM) (Reason and Rouault, 2005; Malherbe *et al.*, 2014), as well as by ENSO (Washington and Preston, 2006; Philippon *et al.*, 2012).

### 2.5.1 Southern Annular Mode

The SAM, which is also known as the Antarctic Oscillation (AAO), describes the movement of westerly wind belt from north to south (30-40°S), which dominate the middle to higher latitudes of the southern Hemisphere (Reason and Rouault, 2005; Bureau of Meteorology, 2012). The change in the position of westerly wind belt has a significant influence on the characteristics (strength and location) of cold fronts and mid-latitude storm systems (Reason and Rouault, 2005), which is an important driver of rainfall in South Africa and southern Australia (Bureau of Meteorology, 2012). This may lead to extreme droughts over the south-western cape of South Africa (Meque, 2015.)

SAM is characterized by positive and negative phases. During a positive SAM phase, the strong belt of westerly winds contract towards Antarctica (Bureau of Meteorology, 2012; Kiem and Verdon-Kidd, 2012). This leads to weaker than normal westerly winds and the dominance of high pressures over South Africa, Southern America and Australia-New Zealand. Winter over west South Africa tend to be dry than average (Reason and Rouault, 2005)

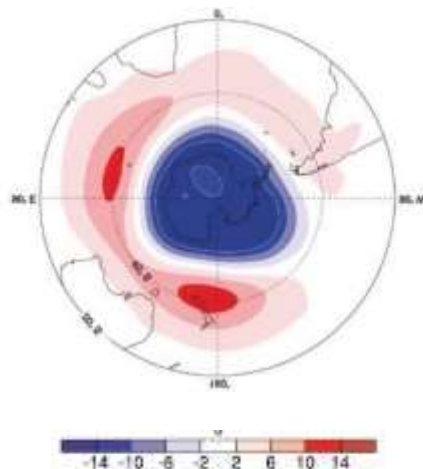


Figure 2. 3: The positive phase of the Southern Annular Mode (SAM), with its influence in the distribution of pressure over Southern Hemisphere (Source: Renwick and Thompson, 2006).

In contrast, a negative SAM phase promotes an expansion of the strong belt of westerly winds towards the equator (Bureau of Meteorology, 2012). The movement of the strong westerly wind belt towards Australia results in more storms and low-pressure systems over Australia.

Negative SAM phase promotes low/negative anomalies pressure systems over southern Africa, which leads to a northward shift in occurrence of COLs, cold fronts and mid-latitude storm systems and increased winter rainfall in west South Africa (Reason and Rouault, 2005), while a positive SAM phase promotes high/positive anomalies pressure systems over southern Africa, which restricts the occurrence of COLs, cold fronts and mid-latitude storm systems (Reason and Rouault, 2005).

The SAM influences winter rainfall through shifting the position of the subtropical jet, changes in the low-level moisture flux upstream over the South Atlantic Ocean and in the mid-level uplift, low-level convergence as well as relative velocity over southern Africa (Reason and Rouault, 2005).

### 2.5.2 El Niño-Southern Oscillation

ENSO is a large scale coupled ocean-atmospheric mode which occurs when the upper tropical Pacific Ocean and the atmosphere above it change from average condition for several seasons. This mode has a significant influence on atmospheric circulation pattern and on weather systems around the globe (Kiladis and Diaz, 1989). ENSO events typically occur every two to seven years and can last for a period of between twelve and eighteen months (Kiladis and Diaz, 1989). ENSO is characterized by neutral, El Niño and La Niña phases.

During the neutral state, easterly trade winds strongly blow strongly towards the west over the surface of the tropical Pacific Ocean, bringing warm moist air as well to the western Pacific and piling up warm water than eastern equatorial. On the other hand, the Pacific Ocean remains cooler, which also results in the thermocline being deeper in the west than the east (Aceituno, 1992). Warm moist air over the western Pacific Ocean and high Sea Surface Temperatures (SSTs) lead to the formation of clouds and rainfall and the ascending branch of the walker circulation.

In an El Niño event, trade winds weaken and may reverse blowing towards central and eastern tropical Pacific Ocean. Warmer than normal SSTs are associated with the deepening of the thermocline over the central Pacific Ocean (Yeh, 2009). High pressure anomalies over the western Pacific leads to more rainfall over the eastern Pacific Ocean.

During a La Niña events, trade winds become strengthened, with more warm SST anomalies moves to the north of Australia. SSTs over central and eastern tropical Pacific Ocean become cooler than average resulting in the thermocline moving towards the surface. It is dominated by higher than normal rainfall as result of enhanced convection and cloudiness.

Just like SAM, ENSO a large-scale climate mode which has a significant influence on the rain-producing weather systems, not only during austral summer but also during the austral winter season over southern Africa. The occurrence of the El Niño event over the Pacific Ocean, is associated with wet austral winters over the southwestern part of South Africa (Philippon *et al.*, 2012). The occurrence of fewer tropical-temperate troughs as well as below-normal rainfall over the eastern and interior regions of South Africa is also associated with El Niño events (Engelbrecht, 2015). It has been indicated that the increased COL frequencies have been observed during the early phase of La Niña (Weldon and Reason, 2014). La Niña events are associated with increased wet-day frequencies during the months of December and January over the Cape south region (Weldon and Reason, 2014). As agriculture is important in South Africa, reliable rainfall forecasts during the austral winter season can be more beneficial for decision making in the agricultural sector. Thus, this study also reflected on the links between the ENSO SAM (large-scale modes), with the appearance of synoptic types during austral winter season.

## 2.6 Forecasting cut-off lows

Even though rainfall over South Africa is attributed to several different types of weather systems, COL events which often occur during the austral spring and autumn have been associated with several cases of extreme rainfall (Taljaard 1985). The simulation of rainfall by numerical weather and climate models is known to have relatively large biases which lead to inaccurate simulations. Known challenges include the overestimation of rainfall over complex topography, early convection initiation, and a lack of severity in simulated thunderstorms (e.g. Keat *et al.*, 2019).

### 2.6.1 Numerical Weather Prediction

NWP models are used to forecast weather up to a few days in advance. Global models used for this time range are currently running with grid spacings of less than 20 km in international meteorological centres. For example, the European Centre for Medium-Range Weather Forecasts (ECMWF) runs its Integrated Forecasting System (IFS) with a grid spacing of 9km, while the UKMO runs the Global Atmosphere (GA) UM with a grid spacing of 10km. In order to obtain higher resolution, Limited Area Models (LAMs) can be used (Houze 2004). These models are only run over a domain of interest, and because of the reduced domain size, they can run with

higher resolution. LAMs are nested within the global models which provide time dependent lateral boundary conditions, and this procedure is called dynamical downscaling. Regional configurations can provide explicit details about small events while the global models can just indicate the possibility of an event about to take place (Prein *et al.* and Coauthors 2015). However, there is still a need to apply global models for forecasting confidence, as the regional models rely on them for large-scale forcing (Zerroukat 2010). Currently, the simulation of rainfall in both Global Circulation Models (GCMs) and LAMs with regards to rainfall-producing weather systems still proves to be a challenge. There are currently biases in predicting the intensity and frequency of precipitation (Jeong *et al.*, 2011). The biases often occur because these models are applied at relatively coarse resolution, where convection processes are not resolved explicitly during the development of small rainfall-producing weather events. Models are then forced to utilize convective parameterization schemes, which is the dynamical treatment of convection and not suitable to represent convective rainfall totals (e.g. Liang *et al.*, 2004).

## 2.6.2 Unified Model

SAWS uses the United Kingdom Meteorological Office (UKMO) UM as its main NWP model. The UM follows a seamless modelling approach where a single model family is applied for prediction across different spatial and timescales (Met Office 2019). Thus, this model can be applied both as a global and a regional model and for NWP, seasonal forecasting, as well as for purposes of simulate climate variability and change with projections that can extend to hundreds of years (Met Office 2019). Weather forecasting using NWP models is on the fundamental equations of fluid dynamics. SAWS started using the UM as its main NWP model in 2006, with a grid spacing of 15km and 12 km, over South Africa and the southern African region, respectively.

Due to improvements in the availability of computational resources the spatial resolution used by models has been improving over time. This means that when NWP started, hydrostatic models were used to forecast weather more recently, the atmospheric community has had to move towards the use of nonhydrostatic models in the recent past to be able to run models with a grid spacing of less than 10 km (Davies *et al.*, 2005). In 2002, a dynamical core named new dynamics was developed by the UKMO and resulted in the UM being the first to solve a virtually unapproximated equation, set the deep atmosphere, non-hydrostatic equations using a semi-implicit semi-Lagrangian method on a regular longitude-latitude grid. Because of the new dynamics, global weather and climate predictions were continuously achieved through a seamless modelling strategy as well as the utilization of a dynamical core at a very high resolution ( $\leq 1.5$  km grid-spacing) (Wood *et al.*, 2014).

Synoptic-scale features were smoothed while the model solution was numerically damped by the application of explicit diffusion and polar filtering as well as the weighting of the semi-explicit to be fully implicit. To maintain the benefits of New Dynamics whilst improving its accuracy, scalability and stability the UKMO developed “ENDGame” (Even Newer Dynamics for General atmospheric modelling of the environment) for both global model and regional configurations (Wood *et al.* 2014). The main atmospheric prognostics include the three-dimension 3-D wind components, Exner pressure and dry density, as well as virtual dry potential temperature. The free tracers in this dynamical formulation include moist prognostic-like mass mixing ration of water vapour and prognostic cloud fields. All these prognostics are discretized onto a regular longitude-latitude horizontally.

### 2.6.3 Application of the 4.4 km Unified Model at SAWS

The model user chooses horizontal and vertical resolutions, but more often the resolution is determined by the available computer power as well as the value of the standard resolutions which tend to be used. Like other operational forecast centres such as Met Office, Japan Meteorological Agency (Narita and Ohmori 2007) and Germany’s National Meteorological Service (Steppeler *et al.* 2003), SAWS has also moved towards higher-resolution model for forecasting short-range weather systems. This is to improve the prediction of different convective systems which are associated with extreme events. At SAWS, the improved computational resources as a result of the procurement of the CRAY XC30 in 2015 made it possible to decrease the grid spacing of the models. SAWS improved the grid spacing used for the UM from 15km and 12km to 4.4km in 2016, and the simulations are made over the whole of southern Africa (from equator). High-resolution models are able to represent mesoscale features and convection explicitly when compared with other coarser resolution models (Holloway *et al.*, 2012).

The skills of different configurations of the UKMO UM composed of 12, 4 and 1 km grid lengths were analyzed over the United Kingdom (Lean *et al.* 2008). The analysis indicated 4 km and 1 km grid length models with more realistic observation of precipitation fields as a result of explicit representation of convection instead of parameterization (Lean, *et al.* 2008). The models were tested in relation to the subjective evolution of the precipitation, the initiation and rainfall amount for several convective cases which occurred during a 2003, 2004 and 2005 summer seasons. As the result its grid size which poorly reproduced convection, the 4 km model poorly simulated large convective cells with delayed initiation (Lean, *et al.* 2008). It is important to examine the skills of a higher-resolution models in producing more realistic and accurate simulations in other parts of

the world, thus in this study we test the skill of the 4.4 km model in simulating deep moist convection in recent COL events over South Africa.

#### 2.6.4 Importance of the model

Increased resolution enables the model to resolve and simulate convection explicitly better than models that rely heavily on parameterizations. Done *et al.* (2004) found a realistic representation of areas associated with deep moist convection when reducing the model resolution towards 1 km for convective systems. Improved forecasts of the 4.4 km resolution model can be used to give a detailed and reliable weather guidance which are essential for decision-making on different timescales for different regions.

High resolution models can be applied for analyzing historical weather observation, in order to manage climate risk (Jayakumar *et al.* 2017). These analyses can be useful for different sectors for example, they can be used in agricultural for activities such as the choice of crops and minimizing the failure of crops. They can also be used to produce forecasts of the routine and hazardous weather conditions. However, the main key question particularly to the operational forecast center, is whether the high-resolution models are able to simulate rainfall accurately during the occurrence of convective weather systems over South Africa.

### 2.7 Impacts of cut-off lows

COLs are important for stratosphere–troposphere exchanges, as well as for deep moist convection. Stratosphere-troposphere exchange during the occurrence of COLs is important for the downward transportation of ozone and other reactive species into the troposphere (Johnson and Viezee, 1981). This can play an important role in the radiative flux balance in the troposphere and lower level of stratosphere, which influences the radiative forcing of the global climate (Ramaswamy *et al.*, 1992). The occurrence of COLs over South Africa is accompanied by an intrusion of stratospheric air into the troposphere. This is also associated with an ozone enhancement. (Barsby and Diab, 1995).

In South Africa, there are several documented cases of sever rainfall associated with the occurrence of COLs. This is because cold air aloft in COLs promotes deep convection, which results in the persistent heavy rainfall. Surface depression which may develop below these systems are also associated with a significant rainfall (Palmen and Newton, 1969). A blocking ridging anticyclone may continue to steer a cold and moist southerly airflow from the Southern Ocean.

In some regions, such as Europe, the Mediterranean and Australia, COLs are associated with heavy precipitation which may persist for a long time (Sabo, 1992). Hu et al. (2010) indicated that most of the convective events which occur over northern China are often associated with the occurrence of COLs. In June and August 1998, COL events led to a record flood which caused a severe damage to the economic activities and societies of northern China (Zhao and Sun, 2007). Over West Africa, a COL system led to rainfall of up to 116 mm per day during the cool season of 9 to 11 January 1981 (Molekwa, 2013). Over South Africa one out of five COLs are normally associated with flood events, particularly over the southern and eastern coastal belts of the country (Taljaard, 1985).

It has been widely accepted that extreme weather events such as heavy rainfalls, snow or thick fog have a significant impact on the performance of the transport system (Nelson and Persaud, 2002). In major cities high intensity rainfall is associated with a significant impact on freeway capacity as well as operational speed (Chin *et al.*, 2002). Thus, it is crucial to consider the regions which are associated with heavy precipitation during the occurrence of COLs, when improving transportation facilities.

Most agricultural activities over southern Africa are rain-fed and extreme rainfalls often impose adverse impacts on the agricultural crops, such as sorghum, millet and maize as well as livestock and other forestry-based activities (Nhemachena *et al.*, 2014). Excess water from extreme rainfall can lead to soil water logging, anaerobicity and effects on the plants growth rate (Gornal *et al.*, 2010). Excess water can also indirectly delay farming operation because agricultural machinery may not work properly on a wet surface (Kettlewell *et al.*, 1999). Crop production is greatly influenced by the distribution of rainfall and is a dominant source of food production over South Africa, which makes it important to simulate areas associated with heavy rainfall patterns over the country.

## 2.8 Summary

Most of the previous studies about COLs described the characteristics of the systems whereas some considered the processes which are responsible for the associated extreme precipitation over the south west region. Some studies have well analyzed the influence of topography and SSTs on the occurrence of COLs managed to quantify the importance and contribution of COLs to the total rainfall over the Eastern Cape Province.

## CHAPTER 3

### DATA AND METHODS

#### 3.1 Introduction

The meteorological characteristics, location and duration of the recent COL events may be evolving in response to the changing climate. It is therefore essential to understand the characteristics of recent occurring events, to improve their predictability.

The aim of this chapter is to present the primary datasets used to analyze the characteristics of the COL as well as their sources. The study employed several long-term (1979 to 2017) seasonal, monthly and daily datasets from secondary data sources. This chapter also indicated the suitable approaches which were used to analyze the meteorological structure, physical and thermodynamic processes associated with occurrence Cut-off Lows (COLs).

#### 3.2 Long-term rainfall and temperature data

Rainfall and both maximum and minimum air temperature data were obtained from the South Africa Weather Service (SAWS). In this study, these long-term datasets were used to analyze the annual distribution of rainfall and temperature patterns over South Africa. This helps to examine the distribution pattern of rainfall and temperature from 1979 to 2017 over the country. Rainfall and temperatures are some of the primary data which are used to analyse the characteristics of COL events, thus is important to understand their long-term distribution over the country.

SAWS is a member of the World Meteorological Organization (WMO), managing the process of meteorological and climatological data over the country since 1936 (SAWS, 2017). Rainfall and minimum temperature are measured at 08:00 South African Standard Time (SAST) every day in the morning, whilst the maximum temperature is recorded at 15:00 South African Standard Time (SAWS, 2017). During the measurements, rainfall accumulates in the bucket of the rain gauge, which is then poured in a calibrated measuring glass where the millimeter reading is recorded (SAWS 2017).

#### 3.3 Satellite data

##### 3.3.1 Climate Hazards Group InfraRed Precipitation with Station data

Climate Hazards Group InfraRed Precipitation with Station (CHIRPS) is a quasi-global rainfall dataset which can a period cover a period of more than 30 years (Katsanos *et al.* 2016). This

dataset incorporates in-situ station data to create and satellite imagery with 0.05 resolution. CHIRPS is often used to create gridded rainfall time series for trend analysis and seasonal drought monitoring (Katsanos *et al.* 2016). CHIRPS was used as observation against the UM simulations for identifying the areas of deep moist convection during the occurrence of COL systems over South Africa. CHIRPS dataset was mostly applied were the ECMWF datasets were unable to create plots against the model.

### 3.3.2 HIRS Out-going Longwave Radiation data

Out-going Longwave Radiation (OLR) is the emission of terrestrial radiation energy from the top of the earth's atmosphere to space as longwave radiation. Characteristics of OLR are greatly influenced by the temperature of the earth and the atmosphere above it, the presence of water vapor in the atmosphere as well as clouds. The flux of energy within an ORL is measured in  $W/m^2$ .

The amount of OLR is typically lower towards the poles (colder regions) as well as over the tropical (regions of convective clouds and thunderstorms), while higher values are found over the desert regions, dry (mid-upper troposphere) ocean regions, which are characterized by hot, dry and clear sky conditions (Fig. 3.1). Hence, lower values of OLR in the tropics and subtropics indicate the presence of deep convective clouds and rainfall.

The long-term daily OLR data was obtain from the High-Resolution Infrared Radiation Sounder (HIRS) radiance observations of the National Oceanic and Atmospheric Administration (NOAA) Television Infrared Observation Satellite (TIROS-N) series and MetOp satellites through The Royal Netherlands Meteorological Institute (KNMI). The OLR retrieval is achieved by using multispectral regression (Urbain *et al.*, 2017) which includes HIRS radiance calibration, OLR inter-satellite adjustments, and temporal integral with OLR diurnal models for a better final product (Lee *et al.*, 2007).

The final product is mapped into  $2.5^\circ$  by  $2.5^\circ$  equal angle grid (144x72, total 10368 grids over the globe) (Gruber and Krueger, 1984). The HIRS OLR is significant compared with other OLR data like the Advanced Very High-Resolution Radiometer (AVHRR) from NOAA Polar Operational Environmental Satellites (POES) (Schreck *et al.*, 2018). HIRS OLR is an intersatellite-calibrated product for better recording of OLR. AVHRR OLR utilizes the day and nighttime records provided by only one satellite leading to difficulties when dealing with huge daily OLR values. The spectral channels of the HIRS consider atmospheric aspects which influence values of OLR for better

recording. HIRS significant for both regional and large coverage weather system which are associated with deep convection (Schreck *et al.*, 2018).

In this study, long-term seasonal OLR data were used to evaluate the seasonal distribution of OLR from 1979 to 2017. Furthermore, daily OLR data were used to analyze areas associated with a deep moist convection during the occurrence of COLs from 2011 to 2017.

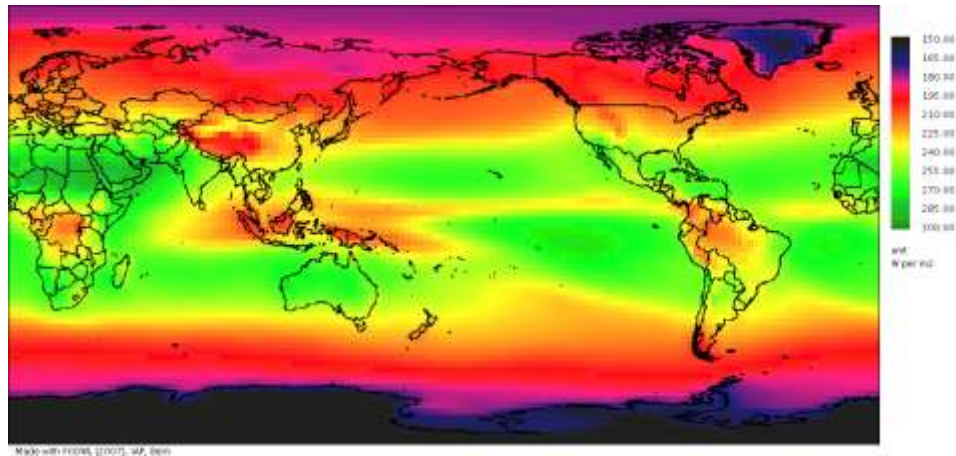


Figure 3. 1: Distribution of Mean annual Outgoing Longwave Radiation (OLR) values in  $W/m^{-2}$  over poles, tropical, deserts and warm dry ocean regions during the period 1974-2006 from NOAA.

### 3.3.3 High cloud cover

Clouds have a significant role in the earth's climate systems. Due to their effects on the characteristics of precipitation, solar and terrestrial radiation. Cloud cover can be defined as a fraction of the sky covered by clouds when detected from a certain angle.

It is crucial to define a geographic area which is typically associated with High Cloud Cover (HCC) and heavy rainfall during the occurrence of COLs over South Africa. Caruso and Businger (2006); and Buckley *et al.* (2007) have shown that mature COLs are usually characterized by clouds over the eastern flank, drawing a comma pattern.

Typically, the warm conveyor is linked to the stratiform clouds over the eastern flank and surrounding the low-pressure center. This is promoted by instability generated by the availability of the cold pool, which enhances the development of cumulus and cumulonimbus (Buckley *et al.*, 2007). Nevertheless, HCC is not often always associated with deep convection. Often fair-weather cirrus, cirrocumulus and cirrostratus may be present due to e.g. upper divergence, the left entrance and right exit of the subtropical Jetstream.

Over southern Africa, COL rainfall is more likely located over the east and polar side of the system and extending from the cold-core center by a few hundred kilometers (Taljaard, 1995). Due to the influence of orography, onshore winds which are linked with COLs and sometimes a low land narrow jet, tend to bring heavy rainfall over the coastal mountains (e.g. Singleton and Reason, 2006a). Daily fields of HCC from ECMWF were used to investigate the location, type and structure of the clouds associated with the occurrence of severe COL systems over South Africa.

### 3.3.4 Satellite imagery

The analysis of satellite imagery when investigating mid-latitude systems which are characterized with warm, cold dry and moist airmasses is very important. Satellite imagery can be used to identify areas which are associated with deep moist convection and cold air at the surface (EUMETSAT 2016). Infrared (IR) satellite images are used in this study instead of visible (VIS) images as they are available throughout 24 hours. Visible images depend on reflection of visible light and are therefore only available during daytime. Infrared images are based on cloud top temperature such that deep convective clouds appear brighter than lower level clouds as they are colder and may contain ice crystals. To identify areas of deep moist convection during the intensive stages of the COL systems, this study used Meteosat Second Generation (MSG) IR 10.8i and MSG Airmass RGB satellite images from the European Organisation for the Exploitation of Meteorological Satellites (EUMETSAT, 2019). EUMETSAT operates meteorological satellites system which include geostationary and polar orbit which observe the characteristics of the atmosphere, ocean and land surface throughout a year (EUMETSAT, 2019). The earth observation data can be provided world-wide for weather, climate and environmental monitoring.

## 3.4 Reanalysis and derived data

This study used the reanalysis datasets from the National Centers of Environment Prediction (NCEP) Reanalysis II and European Centre for Medium-Range Weather Forecasts (ECMWF) for significant analysis of COL characteristics over South Africa. NCEP-NCAR reanalysis II is consists of datasets that are continually representing the state of the earth's atmospheric variables since 1948 (Kalnay *et al.*, 1996).

Reanalysis is a scientific method where observations and numerical model that simulate similar variables are assimilated into an atmospheric model to create more accurate representation about the Earth System. Reanalysis data can be used to analyze evolution of both weather and climate (Bengtsson *et al.*, 2004).

Global Precipitation Climatology Project (GPCP) and OLR datasets from 1979 to 2017 from NCEP Reanalysis II datasets were used for developing long-term rainfall and OLR seasonal patterns over South Africa while the ECMWF provided different daily atmospheric datasets for the observed COL events.

NCEP reanalysis is often updated and assimilation observations into a Numerical Weather Prediction (NWP) model for the representation of the Earth's atmosphere state. Data are represented at a horizontal resolution of  $2.5^\circ \times 2.5^\circ$  at different pressure levels in the vertical. Data are available at 6-hourly intervals, 00:00 Zulu Time (Z), 06:00 Z, and 12:00 Z and 18:00 Z (Kanamitsu *et al.*, 2002).

ECMWF is an intergovernmental organization which contains one of the largest archives of numerical weather prediction data. ECMWF was formed in 1975 to improve Europe's meteorological services and institutions in the production of the medium range timescales forecasts. The center makes available of twice-daily global numerical weather forecasts, analysis of air quality and ocean circulation, hydrological prediction as well as the monitoring of atmospheric composition (Jolliffe and Stephenson, 2012).

The ECMWF website can provide climate analysis, re-analyses current forecast and various observational datasets. The availability of ECMWF products is disseminated through point-to-point distribution, data servers and broadcasting (Gibson *et al.*, 1999).

To improve accuracy and utility of NWP forecasts, ECMWF exploits satellite data for NWP and seasonal forecasting with EUMETSAT, ESA, EU and a European Science community. Atmospheric datasets for atmospheric composition which are useful in for this study, are provided by Copernicus Atmosphere Monitoring Service (CAMS) which combine both atmospheric modelling and Earth observation (Gibson *et al.*, 1999).

### 3.4.1 Geopotential height

Geopotential height is a representation of the height of a particular pressure surface in the atmosphere, utilizing gravity together with latitude and vertical position to adjust geometric height which can be seen from the hypsometric equation, derived from the hydrostatic equation and the ideal gas law:

$$h = Z_2 - Z_1 = \frac{R_d \bar{T}_V}{g} \ln \left( \frac{P_1}{P_2} \right), \quad (\text{Equation 3.1})$$

Where,  $Z_1$  and  $Z_2$  are geometric heights at pressure levels  $P_1$  and  $P_2$ , respectively.  $R_d$  is the gas constant for dry air,  $\bar{T}_V$  is the mean virtual temperature of the layer and  $g$  is gravity.

The daily geopotential height fields at the 500 and 850 hPa level were obtained from the ECMWF. At 500 hPa, the geopotential height was used to identify the closed center associated with the occurrence of a COL. Near the surface at 850 hPa, geopotential height was used to examine the circulation pattern which was associated with different identified COL systems from 2011 to 2017. The near-surface (850 hPa) geopotential height fields are often used to represent the surface circulation over the country because they represent a height of 1.500 m which is just above the height of the interior plateau of South Africa (Engelbrecht, 2016).

### 3.4.2 Potential vorticity

Potential Vorticity (PV) can be defined in terms of the air parcels within two isentropic surfaces. PV consists of the absolute vorticity as well as the measurement of the thickness of a column of air. During the formation of COL, higher PV from the stratosphere is transported towards the base of the trough. In this case, PV in pressure ( $p$ )–coordinate ( $q$ ) is defined as (Hoskins *et al.* 1985)

$$q = -g(fk + \nabla_p \times v) \cdot \Delta_p \theta \quad (\text{Equation 3.2})$$

Where  $g$  represents gravitational acceleration,  $f$  is the Coriolis parameter,  $k$  is the unit vector in vertical,  $\nabla_p$  is the ( $x, y, p$ ) three-dimensional gradient operator,  $v$  is the wind vector, whilst  $\theta$  is the potential temperature.

Potential vorticity data from ECMWF in relation to the closed lows was used to validate the occurrence of the identified system. COLs can be significantly identified by a pool of high potential vorticity in the upper troposphere. Cyclonic (negative) potential vorticity near the upper levels is very important for tracking areas where the COL is intensifying more often at the areas of vertical uplift (Hoskins *et al.*, 1985). This is because areas of convergence in the mid-levels of the atmosphere promote uplift which enhances negative potential vorticity in the upper atmosphere. Therefore, COLs will be characterized by a strong pool of negative potential vorticity in the upper atmosphere which descends towards the surface. This pattern may also be useful to determine the depth and vertical extent of COL events.

### 3.4.3 Vertical vorticity (Omega)

Vertical vorticity depends on some of horizontal wind which determines whether the flow is rising or sinking along a vertical axis in the atmosphere. It is also one of the most important parameters used to analyze the convective activities during COL events. This is because of its capability of showing uplift or subsidence of air parcel. Vertical vorticity is expressed as:

$$\omega = \frac{Dp}{Dt} . \text{ (Equation 3.3)}$$

Where,  $Dp$  is the change in pressure whilst  $Dt$  is the change in time. As the pressure decreases with height in the earth's atmosphere,  $\omega$  is positive for subsidence and negative for uplift. The daily fields of vertical vorticity from the ECMWF is used to investigate the vertical motion air for the development of high cloud cover and heavy rainfalls during the occurrence of COL systems. Areas of negative values of Omega coincide with regions where upliftment is taking place.

#### 3.4.4 Temperature fields

The daily-average temperature fields at 500 hPa from ECMWF were significant for identifying and tracking COLs in South Africa. Since COLs are displaced from the mean westerly winds, they are defined as a cold cored of closed -low at 500 hPa. Near the surface, COLs are also associated with cold conditions. Thus, this study employed daily temperature fields from both 500 hPa and 850 hPa to analyse the temperatures associated with the identified systems.

#### 3.4.5 Relative humidity

Relative Humidity (RH) is defined as the amount of water vapour available in air parcel expressed as a percentage of the amount required for saturation at the constant temperature. RH can be expressed by the following formula: -

$$RH = \frac{e_d}{e_a} . 100 \text{ (Equation 3.4)}$$

Where,  $e_d$  is the actual vapour pressure whilst  $e_a$  is the saturated vapour pressure.

The amount of RH generally depends on the temperature of the day. Low RH is often experienced during the hottest time of the day while high values are experienced during sunrise when temperatures are low.

Relative humidity (RH) was obtained from the European Centre for Medium-Range Weather Forecasts (ECMWF). RH fields were used to evaluate the mean COL structures associated with high relative humidity. Typically, COL structures are linked with wet conditions (positive anomalies) over the eastern flank and drier conditions (negative anomalies) over the western side of the low center (Favre *et al*, 2012). Thus, COL systems are characterized by high values of RH over their eastern flank.

### 3.4.6 Vector winds

Vector winds represent the flow of air masses in the atmosphere. They are described by wind speed and the direction where the wind is blowing from. Over the coastal regions, higher wind speeds are often linked with high rates of evaporation and latent heat fluxes into the atmosphere which, may promote deep convection and heavy rainfall (Raymond *et al.*, 2003). Wind fields at corresponding pressure level, are useful in identifying the cutting off process of the system from the main westerly flow. Zonal wind ( $u$ ) is defined as the latitudinal (west to east) flow of the atmosphere whilst meridional wind ( $v$ ) represents the longitudinal (south to north) flow in the atmosphere.

The components ( $u$  and  $v$ ) of the wind at different atmospheric pressure levels (500 and 850 hPa) were obtained from ECMWF on 23 pressure levels on a  $2.5^\circ$  grid (<http://www.ecmwf.int>). Wind components are reported eight times in 24 hours and are based on surface assimilation, aircraft and satellite data which are quality controlled before being made available to users online. In the present study, wind vector aids in depicting areas of deep moist convection (where low and middle winds converge) during the occurrence of COL events.

### 3.4.7 Convective Available Potential Energy

Convective Available Potential Energy (CAPE) is the amount of energy contained within a parcel of air at a certain distance when measured vertically through the atmosphere. CAPE can be used as an instability index to determine the instability of the atmosphere and its tendency for convection to occur. It is determined by means of integral of a vertical profile of buoyancy and it has been utilized for various studies. CAPE can be used to investigate the convective potential of the tropical atmosphere (Williams and Renno, 1993). It is computed between the Level of Free Convection (LFC) and the Level of Neutral Buoyancy (LNB) within a vertical profile of from the bottom to the top of a layer, respectively.

$$CAPE = \int_{LRC}^{LNB} R_d \times (T_{vp} - T_{ve}) dn_l(p) \quad (\text{Equation 3.5})$$

Where,  $LNB$  is the level of neutral buoyancy of a cloud,  $LRC$  is the level of free convection of a cloud,  $R_d$  is the gas constant of dry air,  $T_{vp}$  is the rising air parcel, and  $T_{ve}$  is the environment within two specific height levels

After rising dry adiabatically, air passes through the Lifting Condensation Level (LCL) and continues to rise pseudo adiabatically promoting the formation of cloud and possibility of rainfall

(Riemann-Campe *et al.*, 2009). The air parcel rises freely between the bottom and top of clouds because its temperature and hence buoyancy are greater than the temperature of its environment.

CAPE values over the Sahara arid zone are typically about  $500 \text{ J kg}^{-1}$ , while over the equator they can reach  $2000 \text{ J kg}^{-1}$ . The minimum values of CAPE are often observed over regions of cold water, where currents are colder than the temperatures of ambient oceans (Meukaleuni *et al.*, 2016). Usually high CAPE characterizes the regions dominated by inter-tropical convergence zone (ITCZ) or subtropical convergence zone such as South Pacific Convergence Zone (SPCZ) or the South Indian Ocean Convergence Zone (SIOCZ). CAPE was used to identify areas associated with high convective potential energy which will verify the occurrence of HCC and heavy rainfalls during COL events over South Africa.

Due to the unavailability of OLR datasets for 2017, daily CAPE datasets from the ECMWF were used to identify areas identity associated with deep moist convection instead. Low values of OLR and high values of CAPE can be used to complement area associated with deep moist convection and rainfall.

A better analysis of the primary parameters (Table 3.1) associated with the occurrence of COL systems may increase the understanding of the variability and evolution of COLs over South Africa.

Table 3. 1: Primary characteristics associated with the occurrence of COL weather systems over South Africa.

<b>Characteristics of COLs</b>	<b>Description</b>
Latitude of occurrence	Latitudes between $20^\circ$ and $45^\circ$ South
Potential Vorticity	Cyclonic PV
Precipitation	Heavy rainfall exceeding 50mm at a given station over a 24-hour period.
Temperature	Cold conditions, maximum temperatures of $15^\circ\text{C}$ or below as they are cold cored systems, with the central air originating from the higher (colder) latitudes.
Wind field	Surface gale force winds exceeding 17 m/s
Depth of systems	Extend from upper levels down towards the lower levels of the atmosphere, 200 hPa - 850 hPa.

Associated surface low level systems	Surface low and/or cold front and sometimes a mesoscale low near surface (Singleton and Reason 2007b). It is possible to have a ridging high-pressure system as well.
--------------------------------------	---

### 3.5 Methods of Analysis

Several studies have successfully developed the climatology of COLs over the country. Singleton and Reason, (2007a) analyzed the variability in the characteristics of COL pressure systems over subtropical southern Africa (20-35° S) from 1973–2002. The study analyzed the seasonality, frequency, duration, location and size of different COL events over the country as well as interannual variability of relationship with ENSO and the semi-annual oscillation. Furthermore, Molekwa (2013) also analyzed the spatial distribution of COL weather systems over eastern and south-eastern parts of the country from 1979 to 2009. Molekwa (2013) Identified 212 COLs events, 60 of the 138 systems which transit over the Eastern Cape Province were linked with significant impacts heavy rainfall. Most of the identified COL events occurred during March-April-May (MAM) and June-July-August (JJA). About 50% lasted for 3 to 4 days, with most of the rainfall occurring in the last day of the events.

In this study, the meteorological structure, physical and thermodynamic processes of COL events which were associated with heavy rainfall from 2011 to 2016 are studied. This was done to examine the characteristics evolution of these weather systems as well as their predictability over South Africa.

#### 3.5.1 Methods of Identification of Cut-off Lows

Geopotential height, temperature and vorticity fields from the ECMWF were utilized to develop a method to identify COLs in this study.

- a) A closed and cold cored low-pressure system should be present in the mid-upper troposphere from 600– 300 hPa.

Usually COLs are defined by a cold-cored depression that is developed by an upper westerly deepening into a closed circulation (Preston-White and Tyson, 1988). To be certain that tracks originate from an extra-tropical origin, cut-off from the westerly waves and characterized of cold core, the test described in Favre *et al.* (2012) is used for this closed-low track dataset.

Some studies have defined COLs on the 300 hPa pressure level with a closed geopotential height contour lasting for more than 24 hours (e.g. Singleton and Reason, 2007b). For this study, the geopotential height fields at 500 hPa were used in identifying and tracking these systems.

Furthermore, the identification of these systems at 500 hPa was used to analyze their distribution over region A and B of the study area. Locations of the COLs were determined according to their closed low on the first day of development.

b) Near-surface synoptic patterns which are associated with the occurrence of COLs

Even though COLs are categorized as low-pressure systems (Taljaard, 1995), their surface synoptic patterns can be characterized by either a strong low-level wind jet, ridging high-pressure systems and cold fronts (Engelbrecht *et al.* 2015). To investigate the near-surface synoptic patterns in relation to the identified COL systems over the land, 850 hPa geopotential fields were used to analyse circulation over the land. Some systems can be dominated by troughs, surface lows or highs or both surface lows and highs. This will be significant for analysing the characteristics of different systems in relation to their near-surface synoptic pattern. Furthermore, the accuracy of the UM in simulating COL systems with different synoptic patterns at 850 hPa.

c) Strong pool of negative potential vorticity field from the stratosphere into the upper troposphere.

COLs are formed by an intrusion of polar stratospheric air with high cyclonic potential vorticity (e.g. Singleton and Reason 2007b). The formation of COL is characterized by the anomalous values of PV making it to be a useful quantity for tracking COLs. This is because of the tropopause folding and the as well as the isentropic advection of stratospheric air from the extra-tropics (Van Delden and Neggers, 2003).

d) A convectively unstable atmosphere and heavy rainfall

Air within COL is colder than its surroundings due to its originating from higher latitudes, which often promote deep convection as the relatively cold air in the middle/upper troposphere helps to destabilize the atmosphere. Typically, rainfall associated with cold cored systems are detected some several kilometers to the northeast, east and southeast of the systems. The analysis of the COL datasets from 1979 to 2011 indicated heavy rainfall over the west of the system (Favre *et al.* 2013).

The duration of a COL is defined as a life span of a system, from the day it is identified with a closed low at 500 hPa, to the day, the closed low dissipated (Molekwa 2013). To analyse the duration of the identified COL events, the duration of systems was categorized into three groups; namely, those that lasted for 1 to 2 days, those that lasted 3 to 4 days as well as those that lasted

for more than 4 days. Mostly COL systems which only last for one to two days are regarded as weak and quick-moving (Prince and Vaughan, 1992).

The study area was divided into two regions (A and B) (Fig. 1.2) to define the location of the systems. A The locations of the COLs were determined according to their closed circulation on the first day of development using the 500 hPa geopotential height fields.

### 3.5.2 Analysis of Cut-off Lows characteristics

Following Singleton and Reason (2007) and Molekwa (2013), who analyzed the characteristics of COLs from 1973 to 2002 and 1979 to 2009 respectively, the current study analyzes the meteorological structure, physical and thermodynamic processes associated with occurrence of severe COLs and their predictability from 2011 to 2017.

From 2011 to 2017, eight COLs were identified using daily geopotential height data fields from the ECMWF. Furthermore, the systems were categorized into two groups according to their synoptic characteristics at 850 hPa. COLs which were linked with low-pressure system at 850 hPa were grouped together whilst those which were associated with a ridging high system were also grouped together. This was done to analyse the influence of high and low-pressure systems at 850 hPa as a driving mechanism during the occurrence of the COLs over the land. Lastly the accuracy of the 4.4 km UM was tested in testing both high and low-pressure associated COLs.

COLs often form over the South Atlantic Ocean and transit across different provinces of the country to the south Indian Ocean. These types of COLs lead to the cold conditions and heavy rainfall cross different parts of the country.

### 3.5.3 Trend analysis

Long-term analysis of trends is also important to determine the pattern of climatological variables over time. Trends may be linear or non-linear and can be used to predict the characteristics of a certain variables in the future. In this study, this method was used to analyze the patterns of rainfall and OLR from 1979 to 2017. A better understanding of long-term OLR and rainfall patterns over South Africa is significant for the identification of extreme values of similar variable associated with the occurrence of severe COL system.

### 3.5.4 Composite analysis

Composite analysis is a method which is used to diagnose the characteristics of one or more variables events of similar nature e.g. El Niño events. Composite analysis can show patterns in a

group better than individual cases (Nash and Endfield, 2008). Seasonal, monthly and daily extremes of different parameters can significantly bring out the daily characteristics COL events as they last for few days. In this study, this method investigates the correlation of the primary datasets during the occurrence of the COL systems.

### 3.5.5 Self-Organizing Maps

A Self-Organizing Maps (SOMs) is the classification and pattern recognition method used to diagnose climate parameters and anomalies that characterized certain events over the study period (Kohonen, 1982). For the purpose of this study, SOMs are used to create charts to investigate the anomalous characteristics of atmospheric and surface primary variables which linked with severe COL systems over South Africa. Firstly, synoptic maps showing anomalous closed geopotential height at 500 and 850 hPa were created. This was done to identify the location of the systems as well as investigating the near surface circulation associated with the identified systems. The maps with the closed lows were further checked against the total precipitation, temperature, CAPE, and OLR charts to complement the occurrence of the weather systems.

### 3.5.6 Unified Model simulations

The study will test the skill of the 4.4km UM data in simulating areas of deep convection and rainfall in COLs. The comparison was made for COL events which were experienced from 2016 to 2017, because the resolution of the UM was increased to 4.4km in 2016, while prior to that a grid spacing of 12km and 15km was used. The data analysed here, was produced on an operational basis at SAWS. The model simulations are at SAWS are updated four times a day, and therefore there is a 6-hour time step between each model run. The 24hr precipitation simulations from the 4.4 km UM are compared with the era-interim 6-hourly total precipitation.

To investigate the skill of the model in simulating location and areas of the deep moist convection of the identified systems, the model simulated geopotential height at 500 hPa and precipitation from simulations initiated with the 00Z, 12Z and 18Z observations are analysed. It may be noted that the simulations initiated from 06Z observations had to be deleted due to storage issue at SAWS and were therefore unavailable for this study. All three model outputs were compared with the observed 6-hourly total precipitation from ECMWF.

### 3.5.7 Visual inspection

This is the process of evaluating the accuracy of a forecast in predicting certain variables. This is done by comparing forecast with observation all together to determine the accuracy of the model (Cassola *et al.*, 2015). Even though the result of the method is not quantitative, it can provide a

better pattern of the variable being analyzed. It is recommended that the method must be applied with caution in any formal verification procedure to avoid biasness during interpretation (WMO,2000). In this study, this method was significantly applied to identify the accuracy of the model in simulating the areas associated with the occurrence of deep moist convection. The 6-hourly closed geopotential height at 500 hPa and precipitation charts were verified with the observed 6-hourly closed geopotential and total precipitation from ECMWF.

### 3.5.8 Case study approach

A case study approach is defined a way of examining the characteristics of a certain event, phenomenon, or other observations over a certain period. In this study, a case study approach was used to examine the characteristics which were associated with the occurrence of COL events from 2011 to 2017. The approach further examines if the model was accurate in simulate the experienced weather characteristics which were associated with the events.

## 3.6 Data display

### 3.6.1 The Grid Analysis and Display System

Grid Analysis and Display System (GrADS) is an interactive desktop tool that is used for accessing, manipulation and visualization of earth science data. It was developed in 1988 by Center for Ocean-Land-Atmosphere studies, institute of Global Environmental and Society at George Mason University. The format of data can be binary, NetCDF, HDF-SDS, or GRIB files (Doty 1995). GrADS may be used to overlay certain variables together for better analysis of their correlation. For this study, GrADS was used to map spatial patterns of weather and climate variables at a different atmospheric level. Furthermore, it was used to plot line graphs comparing the simulated and observed rainfall.

### 3.6.2 Royal Netherlands Meteorological Institute Climate Explorer

The KNMI climate explorer is a web application which one can use to statistically analyse climate data <https://climexp.knmi.nl/start.cgi> . Initially in 1999, it was used to analyse ENSO teleconnections and then developed to an analysis tool of more than 10 TB of climate data over the years. Most of its observational data are updated every month with more data provided by external sites on request. Available data is generally split between time series and spatial field. Station data, climate indices, reanalysis products, climate model output, seasonal and decadal forecasts can be accessed through this tool (Trouet, 2013). Furthermore, the explorer consists of

a set of shell scripts and Fortran programs and runs under Linux and Mac OS X. In this study, KNMI climate explorer was used to access rainfall and OLR daily data.

### 3.6.3 National Aeronautics and Space Administration Giovanni

Nasa Giovanni is an online web application which may be used to visualize, analyze and obtain remote sensed data particularly from National Aeronautics and Space Administration (NASA) satellites. Giovanni was derived from Goddard Earth Sciences Data and Information Service Center. <https://giovanni.gsfc.nasa.gov/giovanni/>

Giovanni can be used to visualize time-averaged map, area-averaged time series, scatter plot, vertical profiles and accumulation map. This web application provides data for aerosols, atmospheric chemistry, temperature and moisture as well as rainfall. It can also provide an output from assimilation models covering atmospheric, oceanographic and land surface parameters (Acker *et al.*, 2014). Giovanni was used to obtain precipitation satellites data associated with the identified COL events to complement the accuracy of the observational data

This online web application is often preferred for high school and undergraduate research as it provides uncomplicated access to remote sensed data (Acker *et al.*, 2014). Through manipulating imagery, students tend to gain knowledge on investigating Earth's interconnected geophysical and biological components through using remote-sensing data (Lloyd *et al.* 2008).

NASA satellites consist of an advanced radar (radiometer) systems for accuracy measurement of precipitation from space. Thus, Giovanni can provide a vertical profile of precipitation from the surface up to a height of about 20 km.

## 3.7 Summary

The primary datasets of this study were obtained from secondary sources, which include KNMI, ECMRWF and NCEP NCER Reanalysis II. The annual and seasonal cycles, as well as the spatial patterns analysis for both rainfall and OLR from 1979 to 2017, were achieved by using KNMI and NCEP Reanalysis II datasets. The identification of the COL weather systems and analyses of their associated meteorological structure, physical and thermodynamic processes was achieved by using daily data fields the ECMWF. Furthermore, the observational datasets which were used against the simulations of the model were also obtained from the ECMWF. Self-organized maps and line graphs showing the characteristics primary variable of the COL systems were created using GrADS. Furthermore, the characteristics of variables for the identified systems were verified by quick plots created on KNML Climate Explorer and Nasa Giovanni online web applications.



## Chapter 4

# Evolution and meteorological structure of recent cut-off lows over South Africa

### 4.1 Introduction

In this chapter, Cut-off low (COL) events which were associated with deep moist convection and heavy rainfall events from 2011 to 2016 were identified and analyzed. At first, seasonal mean cycles and patterns of global precipitation climatology project (GPCP) rainfall as well as the outgoing longwave radiation (OLR) from 1979 to 2017 over South Africa. GPCP and OLR are the primary datasets employed in this study. The chapter seasonal distribution of COLs during this study period is determined whilst systems are analyzed as case studies for their dynamic and thermodynamic structure and their associated impacts over the affected area.

### 4.2 Mean annual cycles of rainfall and Outgoing Longwave Radiation over South Africa

South Africa is characterized by high interannual rainfall variability, which may be linked to fluctuation of sea surface temperatures (SSTs) in several local and remote ocean regions. Changes in temperatures of the surrounding ocean basins have a significant influence on the distribution of rainfall over the country. Warm SSTs ( $>28^{\circ}\text{C}$ ) over southwest Indian Ocean and the Mozambique Channel are conducive for tropical cyclogenesis which may lead to the heavy rainfalls over the region.

As defined in chapter 1, region 1 of the study area tends to receive most of its rainfall during the mid-summer season. Over this region, the December and January months tend to record average rainfall of between 120 mm to 130 mm (Fig. 4.1). These months are characterized by a significant number of heavy rainfall days (Rouault and Richard 2003). The period from April to September is predominantly dry with little rainfall. Rouault and Richard (2003) found this region to exhibit the biggest difference between summer and winter rainfall. However, a COL event may occur and provided heavy anomalous rainfall during the dry season.

High rainfall during the early austral summer rainfall leads to lower values of OLR ( $\sim 250\text{Wm}^{-2}$ ) over the region (Fig. 4.1). The strength and location of the continental lows, tropical cyclones, cloud bands have a significant influence on the rainfall characteristics over the region. As a result

of high rainfall, the region plays a significant role for over a third of South Africa's Gross Domestic Product (GDP) (Dyson, 2009).

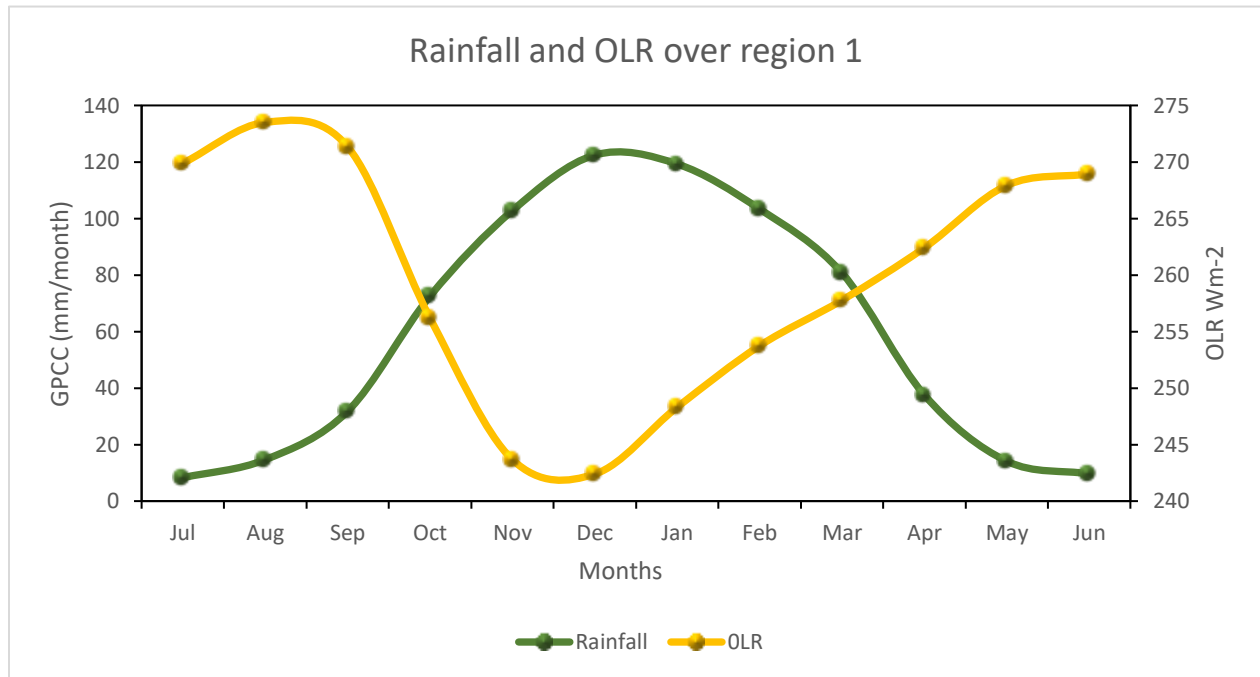


Figure 4. 1: Long-term mean annual global precipitation climatology project (GPCP) rainfall (mm/month) and Out-going Longwave Radiation (OLR) (Wm/2) cycles over region 1.

Region 2 of the study area covers the central and western interior of the country and can be referred to late summer region. Unlike region 1, this region tends to receive peak amount of rainfall during December, January and March with an average of about 75 mm (Fig. 4.2). The western areas of this region tend to me wetter during austral winter seasons when compares to the most central areas (Rouault and Richard 2003). The region tends to experience high OLR values during austral winter months due to low rainfall activity (Fig. 4.2).

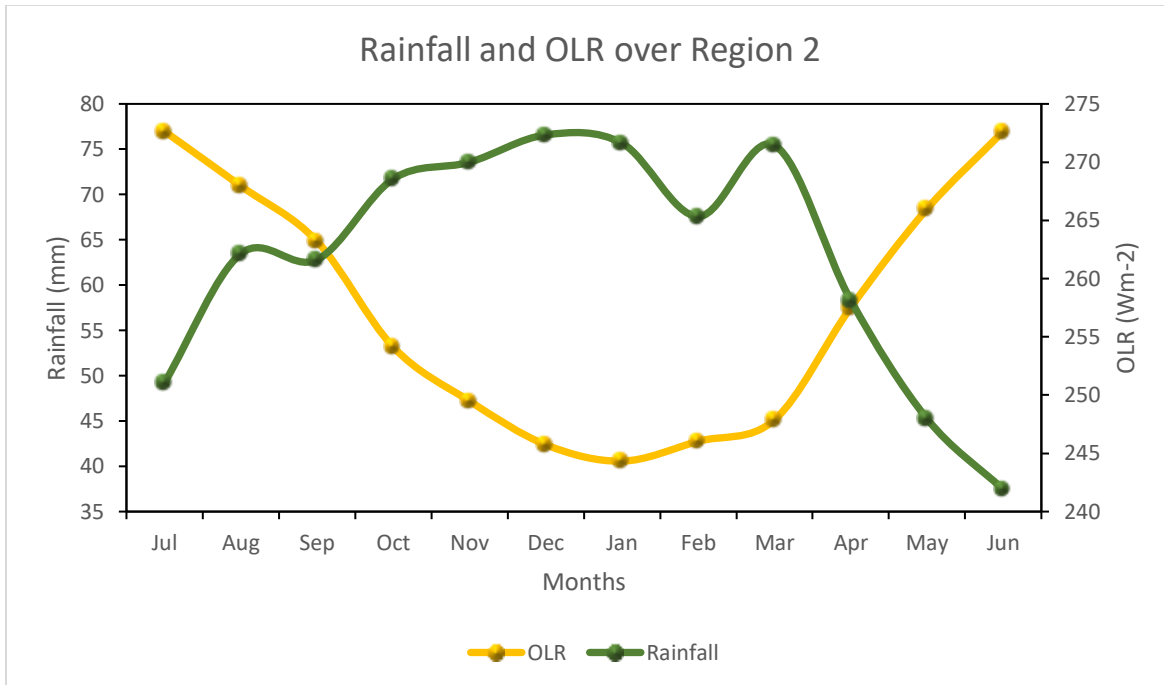


Figure 4. 2: Long-term mean annual global precipitation climatology project (GPCP) rainfall (mm/month) and Out-going Longwave Radiation (OLR) (Wm/2) cycles over region 2.

Region 3 tends to receive rainfall throughout the year, with the maximum amount during June, July, August and March with a monthly average rainfall of 51 mm to 61 mm (Fig. 4.3). This region covers the smallest portion of the country and is referred to as the Cape south coast (Engelbrecht *et al.* 2015). A sharp drop in the average monthly rainfall from 57 mm to 24 mm is observed during summer months (Fig. 4.3). February and December tend to be dominated by the lowest average rainfall, with the highest values of OLR.

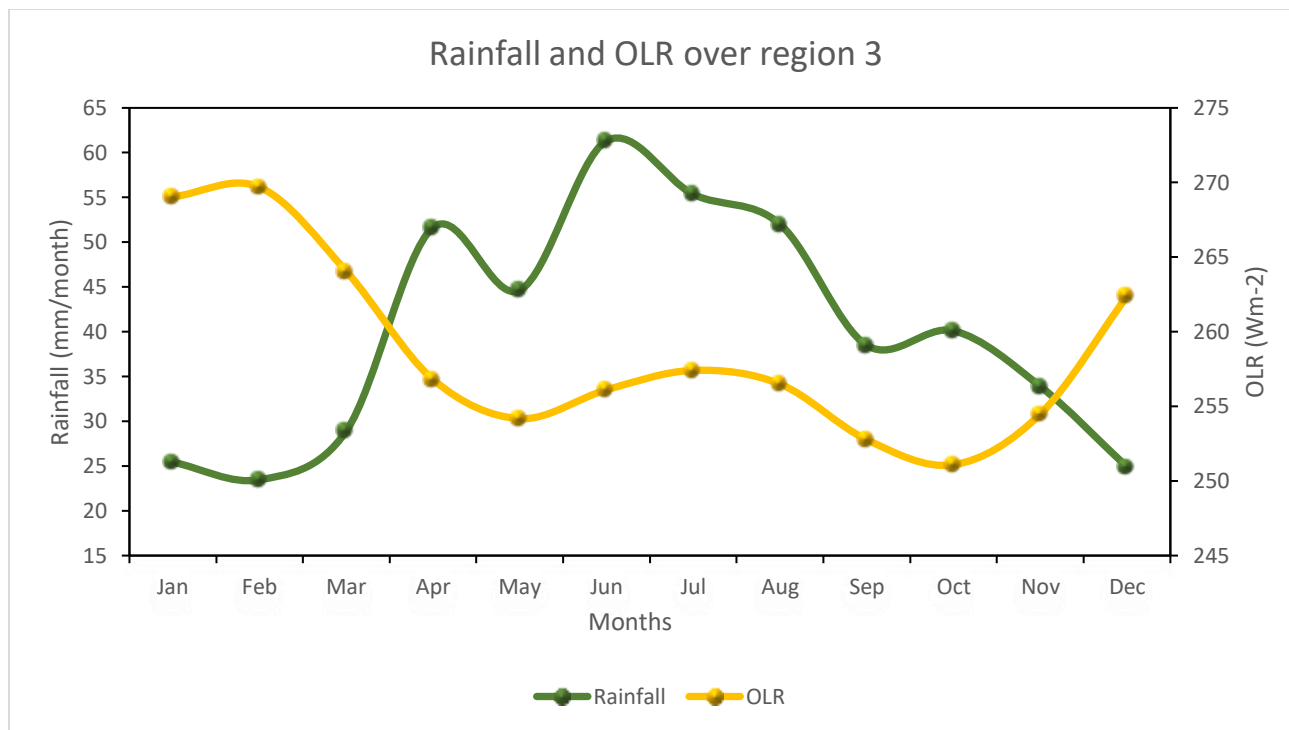


Figure 4. 3: Long-term mean annual global precipitation climatology project (GPCP) rainfall (mm/month) and Out-going Longwave Radiation (OLR) (Wm/2) cycles over region 3.

Region 4 (Fig1.3) of the study area covers areas which receive their highest rainfall during austral winter season. Rainfall activity tends to peak during June-August, with a monthly rainfall amount of about 50 mm per month (Fig. 4.4). The equatorial migration of the subtropical highs and attendant cold fronts results in winter rainfall. Some cold fronts may also co-occur with an upper COL. The recent decrease in autumn (March-May) rainfall over the southwest Cape may also suggest a shift in the seasonality of weather systems affecting that region. Ridging highs also contribute to rainfall over this region and the entire escarpment areas up to the northeast of the country. The region is characterized by high values of OLR during the austral summer with low figures during the austral winter season (Fig 4.4).

The relationship between rainfall and OLR patterns tends to be weaker when moving away from the tropics. At some points, the values of OLR show a direct relationship with rainfall pattern (Fig. 4.3). As a result, OLR alone cannot be useful to analyze the rainfall pattern of regions far removed from the deep tropics.

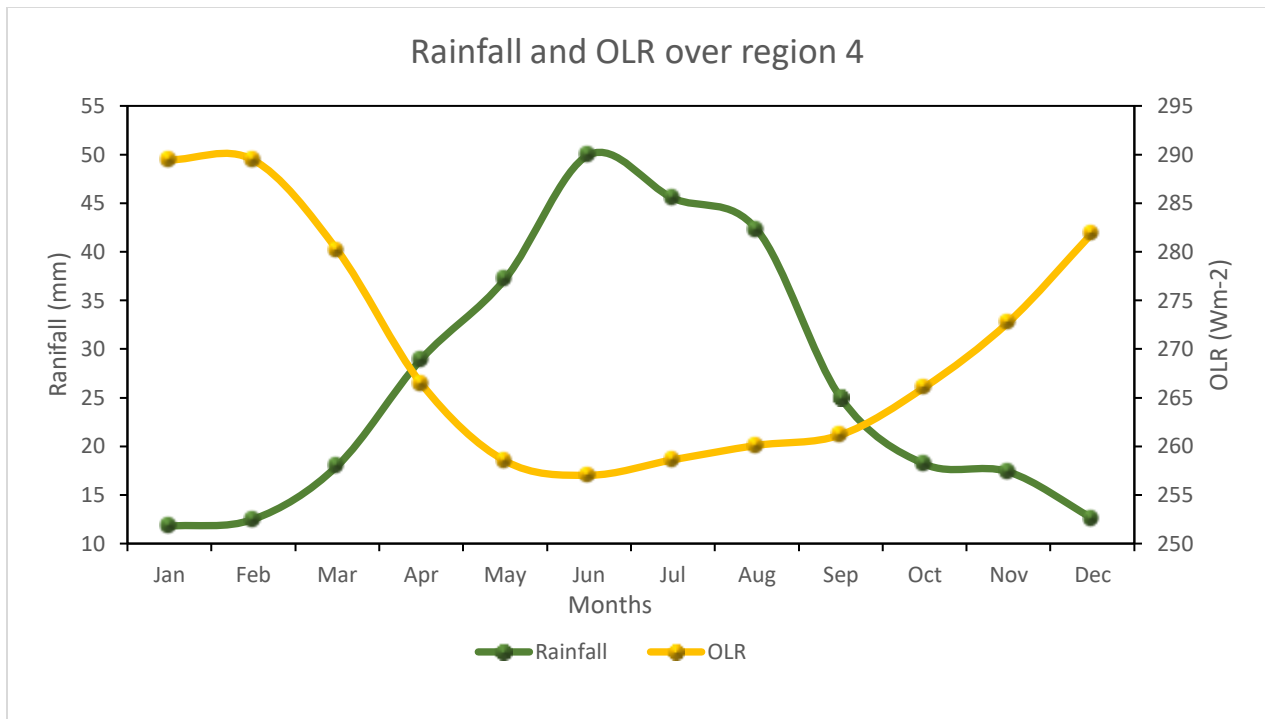


Figure 4. 4: Long-term mean annual global precipitation climatology project (GPCP) rainfall (mm/month) and Out-going Longwave Radiation (OLR) (Wm/2) cycles over region 4.

### 4.3 Long-term seasonal patterns of rainfall and OLR variabilities over South Africa

#### 4.3.1 Austral Summer season

The long-term mean (1979-2017) seasonal patterns of rainfall during the austral summer season (DJF) indicates that eastern South Africa is relatively wet, especially on the escarpment with a sharp gradient to the western interior and Atlantic coast (Fig. 4.5 a). Rainfall over the north eastern parts of the country peaks during the at 6 mm/day during January (Fauchereau *et al.* 2003). The polewards shift of the Inter Tropical Convergence Zone (ITCZ) in summer has a significant influence on the seasonal distribution of rainfall over the region. The displacement of the ITCZ about 20° over Mozambique and Madagascar promotes the inflow of the north-easterly winds to interior of South Africa to the development of tropical-temperate cloud bands (Hart *et al.* 2010). High rainfall activities over the north eastern parts of the are country also promoted by the development of low-pressure systems over land (Reason *et al.* 2006).

It is during this period when most parts of the Kalahari, and northern Namibia, Western, Northern and Eastern Cape Provinces are characterized by low rainfall (Fig. 4.5 a). As expected, regions of high rainfall over the north-eastern parts of the country are observed with the low values of

OLR, mostly ranging from 230 to 260 W/m<sup>2</sup>. This is a result of convective activities which lead to substantial cloud cover over the region. Parts of the Northern, Western and Eastern Cape provinces are characterized by high values of OLR, ranging from 270 to 290 W/m<sup>2</sup> due to low rainfall (Fig. 4.5 b).

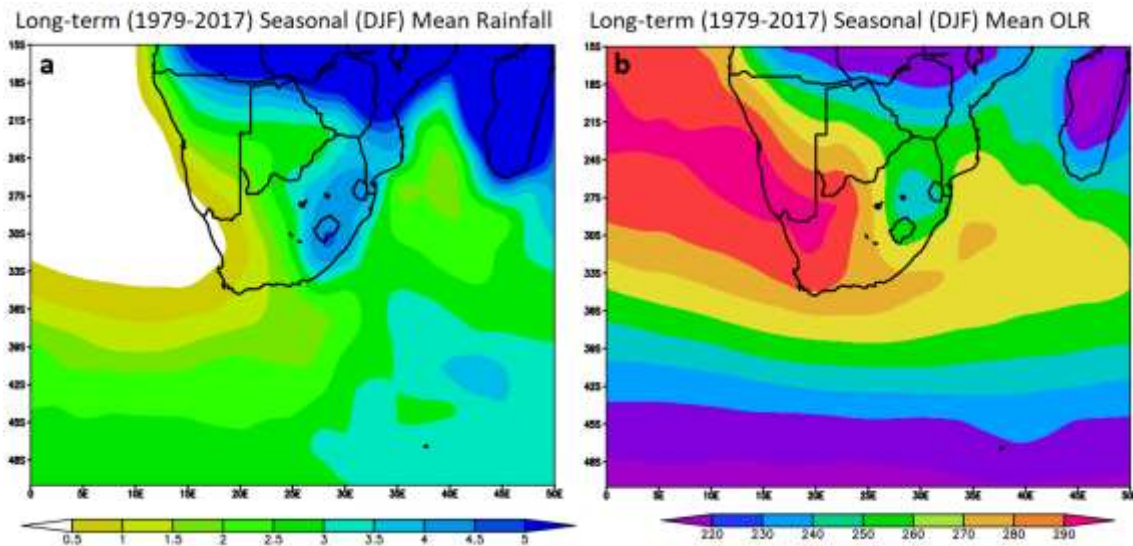


Figure 4. 5: Long-term summer seasonal (a) global precipitation climatology project (GPCP) rainfall (mm/month) and Out-going Longwave Radiation (OLR) (Wm/2) distribution over South Africa.

#### 4.3.2 Austral autumn season

Over southern Africa, the autumn season is characterized by a decrease in the amount of rainfall from the austral summer seasonal maximum rainfall (Fig. 4.6 a). This decrease can be clearly observed over the most parts of Limpopo, Mpumalanga, Gauteng and North West, Free State and Eastern Cape provinces compared to summer (Fig. 4.6 a). A slight increase in rainfall can be observed over the several parts of the Western Cape Province (Fig. 4.6 a). The increase of rainfall over the Cape south coast is often associated with a slight northward shifting of temperate weather systems. Over the north eastern parts of the country, the decrease in the amount of rainfall correlates with the increasing values of OLR by 10 W/m<sup>2</sup>. The values of OLR also observed, decrease from 290 to 270 W/m<sup>2</sup> over the south coastal regions (Fig. 4.6 b).

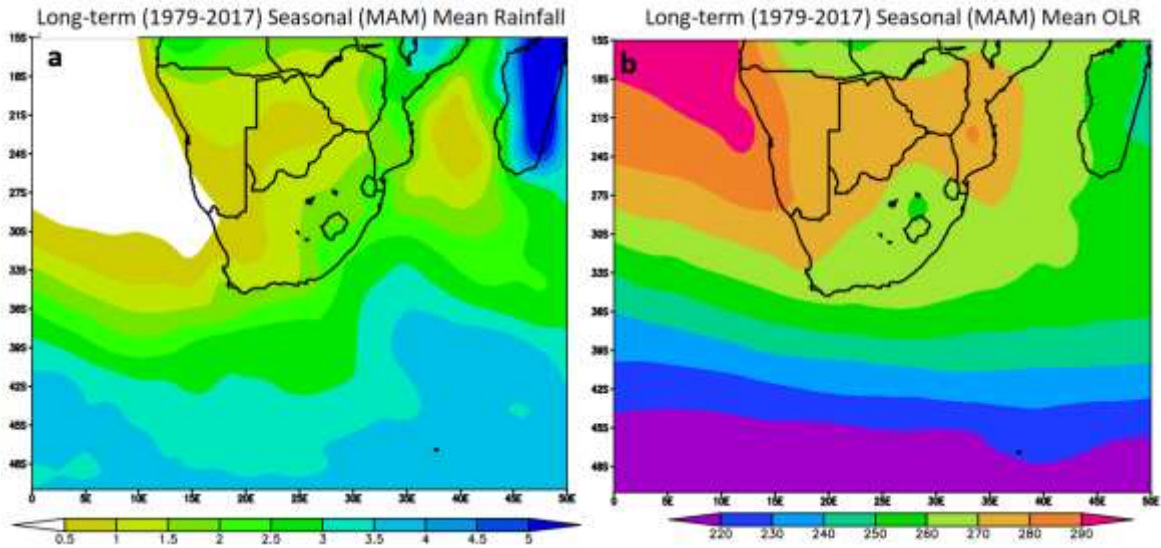


Figure 4. 6: Long-term Autumn seasonal (a) global precipitation climatology project (GPCP) rainfall (mm/month) and (b) Out-going Longwave Radiation (OLR) ( $Wm/2$ ) distribution over South Africa.

#### 4.3.3 Winter (JJA) season

The spatial rainfall distribution for austral winter season shows most interior parts of the country experiencing dry conditions, whilst the Cape south coast is characterized by wet conditions (Fig. 4.7 a). This is because of little or no convective activities over the interior, which is often by the dominance of high-pressure system over the land and the South Indian Ocean. The equator ward shifting of the South Atlantic and South Indian Ocean High pressure cells tend to facilitates the northeast shifting of temperate weather systems such as extratropical cyclones, cold fronts and cut-off lows towards the country. As the result, most parts of Western and Eastern Cape provinces experience more rainfall when compared to other parts of the country (Fig. 4.7 a). The northern and several central parts of the country tend to be characterized by clear skies, which promote high values of OLR ranging from 270-280  $W/m^2$  (Fig. 4.7 b).

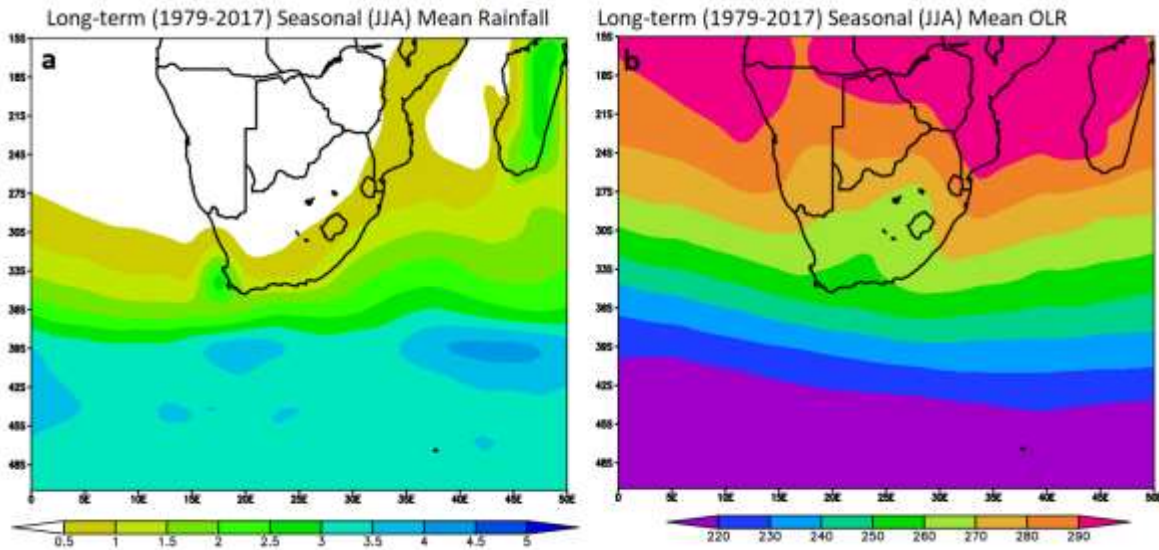


Figure 4. 7: Long-term seasonal Winter (a) global precipitation climatology project (GPCP) rainfall (mm/month) and (b) Out-going Longwave Radiation (OLR) (W/m<sup>2</sup>) distribution over South Africa.

#### 4.3.4 Austral spring season

During austral spring, most parts of the country tend to be characterized by wet conditions, with high rainfall activities over the Eastern Cape and KwaZulu-Natal provinces. During this season, most parts of the Western Cape and North West provinces experience dry conditions (Fig. 4.8 a). Most of the eastern coastal areas tend to get moisture from South Indian Ocean (Fig. 4.8 a). In response to increased cloud cover over most parts of the country, parts of Gauteng, Free State, Kwazulu-Natal, Eastern Cape and Limpopo provinces, show low values of OLR of less than 280 W/m<sup>2</sup> (Fig. 4.8 b). High values of OLR are observed over the northern parts of Western and Northern Cape provinces (Fig. 4.8 b).

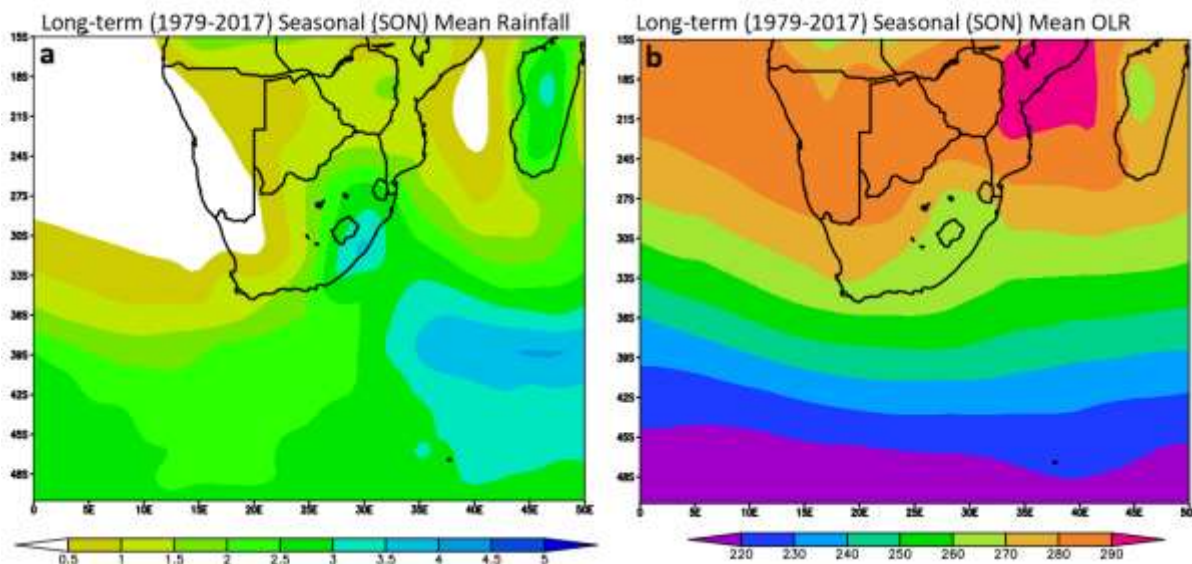


Figure 4. 8: Long-term spring seasonal (a) global precipitation climatology project (GPCP) rainfall (mm/month) and (b) Out-going Longwave Radiation (OLR) (W/m<sup>2</sup>) distribution over South Africa.

#### 4.4 Seasonal distribution and duration of identified Cut-off Lows systems

##### 4.4.1 Seasonal distribution of identified Cut-off Lows systems.

The seasonal distribution of the COLs which were associated with heavy rainfalls from 2011 to 2017 over South Africa is indicated in Figure 4.9, 60% of the observed COL systems occurred during June-July-August (JJA) followed by September-October-November (SON) with 30% and March-April-May (MAM) with 10% while there was no system associated observed in December-January-February (DJF). These findings are in-line with the findings of Singleton and Reason (2007a) who indicated a shift in the seasonal distribution of COLs from March-May to June-August. The analysis of 7-years of COL systems which were associated with heavy rainfall shows a slightly different pattern from the findings of the previous studies such as Molekwa (2013) where high seasonal distribution of COLs was observed during MAM with the least occurrence during DJF. Climatology of COLs presented by Taljaard (1985) and Singleton and Reason (2007a) from 1973 to 1982 and 1973 to 2002, respectively, found that an average of 11 COLs occur per year with highest number experienced in austral autumn (MAM) season. Tyson and Preston-White (2000) also found that the frequency of COLs shows a semi-annual variation with highest number in March to May and September to November.

In the current study, COLs which was coupled with the dominance of high-pressure circulation near the surface (850 hPa) were identified with the occurrence of ridging highs, whilst those which

were coupled with both low- and high-pressure circulation patterns were observed with the occurrence of cold fronts. There was no event which was identified with only low-pressure circulation pattern near the surface. From the 60% of the total COL systems during the JJA season, 40% were observed with the occurrence of cold fronts, whilst 20% were coupled with the dominance of ridging high systems at 850 hPa. During the SON 20% of the systems were coupled with a surface ridging high and 10% with both low- and high-pressure circulation (Fig. 4.9).

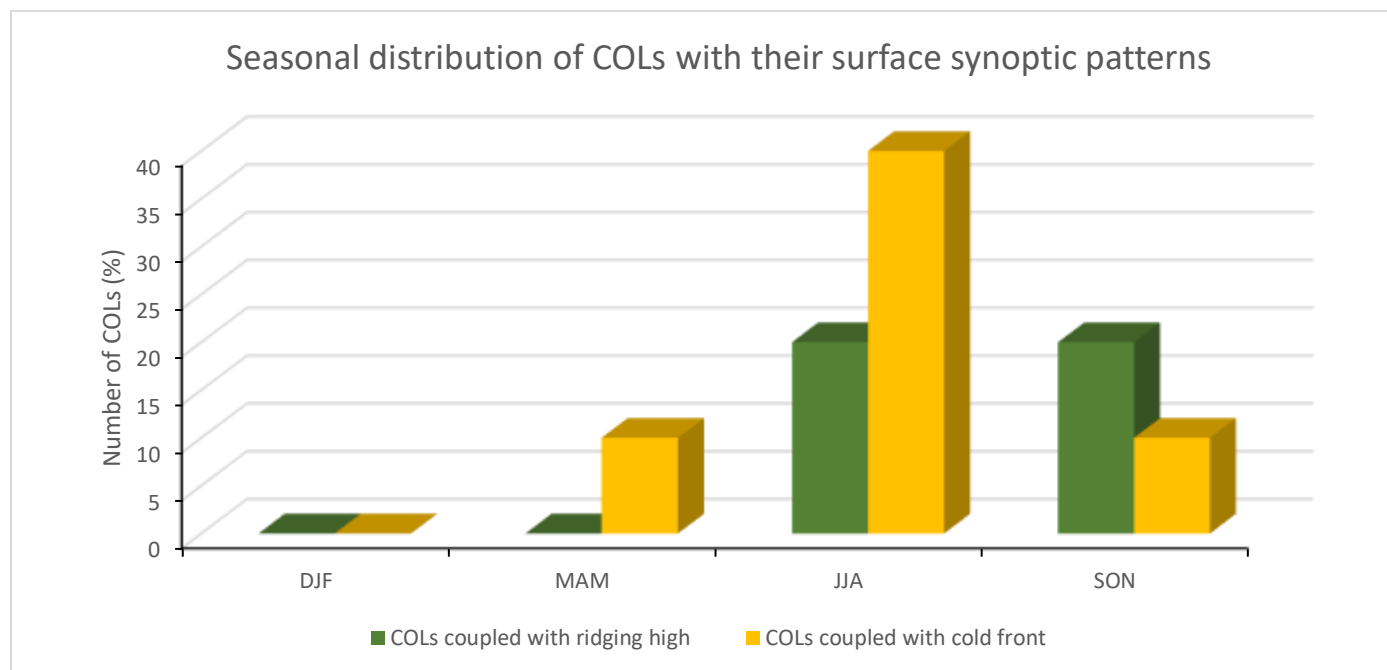


Figure 4. 9: Seasonal distribution in percentage of Cut-off Lows (COLs) with their synoptic near surface patterns from 2011 to 2017

#### 4.4.2 Seasonal distribution of Cut-off Lows over region A and B

There is a shift in the preferred geographical regions for the development of COLs over South Africa. In this study, the highest number (70%) of COLs developed over Region A (-22°S to -32°S) with a least number (30%) of COLs developed over region B (32°S-34°S) (Table 4.1). All identified COL systems were observed to transit across both region A and B of the study area. Over region A and B, the highest number of COL events 40% and 20% respectively, were observed during JJA with no event observed during DJF during this study period. SON was recorded as the second season with the highest occurrence of COL events with 20% and 10% respectively over both region A and (Fig. 4.10).

Table 4. 1: Number of Cut-off Lows (COLs) over region A and B with their seasons of occurrence from 2011 to 2017

Seasons	DJF	MAM	JJA	SON	TOTAL
Region A	0	1	4	2	7
Region B	0	0	2	1	3
<b>TOTAL</b>	0	1	7	3	<b>10</b>

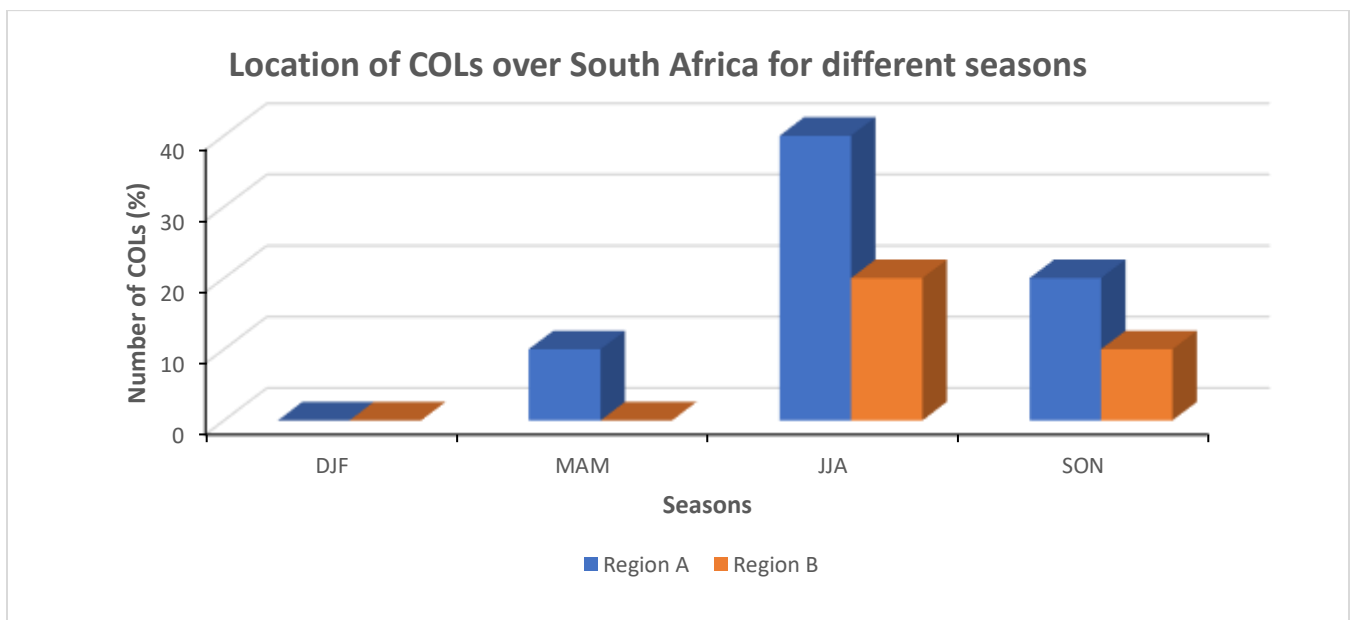


Figure 4. 10: The seasonal distribution of Cut-off Lows (COLs) in percentage over region A and B from 2011 to 2017

#### 4.4.3 Duration of the Cut-off Lows during different seasons in South Africa

Long-term analysis of the characteristics of COLs by Molekwa (2013) found that most COLs lasted for 2-4 days over the country. 64% of COL systems which last for more than 24-hours have been associated with a significant influence on the total rainfall over certain parts of the country. Furthermore, the analyses indicated that high contributions of rainfall associated with the occurrence of COLs has observed over the coastal regions with approximate 40% and less 10% annually over the most interior parts of the country. In this study, most (60%) of the identified COLs lasted for 3-4 days with 40% of them observed during the JJA about 10% occurred during MAM and the SON seasons respectively (Fig. 4.11). 30% of the total identified systems lasted

for more than 4 days with 20% observed during JJA and 10% during the SON seasons (Table 4.2). Very few COL systems lasted for 1-2 days during SON season in this study period (Fig. 4.11). The SON season was the only season which was identified with all three categories of COLs (Fig. 4. 11).

Table 4. 2: Number of Cut-off Lows (COLs) associated with heavy rainfall from 2011 to 2017 in three duration categories.

Seasons	DJF	MAM	JJA	SON	TOTAL
1-2 days	0	0	0	1	1
3-4 days	0	1	4	1	6
>4 days	0	0	2	1	3
<b>TOTAL</b>	0	1	6	3	<b>10</b>

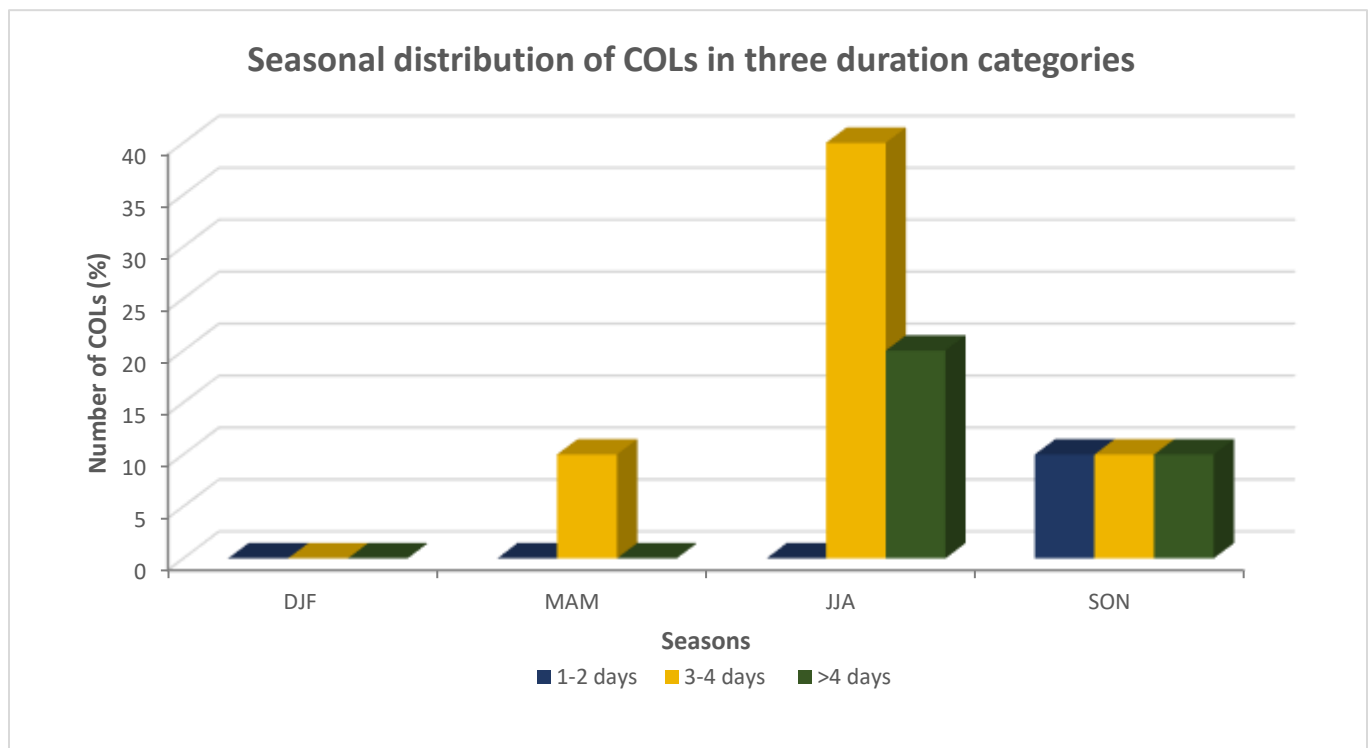


Figure 4. 11: Seasonal distribution of Cut-off Lows (COLs) in percentages from 2011 to 2017 in three categories over South Africa

## 4.4 Observed Cut-off Lows systems

Following the categories of COL systems according to their near surface circulation, this section examined the COL events which were associated with an anomalous meteorological structures and extreme rainfall from each category. The first event which was analyzed occurred from 13<sup>th</sup> to 15<sup>th</sup> July 2012 and was dominated by strong ridging highs near the surface. The second event occurred from 12<sup>th</sup> to 15<sup>th</sup> May 2016 and was accompanied by a cold front. Furthermore, satellite images were used to complement the occurrence of the near surface systems and to identify areas of convective clouds associated with the identified systems.

### 4.5.1 Event of 13-15 July 2012

On 13<sup>th</sup> July 2012, a steep upper-trough at 500 hPa was identified lying over the parts of Northern and Western Cape provinces, accompanied with cold temperatures of between -34 to -18°C due to the air for higher latitudes (Fig. 4.12 a and b). A surface high-pressure system was identified located over south-west of the country, promoting onshore flow and cold conditions of -4 to 16°C temperatures at 850 hPa over along some parts of the Western Cape Province and over the south Cape coast region (Fig. 4.12 c and d). At this stage, negative values of vertical velocity ( $\Omega$ ) were observed over the south east of the trough following the enhanced vertical motion (Fig. 4.13 e). The area also significant cloud at 18:00 UTC (Fig. 4.13 f).

On 14<sup>th</sup> July, the system was located behind two high-pressure systems located over the South Atlantic and South Indian Oceans respectively with a weak surface low over the interior (Fig. 4.14 c). The circulation which brought in cold air from the higher latitudes and led to cold conditions of -4 to 18°C temperatures over the country with lowest temperatures of -2°C over the western parts of the Northern, Western and Eastern Cape Provinces (Fig. 4.14 a and d). Following the cyclonic circulation over the center, the system was characterized by an inverted comma shaped cumulonimbus and thin cirrus clouds over the east of the country (Fig. 4.15 f).

The cumulonimbus clouds and thin cirrus cloud over and south of the south coast and over the western interior of the country marked the tear-off stage where the system detached from the main westerly wave (Fig. 4.15 f). After being teared way from the main westerly flow, the system promoted the development of showers and thunderstorms, with onshore flow from the two surface high pressure system which led to a heavy rainfall amount of about 120 mm. Areas which were associated with deep convection and heavy rainfall were complemented by low values of OLR (Fig. c) and negative pool of omega (Fig. e) over the south eastern coast of the country.

The location of the system over the eastern parts of the country with strong high-pressure circulation pattern near the surface marked the dissipating stage of the system on 15<sup>th</sup> July (Fig. 4.16 a). The location of the high-pressure system promoted the spread of cold air over the southern and central parts of the country (Fig. 4.16 c and d). Similar to the early stage, the system is no longer characterized by a closed circulation but more of zonal flow. The system was still characterized by cold air with a dissipating unshaped low level stratiform cloud (Fig. 4.17 b). This resulted in moderate rainfall amount of about 80 mm over the south eastern parts of the KwaZulu-Natal and Eastern Cape Provinces (Fig. 4.17 d).

#### 4.5.2 Event of 12-15 May 2016

On the 12<sup>th</sup> May 2016, a deep upper-air trough developed over the South Atlantic Ocean, just to the west of South Africa (Fig. 4.18 a). Over the surface the system was coupled with a low-pressure circulation over the South Atlantic Ocean and the trailing edge of an anticyclone circulation over the South Indian Ocean (Fig. 4.18 c). This circulation patterns led to low temperatures of between 10°C and 18°C over the several parts of Limpopo, Mpumalanga, Gauteng, Kwazulu-Natal, Eastern, Western and Northern Cape Provinces. The upper air trough led to the development of thick clouds over the western parts of the Northern and Western Cape Provinces and low values of OLR ranging from 220 to 230 W/m<sup>2</sup> but no rainfall observed over the country at this stage (Fig. 4.19 b, c and d).

The system deepened into a full closed low coupled with a cold front located over the southwestern interior of the country on 13<sup>th</sup> May 2016 (Fig. 4.20 a). At this stage, the low had been cut off from the main westerly flow and promoted convergence and enhanced uplift. over its eastern side, the system was characterized by a clear cyclonic PV and a pool of air of between -14°C to -18°C temperatures (Fig. 4.20 a and b). Severe cold conditions of between 4°C to 12°C temperatures were recorded over the parts of the Northern and Western Cape Provinces as well as the southern parts of Namibia (Fig. 4.20 d). The enhanced vertical motion promoted the development of complex cumulonimbus and cirrus clouds moderate to heavy rainfall over the central parts of the country (Fig. 4.21 e and f).

On 14<sup>th</sup> May 2016, the core of the system was located over the Northern Cape and North West Provinces (Fig. 4.22 a). Over its center, temperatures dropped to -16°C with a small pool of cyclonic negative potential vorticity of a value of  $-1.6 \times 10^{-6} \text{ m}^{-2} \text{ s}^{-1} \text{ K kg}^{-1}$  (Fig. 4.22 a and b). Cold conditions of between 6 °C to 12°C were observed over the Northern Cape and North West Provinces (Fig. 4.22 d). The system was characterized by high moisture content and cloud cover over its eastern side (Fig. 4.23 a and b). This led to rainfall amount of between 30 mm to 40 mm

over the parts of Northern Cape, North West and Gauteng and Free State Provinces (Fig. 4.23 d).

#### 4.5.3 Associated weather and effects

The COL system which occurred on from 13<sup>th</sup> to 15<sup>th</sup> July 2012 was associated with very cold conditions of less than 10°C over parts of the Northern, Western, Eastern Cape and Free State provinces from 13<sup>th</sup> to 14<sup>th</sup> July (SAWS 2012). The amount of 50 mm of rainfall over 24 hours with heavy snow over were certain areas of the affected provinces (SAWS 2012). There were several cases of people who died from drowning as a result of flooding and exposure to the extreme cold conditions. Destructive winds which damaged buildings and electricity power lines over parts of the Eastern Cape Province.

The second weather system led to heavy rainfall of between 25 and 100 mm over 24 hours in the Northern Cape Province. Most of the impacts were experienced over the northern parts of the Western and Northern Cape Provinces as it remained quasi-stationary during its development stages (EUMETSAT 2016).

#### 4.5.4 Conceptual Model

A Conceptual Model (CM) from EUMETSAT (2012) was used to show typical geopotential height and cloud patterns which are associated with the occurrence of the severe COL systems over South Africa. The model consists of four stages (EUMETSAT 2012).

In the first stage, the upper trough marks the development of the system with the formation of cirrus and CB clouds over east of the trough (Fig. 4.24 a). Typically, the trough is also characterized by the low-level cold air with the center covered by the cumulus clouds.

The deepening and tearing off of the trough mark the second stage model. There is an enhancement of cirrus and cumulonimbus clouds during this stage. Due to the cyclonic circulation the stage tends to be dominated by inverted comma shaped cumulonimbus and cirrus clouds over the eastern and southern part of the upper low (Fig. 4.24 b).

When the core of the COL is clearly visible, the third stage, the southern and western side of the upper trough is covered by low level stratiform clouds (Fig. 4.24 c). The inverted comma clouds which developed during the tear-off stage become clearly visible during this cut-off stage.

In the final stage, the closed circulation of the upper air returns to the zonal flow (Fig. 4.24 d). The system can still be coupled with a low-level cumulus cloud below the upper trough, with no more inverted comma shaped clouds to mark the dissipating stage.

## 4.6 Summary

To achieve the first objective, COL systems were identified using geopotential height at 500 hPa. Out of the 10 identified systems, five were coupled with surface high-pressure, whilst other five were linked with both low- and high-pressure systems near the surface. The presence of a surface high-pressure system during the occurrence of COL systems promoted the vertical uplift of air. As a result, the identified and analyzed systems were associated with negative values of vertical velocity and the development of inverted comma-shaped cumulonimbus and cirrus convective clouds over their east and southern sides. The development of convective clouds promoted the occurrence of thunderstorms and heavy rainfall. Areas of deep moist convection coincide with negative values of potential vorticity and negative anomalies OLR. The analysis of the seasonal distribution of the COL systems over region A reveals that the highest occurrence of COLs is experienced during JJA followed by SON. The lowest number of COLs occurred during DJF over South Africa. High occurrence of COL systems was identified over the regions categorized under A than in regions under B. A number of systems lasted for 3-4 days followed by systems which lasted for more than four days with few cases lasting for 1-2 days. COLs which are coupled with surface low- and high-pressure systems are more common and tend to occur during JJA and SON seasons in South Africa. There is a noteworthy shift on the occurrence of COL systems from MAM to JJA and towards northeastern parts of the country, when compared with the finding of the previous studies such as Molekwa (2013) and (Singleton and Reason, 2007b).

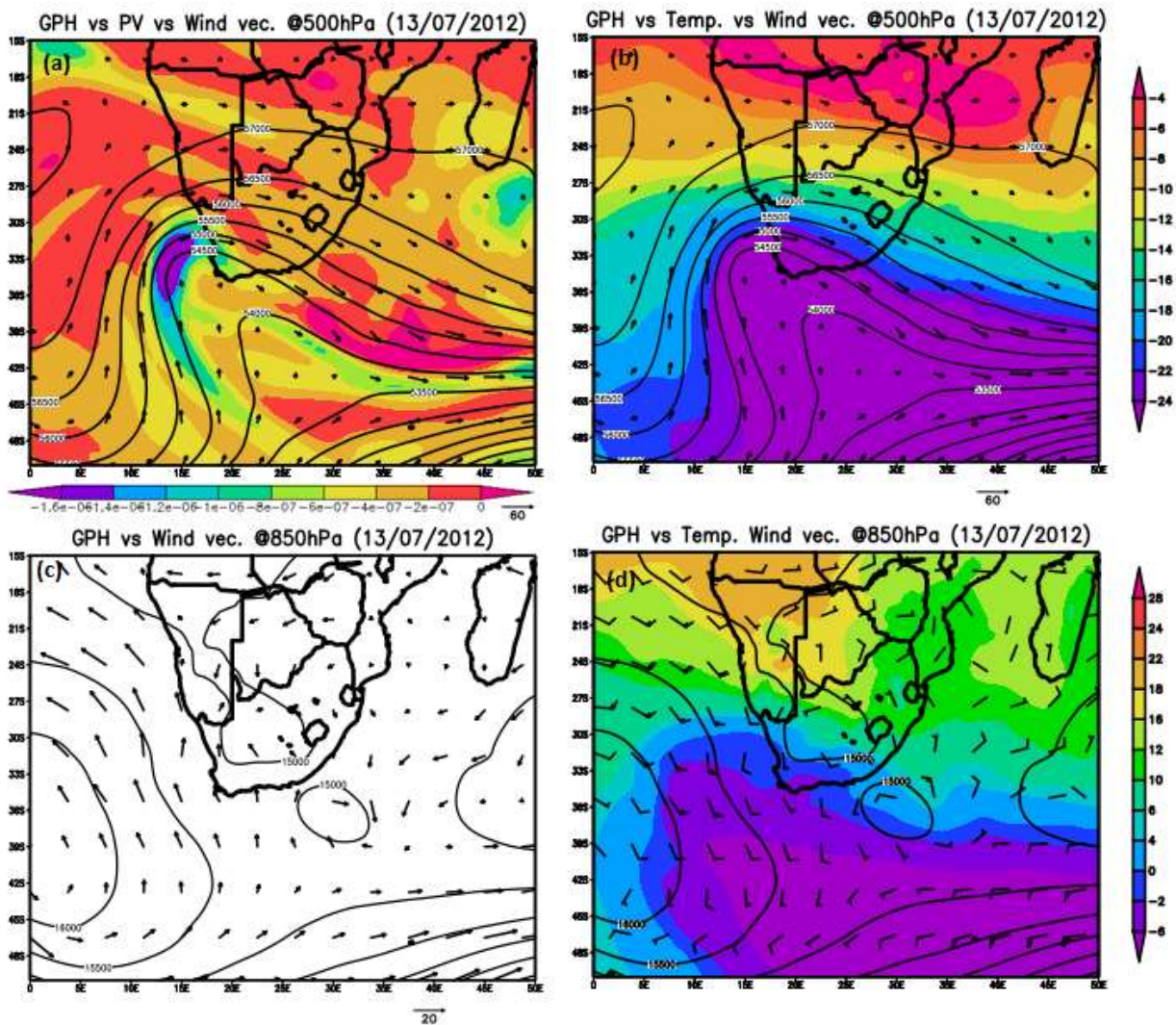


Figure 4. 12: Geopotential height (hPa) vs potential vorticity at 500 (a), Geopotential height (hPa) vs Temperature (°C) at 500hPa (b), Geopotential Height (hPa) vs Winds at 850hPa (c) and Geopotential Height (hPa) vs Temperature (°C) at 850hPa (d), **13 July 2012**

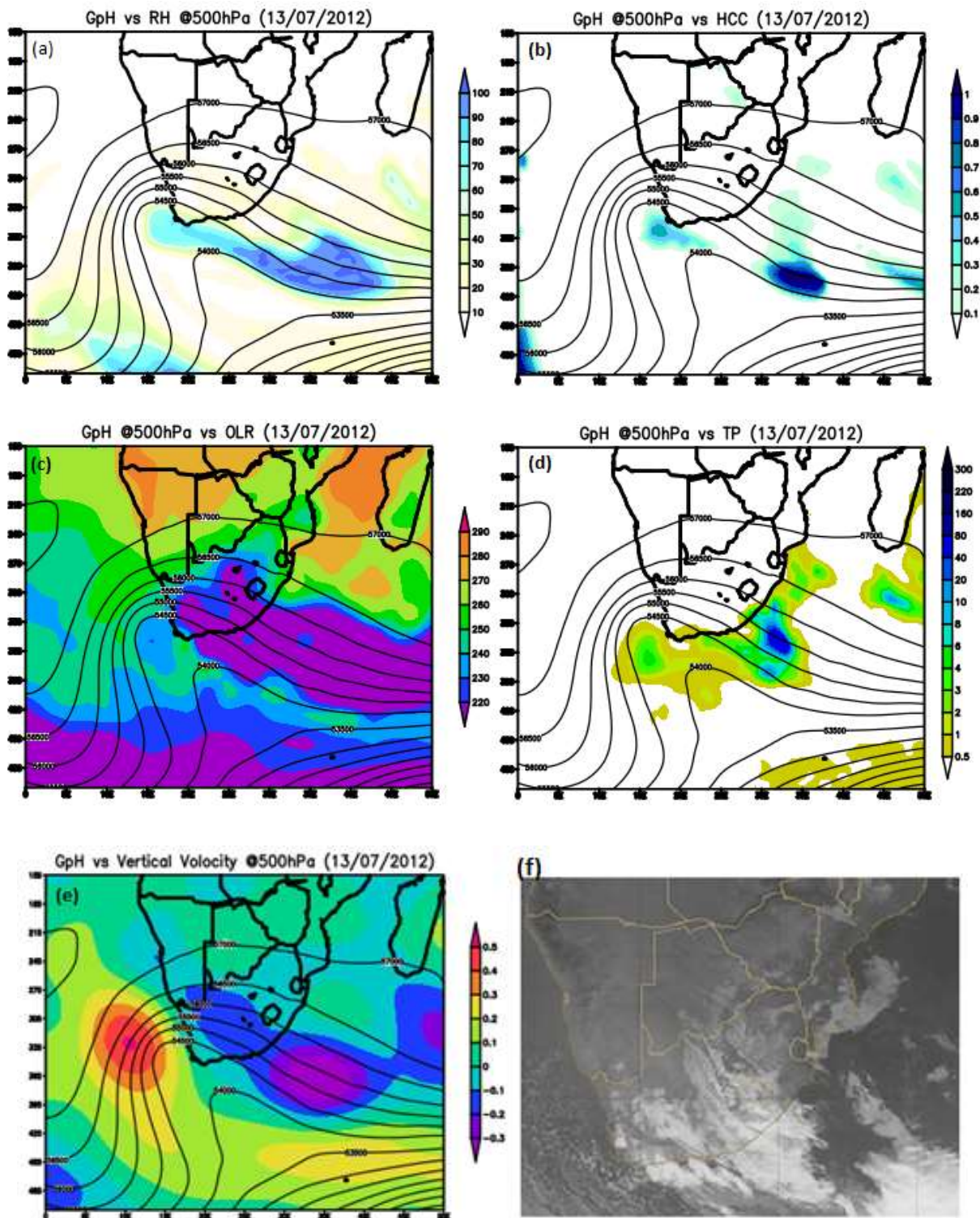


Figure 4. 13: Geopotential height (hPa) at 500 (hPa) vs Relative humidity (a), High Cloud Cover (HCC) (d), Out-going Longwave Radiation (OLR) (c), Total rainfall (mm/day) (d), Vertical velocity (e) and Infrared image of COL at 18:00Z *copyright (2019) EUMETSAT* (f), **13 July 2012**

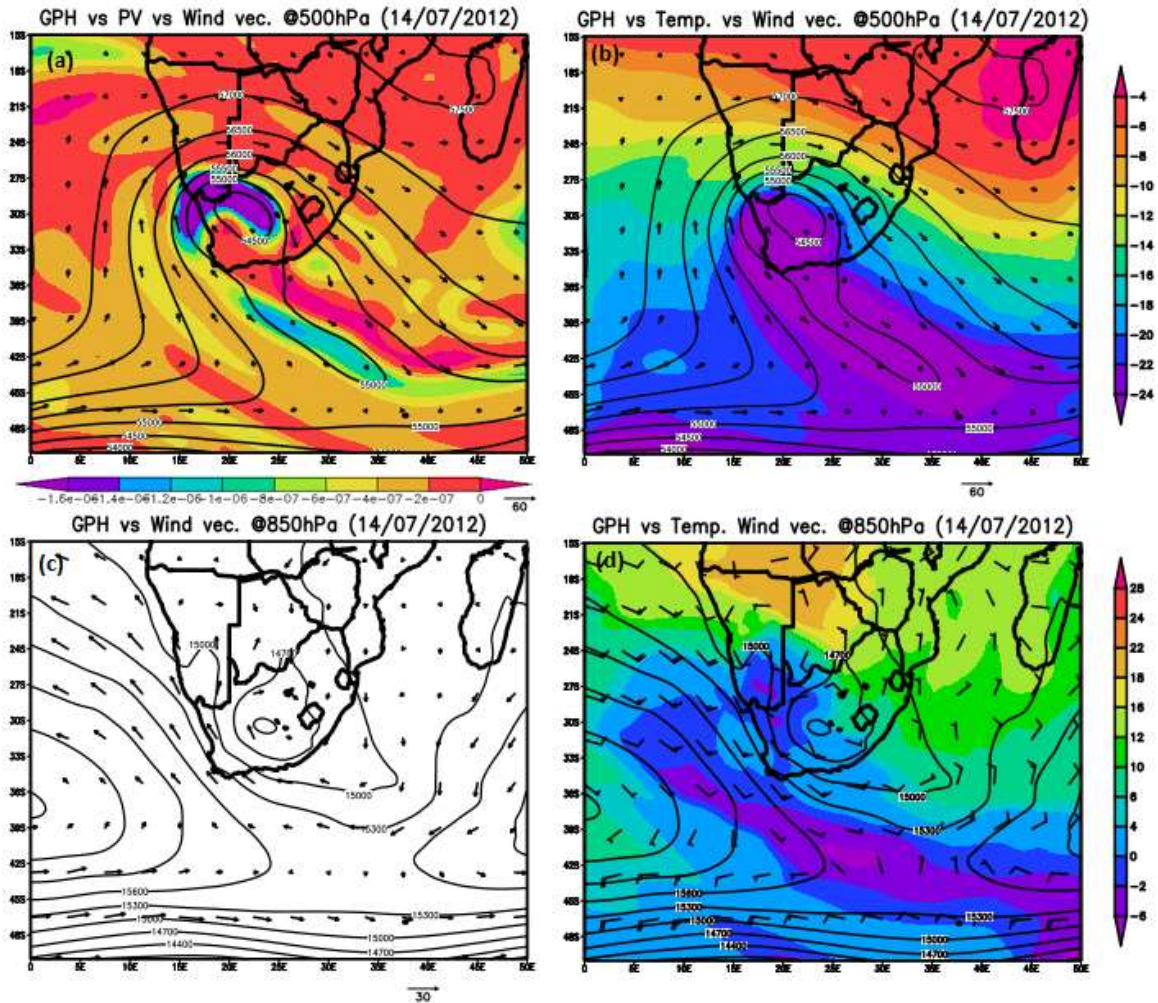


Figure 4. 14: Geopotential Height (hPa) vs Potential vorticity at 500 (a), Geopotential Height (hPa) vs Temperature (°C) at 500hPa (b), Geopotential height (hPa) vs Winds at 850hPa (c) and Geopotential height (hPa) vs Temperature (°C) at 850hPa (d), **14 July 2012**

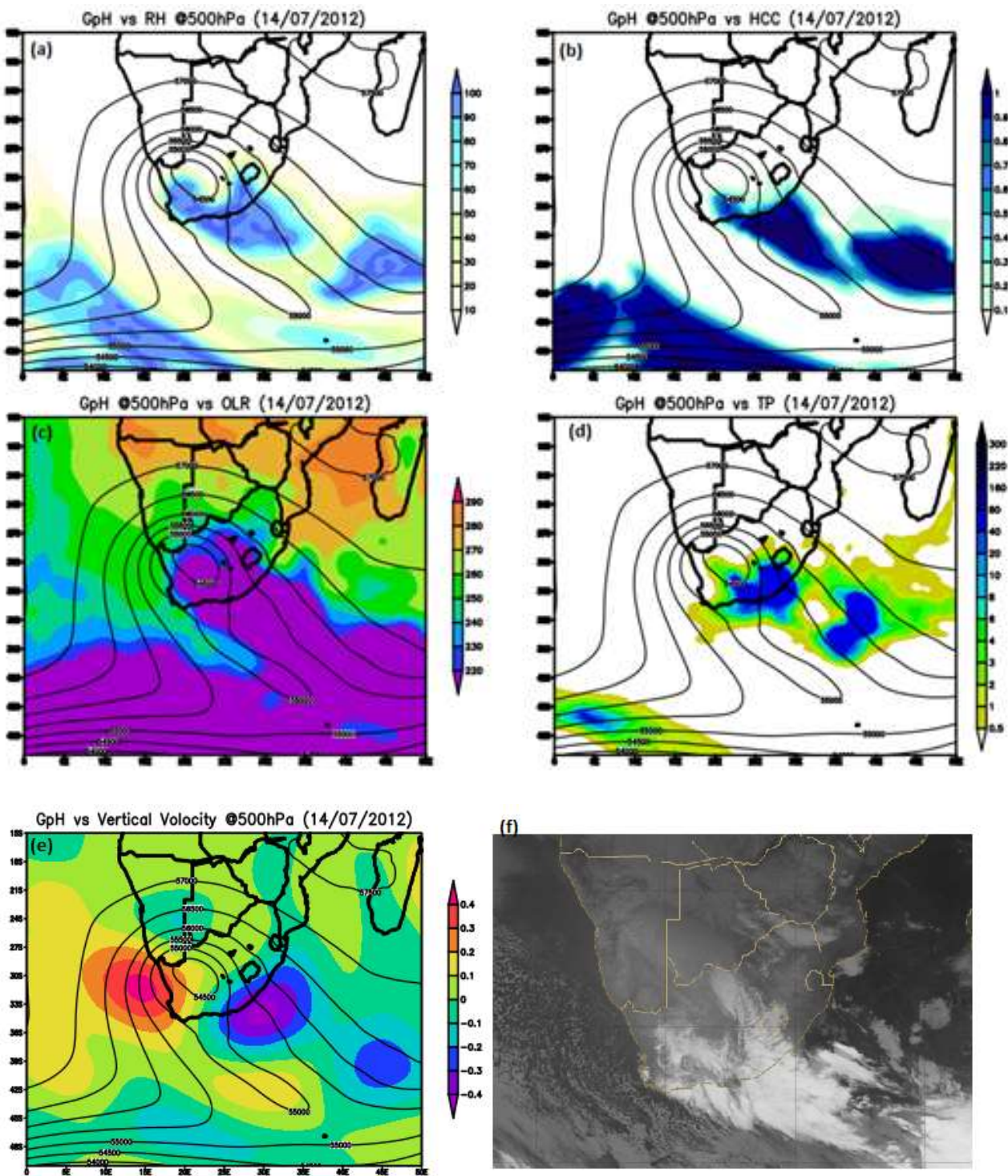


Figure 4. 15: Geopotential Height (hPa) @ 500 (hPa) vs Relative humidity (a), High Cloud Cover (HCC) (d), OLR (c), Total rainfall (mm/day) (d) Vertical velocity (e) and Infrared image of COL at 10:00Z copyright (2019) EUMETSAT (f), 14 July 2012

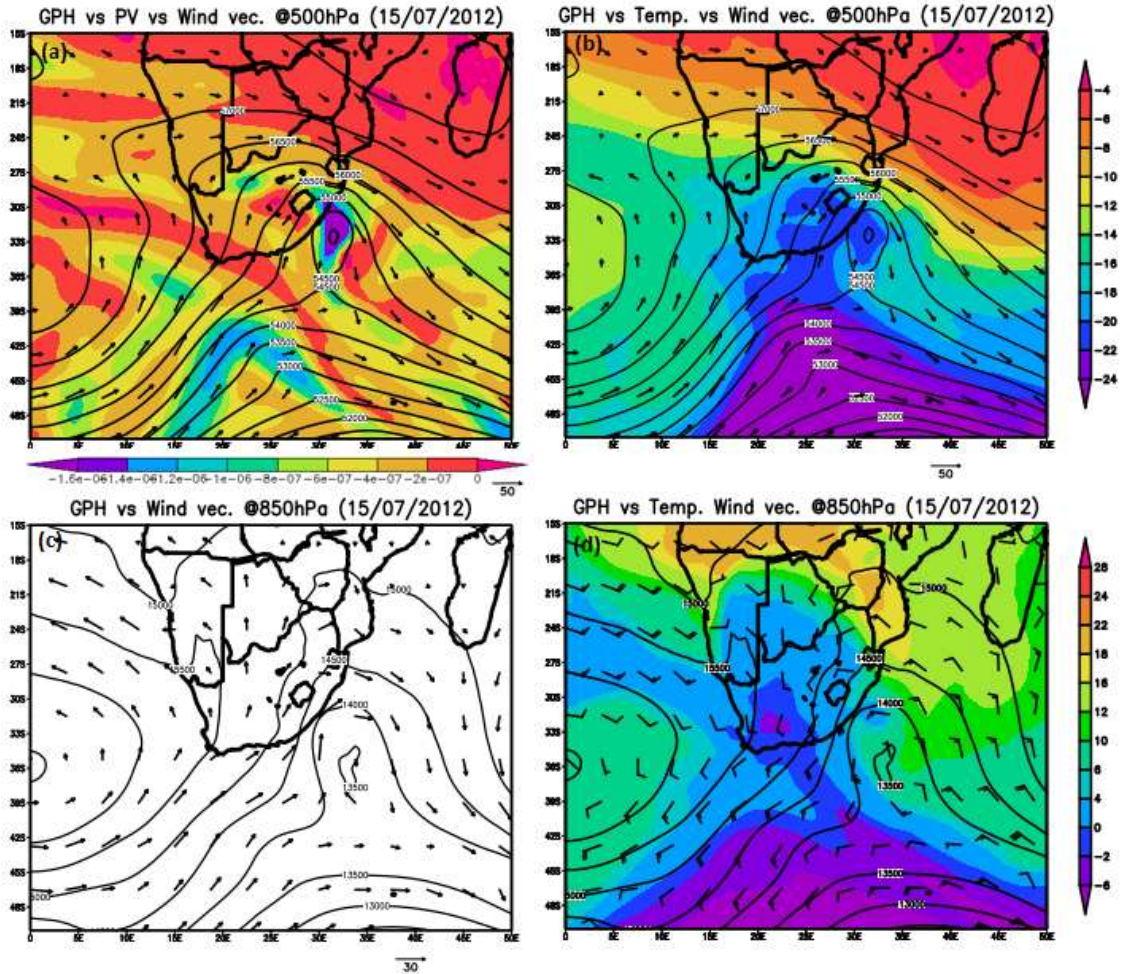


Figure 4. 16: Geopotential height (hPa) vs Potential vorticity at 500 (a), Geopotential height (hPa) vs Temperature (°C) @500hPa (b), Geopotential height (hPa) vs Winds at 850hPa (c) and Geopotential height (hPa) vs Temperature (°C) at 850hPa (d), **15 July 2012.**

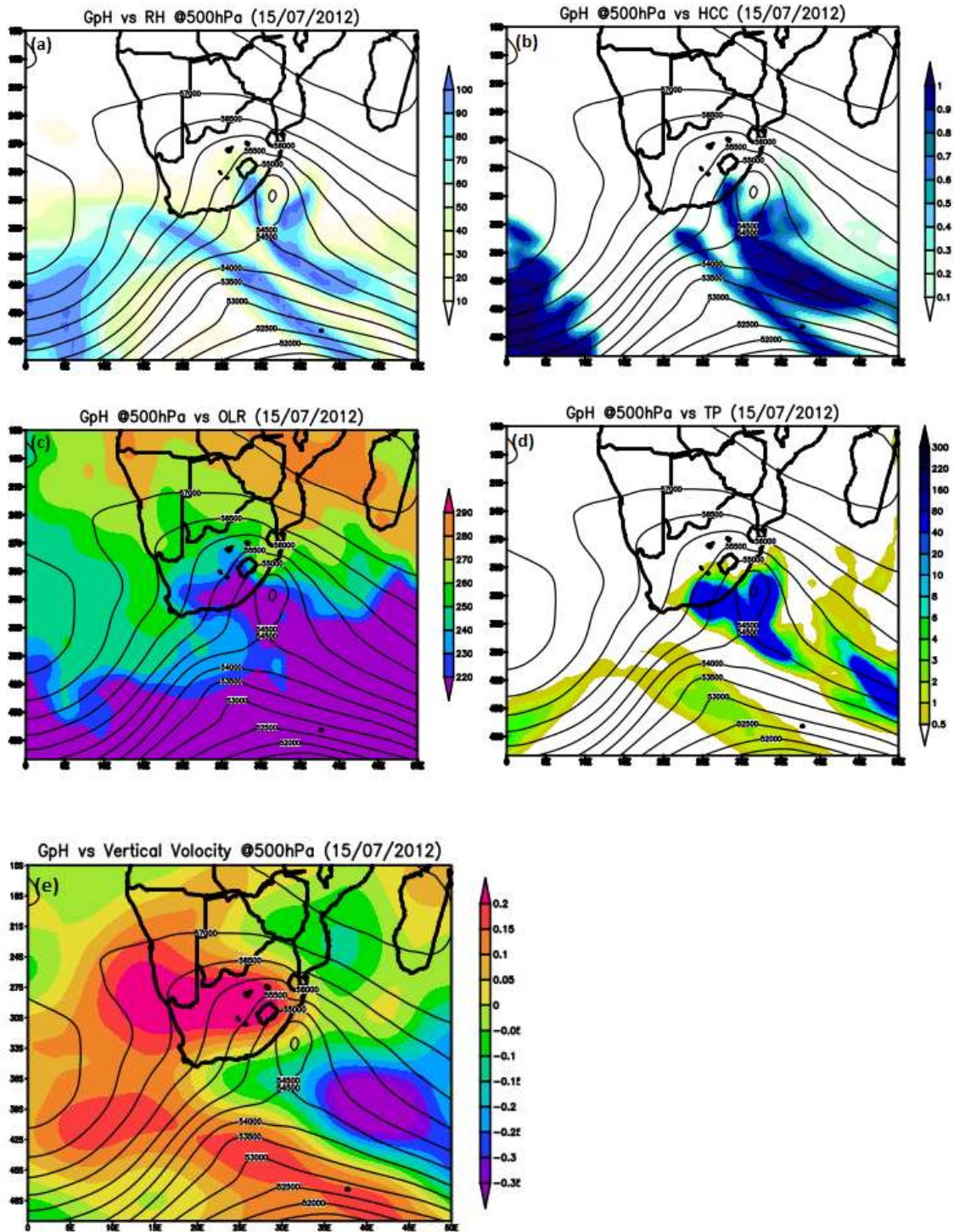


Figure 4. 17: Geopotential Height (hPa) at 500 (hPa) vs Relative humidity (a), High Cloud Cover (d), Out-going Longwave Radiation (OLR) (c), Total rainfall (mm/day) (d) Vertical velocity (e), **15 July 2012**

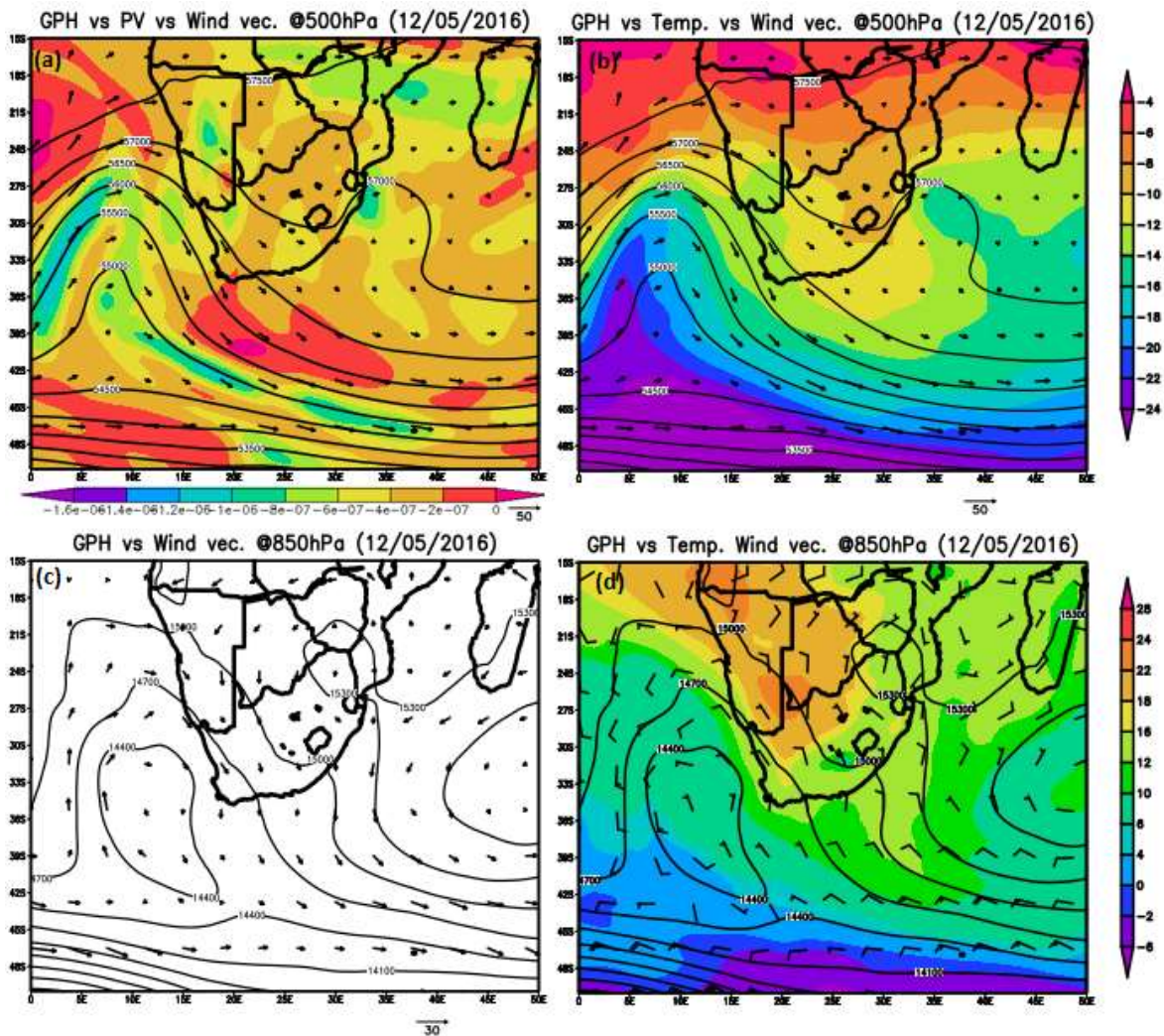


Figure 4. 18: Figure 1.26: Geopotential height (hPa) vs Potential vorticity at 500 (a), Geopotential height (hPa) vs Temperature ( $^{\circ}$ C) at 500hPa (b), Geopotential height (hPa) vs Winds at 850hPa (c) and Geopotential height (hPa) vs Temperature ( $^{\circ}$ C) at 850hPa (d), **12 May 2016.**

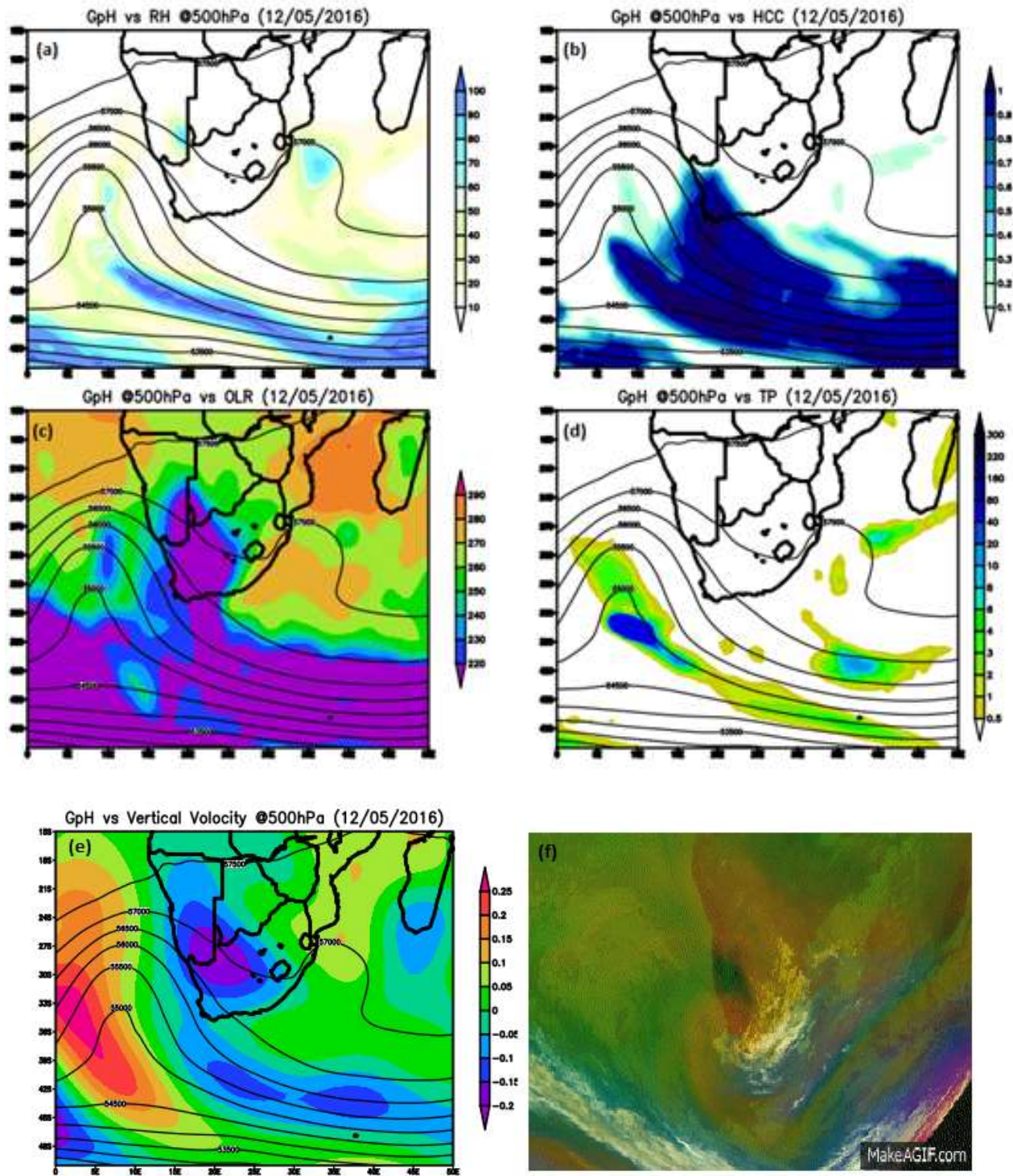


Figure 4. 19: Geopotential height (hPa) at 500 (hPa) vs Relative humidity (a), High Cloud Cover (HCC) (d), OLR (c) and Total rainfall (mm/day) (d), Vertical velocity (e) 00:00Z Meteosat-10 Airmass Red Green Blue (RGB) snapshot, copyright (2019) EUMETSAT (f), 12 May2016.

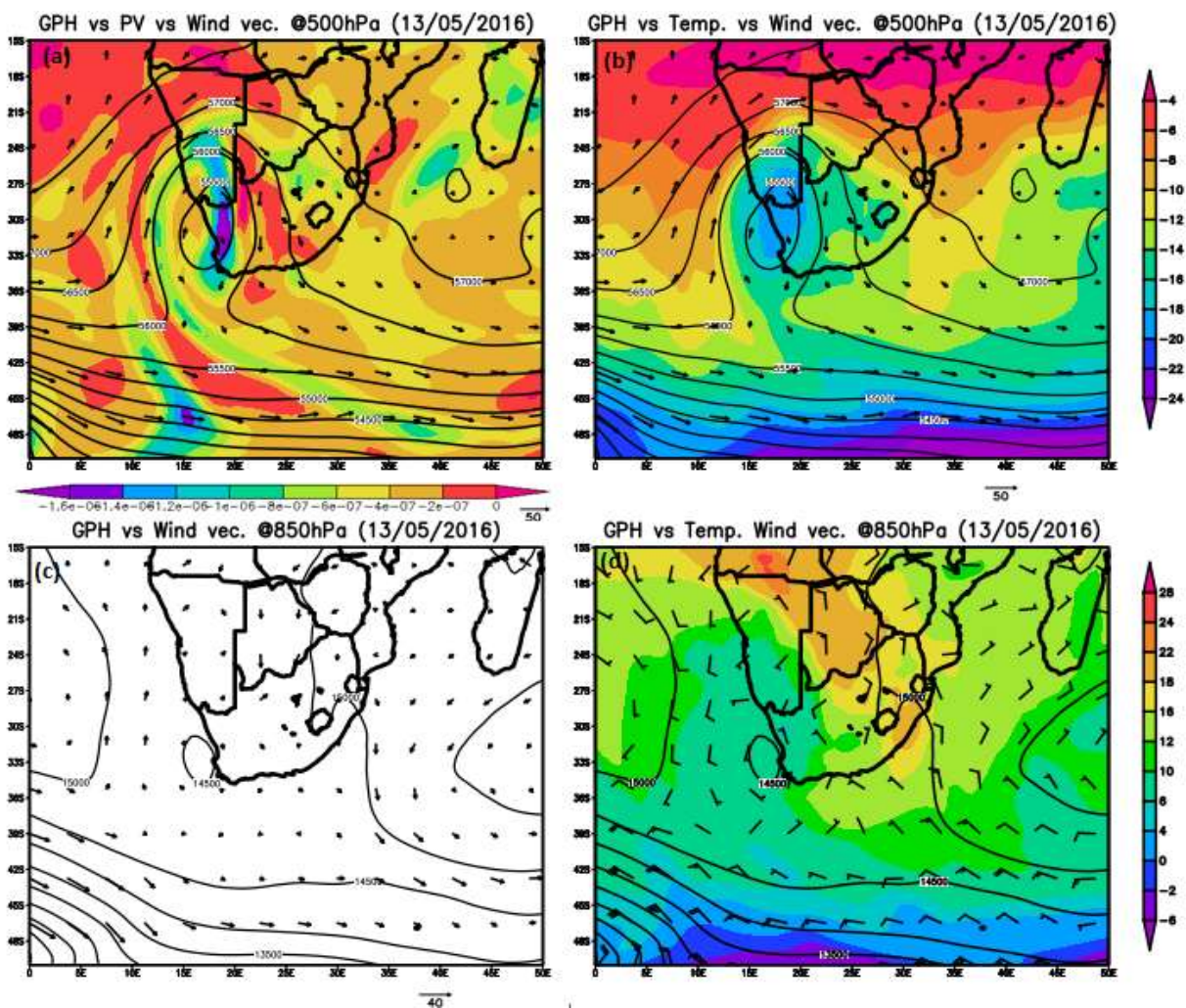


Figure 4. 20: Figure 1.26: Geopotential height (hPa) vs Potential vorticity at 500 (a), Geopotential height (hPa) vs Temperature (°C) at 500hPa (b), Geopotential height (hPa) vs Winds at 850hPa (c) and Geopotential height (hPa) vs Temperature (°C) at 850hPa (d), **13 May 2016.**

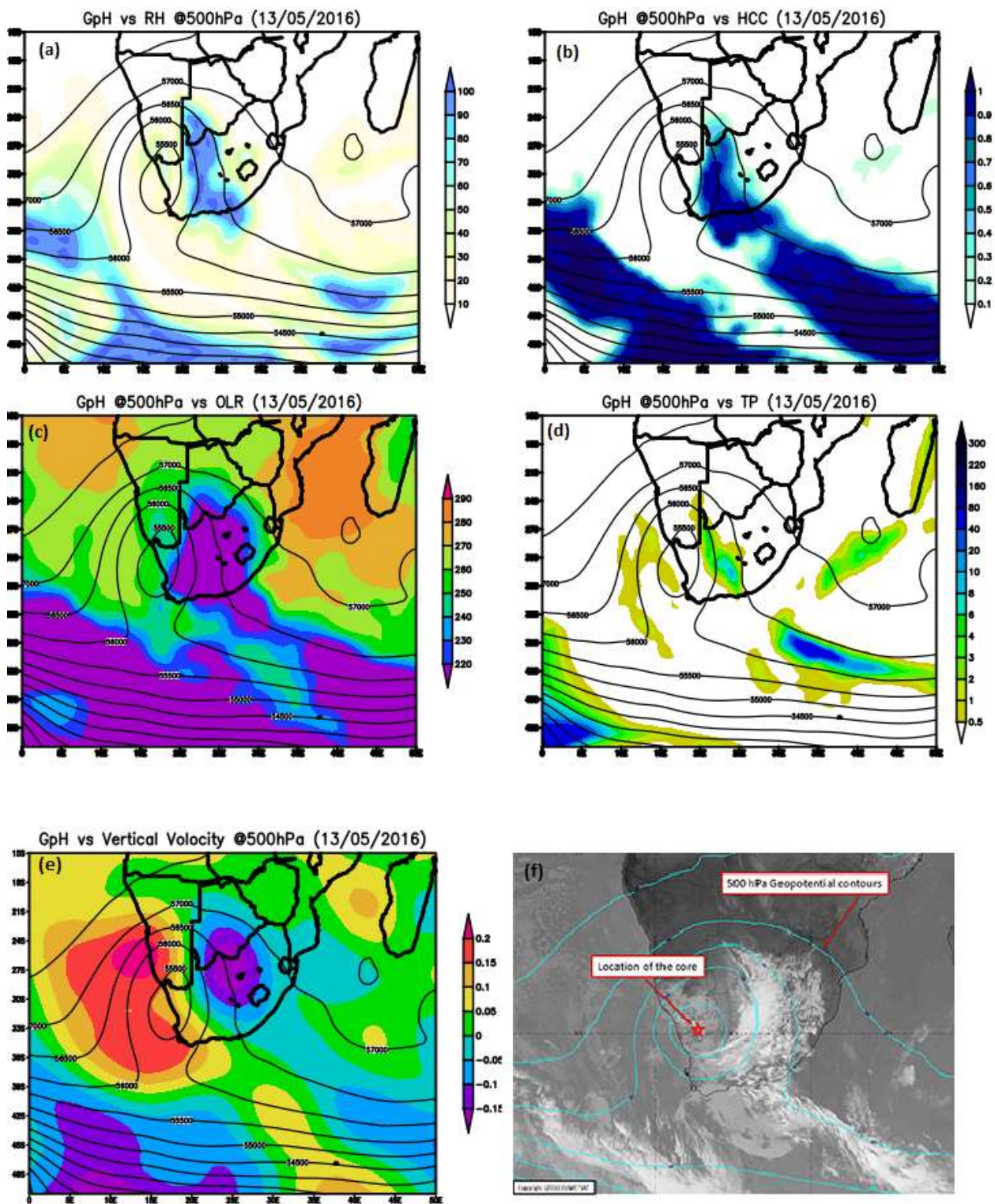


Figure 4. 21: Geopotential Height (hPa) at 500 (hPa) vs Relative humidity (a), High Cloud Cover (d), OLR (c), Total rainfall (mm/day) (d), Vertical velocity (e) and Infrared image of cold front and COL at 12:00Z, *copyright (2019) EUMETSAT* (f), **13 May2016**

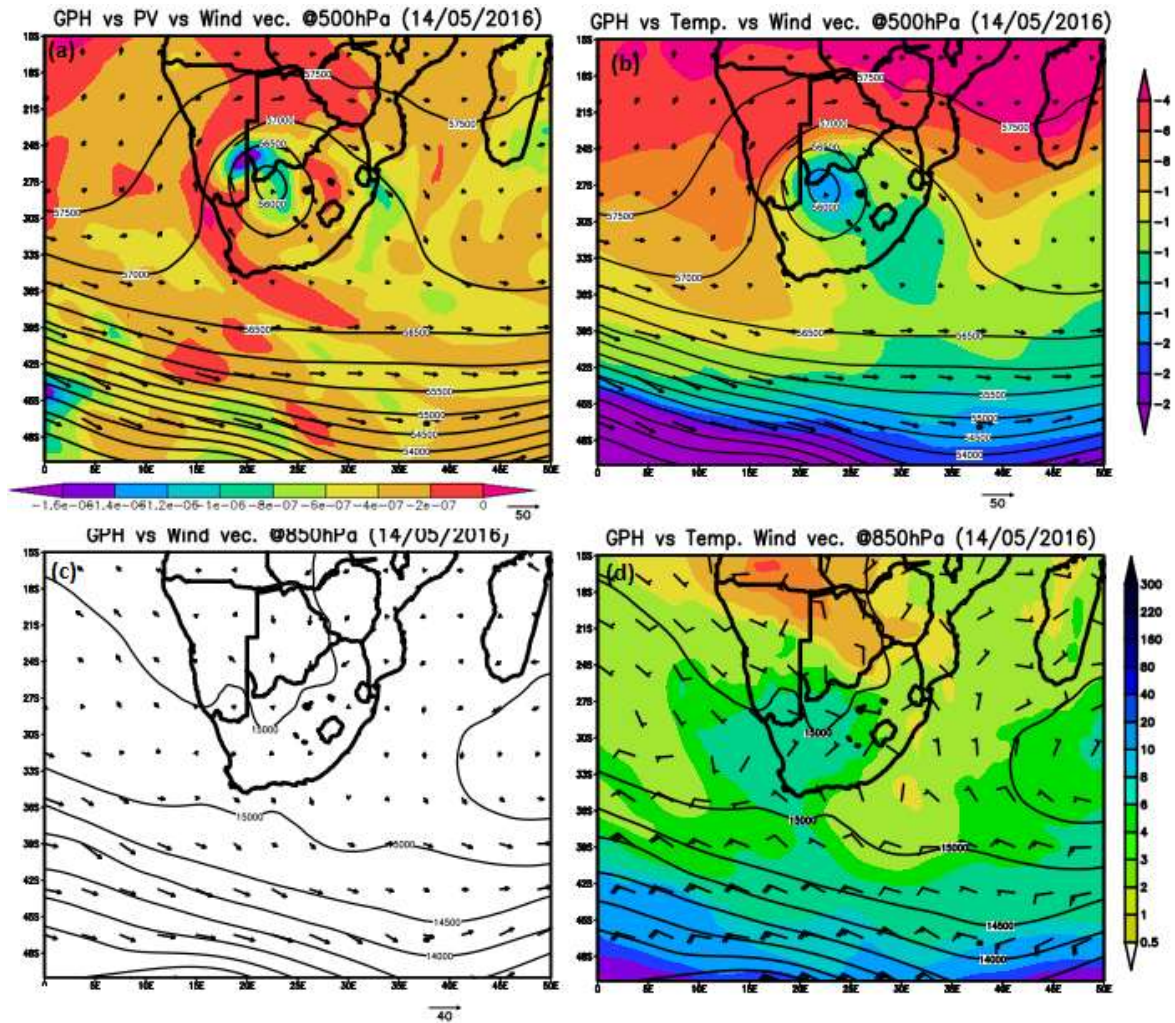


Figure 4. 22: Figure 1.26: Geopotential height (hPa) vs Potential vorticity @ 500 (a), Geopotential Height (hPa) vs Temperature (°C) at 500hPa (b), Geopotential height (hPa) vs Winds at 850hPa (c) and Geopotential height (hPa) vs Temperature (°C) at 850hPa (d), **14 May 2016**.

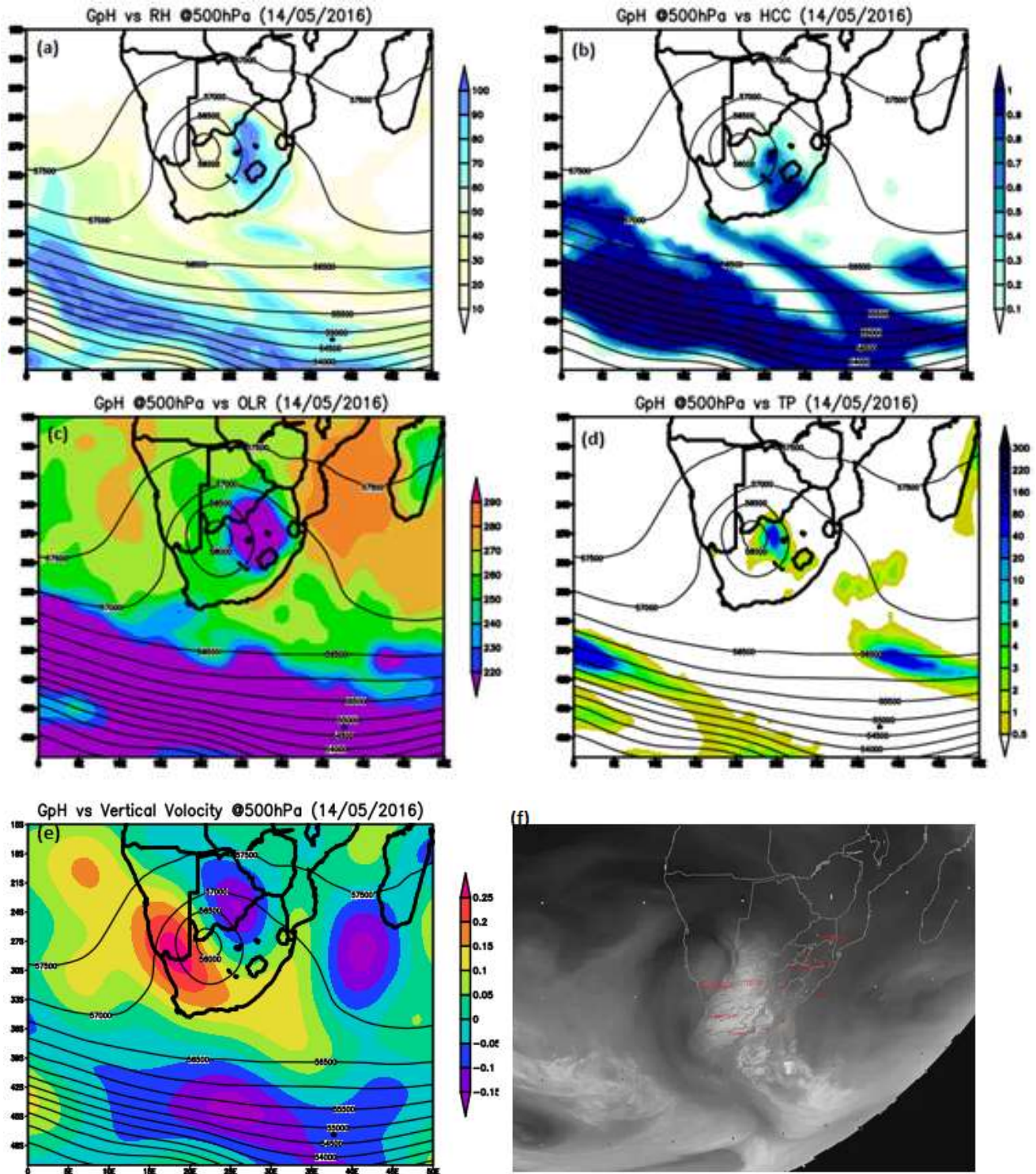


Figure 4. 23: Geopotential Height (hPa) at 500 (hPa) vs Relative humidity (a), High Cloud Cover (HCC) (d), Out-going Longwave Radiation (OLR) (c), Total rainfall (mm/day) (d), Vertical velocity (e) and Infrared image of a COL at 18:00Z, *copyright (2019) EUMETSAT (f), 14 May2016*

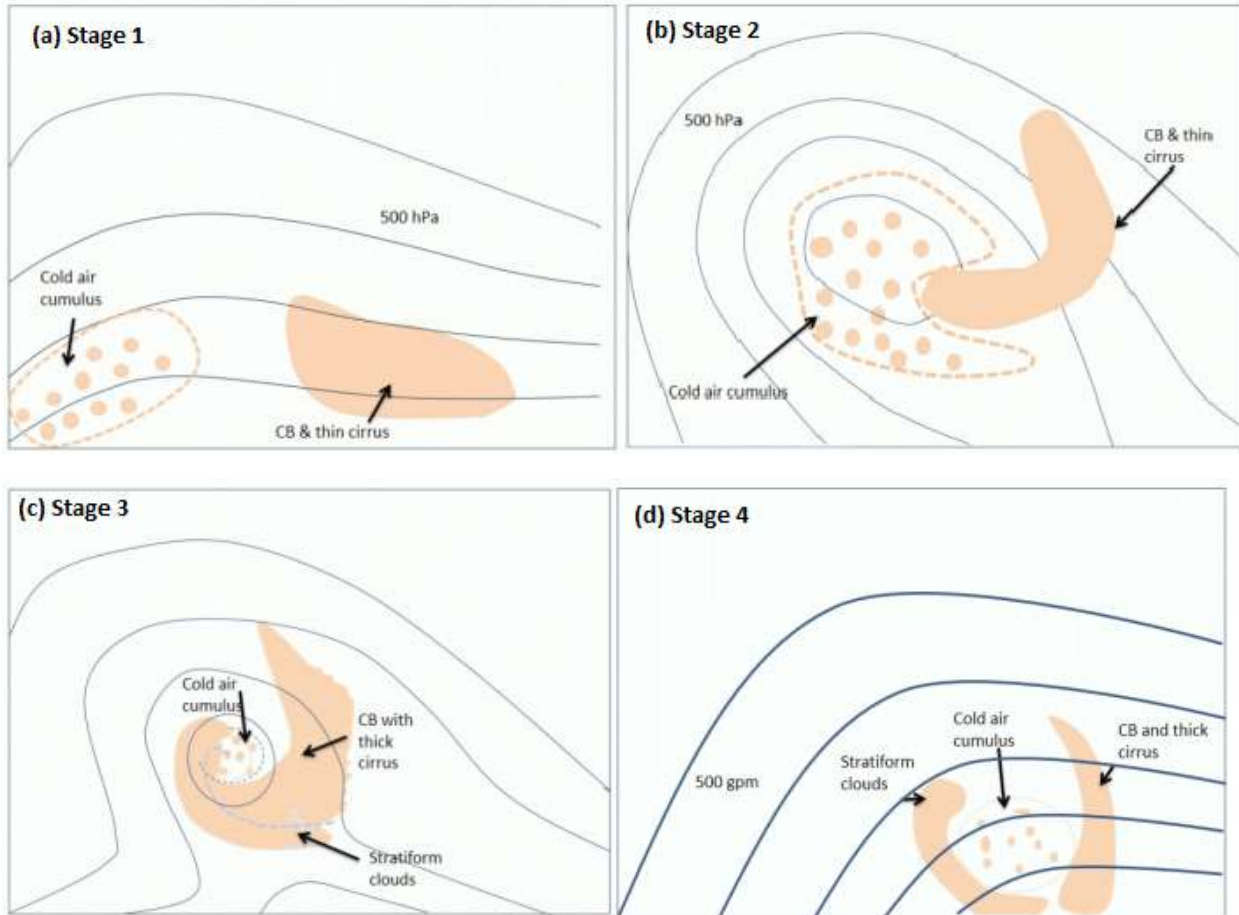


Figure 4. 24: The four stages indicating geopotential heights at 500 hPa and typical cloud patterns, as observed during the occurrence of the COL systems (source: EUMETSAT 2012).

## Chapter 5

### Unified Model Cut-off Low rainfall simulations

#### 5.1 Introduction

This chapter analyses the accuracy of the total precipitation simulations obtained from the Unified Model (UM) run at the South African Weather Service (SAWS) with a grid spacing of 4.4km for areas of deep moist convection associated with cut-off low (COL) systems. The model outputs were compared with total precipitation from the European Center for Medium-Range Weather Forecast (ECMWF). Where ECMWF was unable to produce accurate plots, (Climate Hazards Group InfraRed Precipitation with Station data) CHIRPS dataset was used. Three sets of simulations are available for each day that the simulations were produced with observations from 00Z, 12Z and 18Z used to initialize the model. The simulations of the onset, position and amount of the rain in relation to the center of the identified COL systems using UM were also analyzed. The days and location where the systems were associated with high figures of rainfall, were further plotted as line graphs to validate the skills of the model runs against the observations. Furthermore, the study investigated the accuracy of the model in simulating these characteristics in relation to the different near-surface pressure of the observed COL weather systems.

The 4.4 km resolution model became operational in April 2016 at SAWS and therefore the only data that was available when the analysis of the study was conducted is only for two years. The model data produced in operational model was extracted for all days of the events which were identified in the years 2016 and 2017. Thus, the study analyzed the simulated geopotential height and rainfall associated with the identified COLs from 2016 to 2017. The first two events which were analyzed occurred on the 14<sup>th</sup> to 16<sup>th</sup> May 2016 and 26<sup>th</sup> to 27<sup>th</sup> July 2016 and were both coupled with a near-surface low- and high-pressure circulation patterns. The last two systems occurred on 10<sup>th</sup> to 11<sup>th</sup> October 2017 and 15<sup>th</sup> to 17<sup>th</sup> November 2017 and were coupled with a near-surface high pressure pattern.

#### 5.2 Testing Unified Model simulating Cut-off Low events from 2016 to 2017

##### 5.2.1 Event of 14-16 May 2016

From 14<sup>th</sup> to 15<sup>th</sup> May 2014, the UM simulated the transit of a COL with a significant rainfall over the most parts of South Africa (Fig. 5.1 a, b and c). On 14 May, the model simulated the center of the system located over the northern parts of the North West Province. The simulated rainfall associated with the system was between 30 mm and 60 mm over parts of North West, Gauteng, Free State and Mpumalanga provinces (Fig. 5.1 a, b and c). The 00Z, 12Z and 18Z represent different lead times as the event approaches, with the longest lead being 30 hours associated with 00Z run made the previous day. The simulation with the shortest lead time is the 18Z one, and represents a lead time of only 12 hours, while the 12Z run has a lead time of 18 hours. The visual inspection was used to compare the 00Z, 12Z and 18Z runs of the model against the observation. All the model runs simulated the largest amount of rainfall towards the east of the centre of the system as expected. This is because that is where the most convergence is expected at the surface, associated with strong uplift. There are very small differences in the 3 simulations with the centre of the COL being located at almost the same point. The intensity of the system as indicated by the lowest GPH is similar across all the simulations. The centre of the system as seen in the observations is almost by the simulations, however the observed system is a bit to the west, and the intensity of the observed system is stronger when compared to the simulation. The location of the observed rainfall is also shifted a bit to the west compared to the simulations which is informed by the position of the COL itself (Fig. 5.1 d). When comparing to the observations used, the model overestimated rainfall. Figure 5.2 shows the diurnal cycle of the precipitation as experienced on 14 May between 35°S and 23°S, and along the 27° E line. The model simulated the maximum rainfall to occur slightly earlier than observed, especially in the 00Z simulation which has the longest lead as already mentioned. The timing of the maximum rainfall in the 12Z and 18Z runs almost matches that in the observation, however the peak is higher in the model, which shows that the model overestimates rainfall. The observed rainfall is also more long-lived, compared with to the simulated one, and starts earlier and ends later.

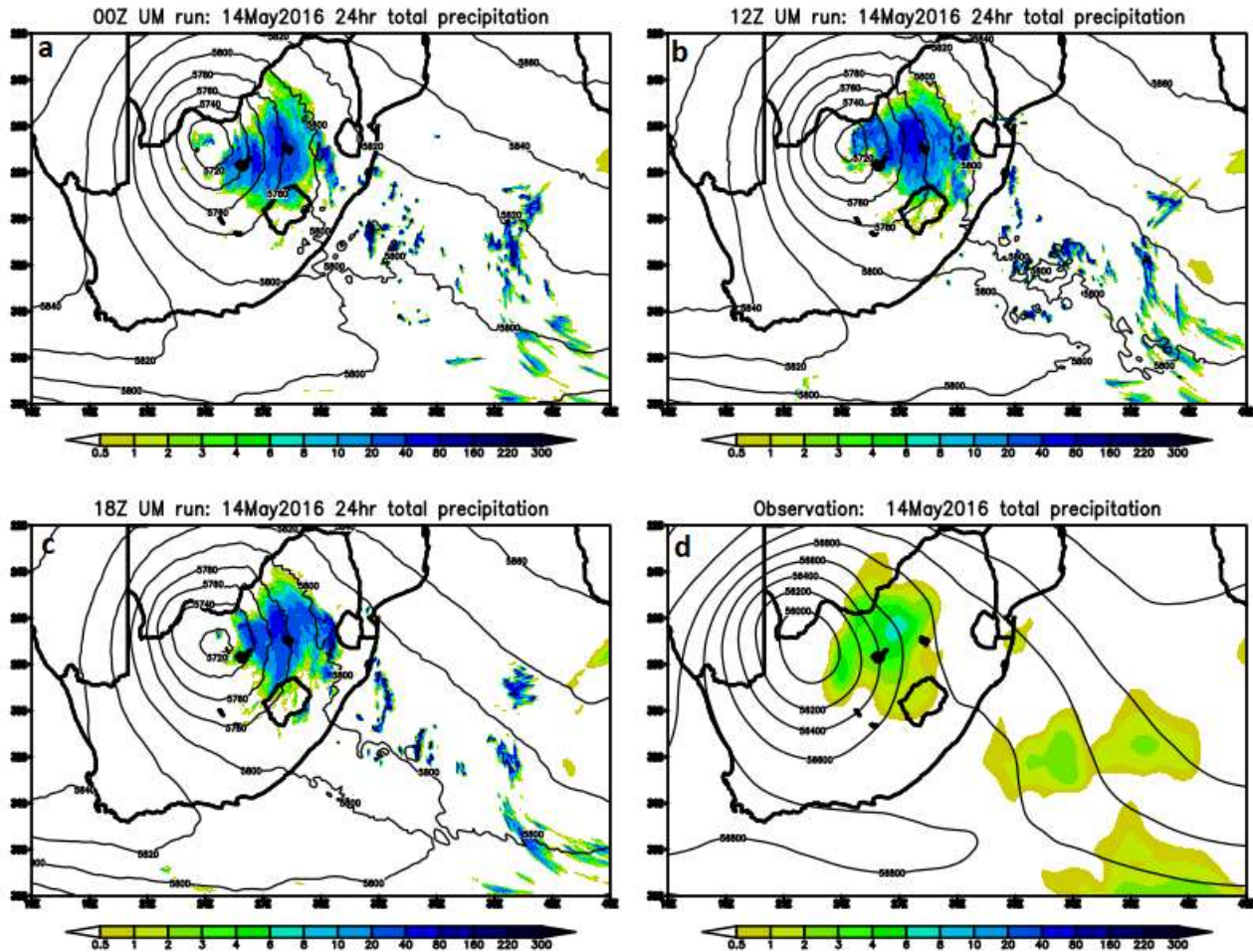


Figure 5. 1: 24hr. Total precipitation at (a) 00Z, (b) 12Z and (c)18Z runs of the 4.4 km Unified Model (UM) vs (d) observation on 14 May 2016.

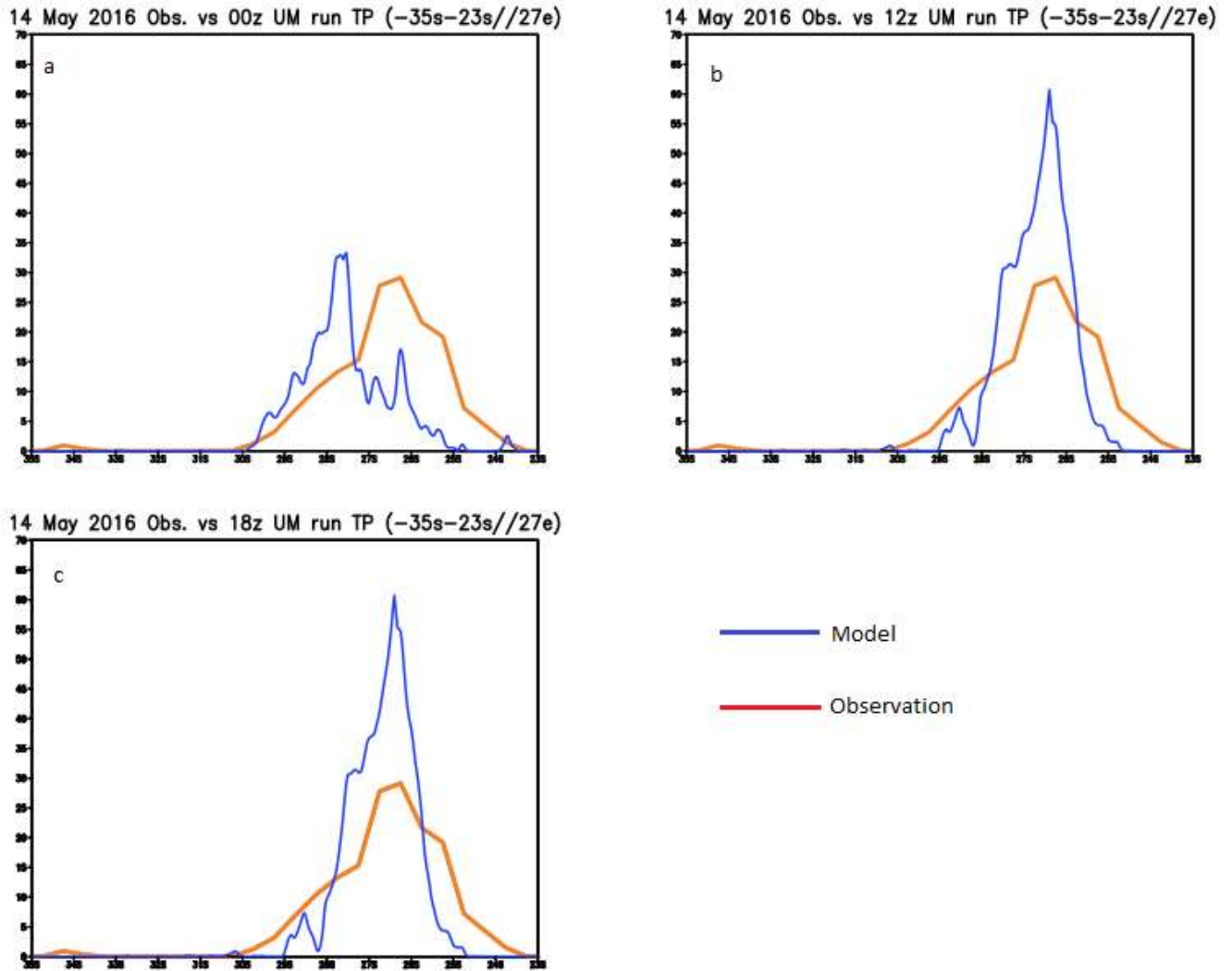


Figure 5. 2: 4.4 km Unified Model (UM) run simulations vs observation 24 hours total precipitation at  $-32^{\circ}\text{S}$  to  $23^{\circ}\text{S}$ // $27^{\circ}\text{E}$  on **14 May 2016**.

On the 15<sup>th</sup> May 2016, the centre of the system was observed to be located over the North West Province. The 15 May simulations are more variable than the 14 May ones, with centres of the system being located at different locations. The 12Z simulations showed the system located over the north-eastern parts of the North West Province, while the two other simulations placed the centre of the system over Botswana. The pattern of the simulated rainfall is even more diverse, with the shorter lead forecasts placing it a bit closer to the observations. The 00Z captured the system the least accurate and placed the rainfall more towards the eastern part of the country, with very little rainfall over the north western parts of the country. The rainfall is observed to extend from the Botswana- South Africa border and includes parts of Limpopo, North West, Free State

as well as Mpumalanga Province, and ends just before the border with the King of Eswatini. The 12Z and 18Z runs place the rainfall simulations further north than observed.

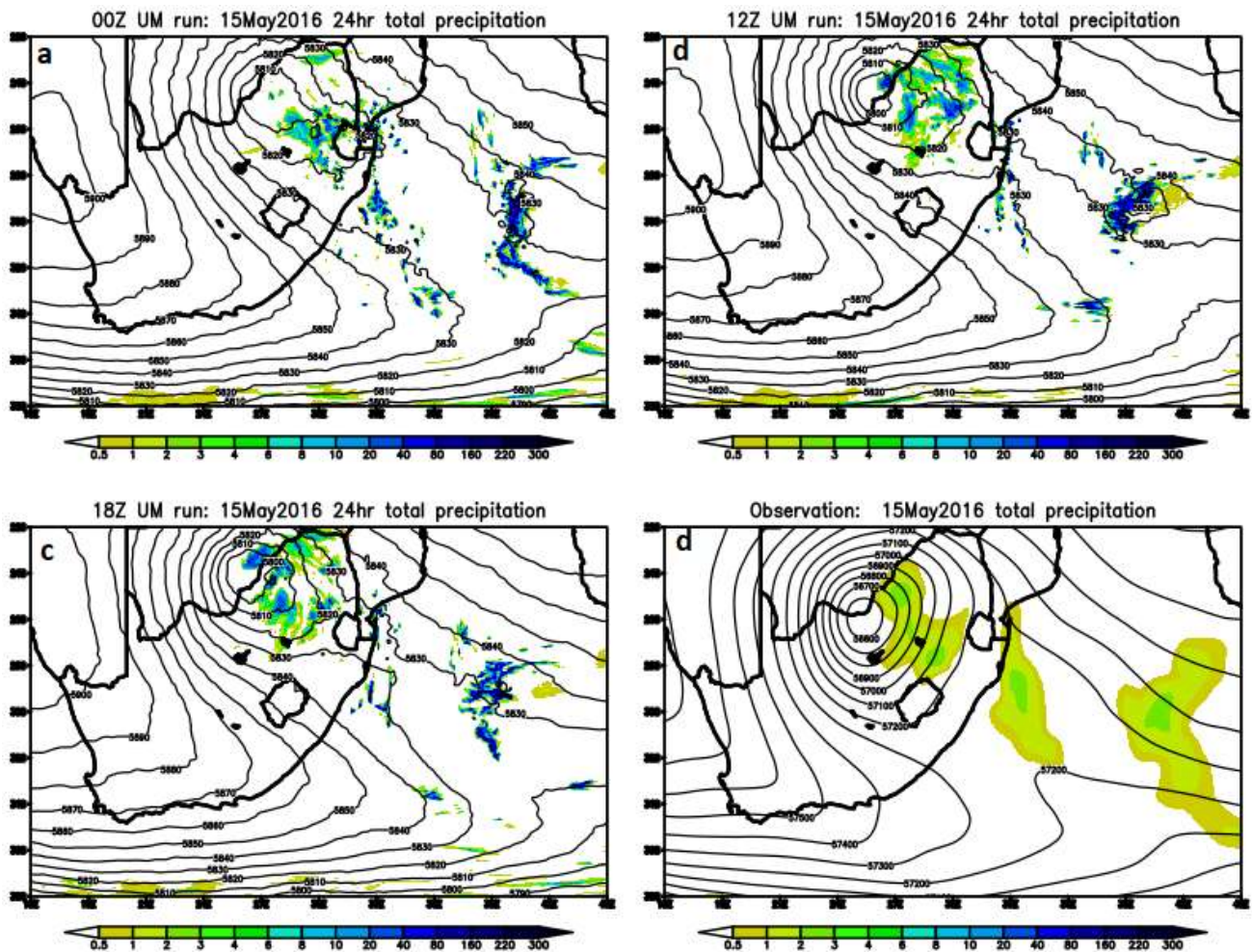


Figure 5. 3: 24hr. Total precipitation at (a) 00Z, (b) 12Z and (c)18Z runs of the 4.4 km Unified Model (UM) vs (d) observation on **15 May 2016**.

On 16<sup>th</sup> May, geopotential height at 500 hPa simulated the dissipation of the system over the Indian Ocean, with no rainfall simulated over the country in all runs of the model (Fig. 5.4 a, b and c). However, the model simulation on the 00Z and 12Z runs showed amount of between 1 mm to 80 mm rainfall whilst the 18Z run simulated amount of 1 mm to 40 mm over the South Indian Ocean (Fig. 5.4 a, b and c). Unlike the simulation, observation indicated rainfall amount of between 1 mm to 8 mm over the eastern coastal regions and Indian Ocean (Fig. 5.4 d).

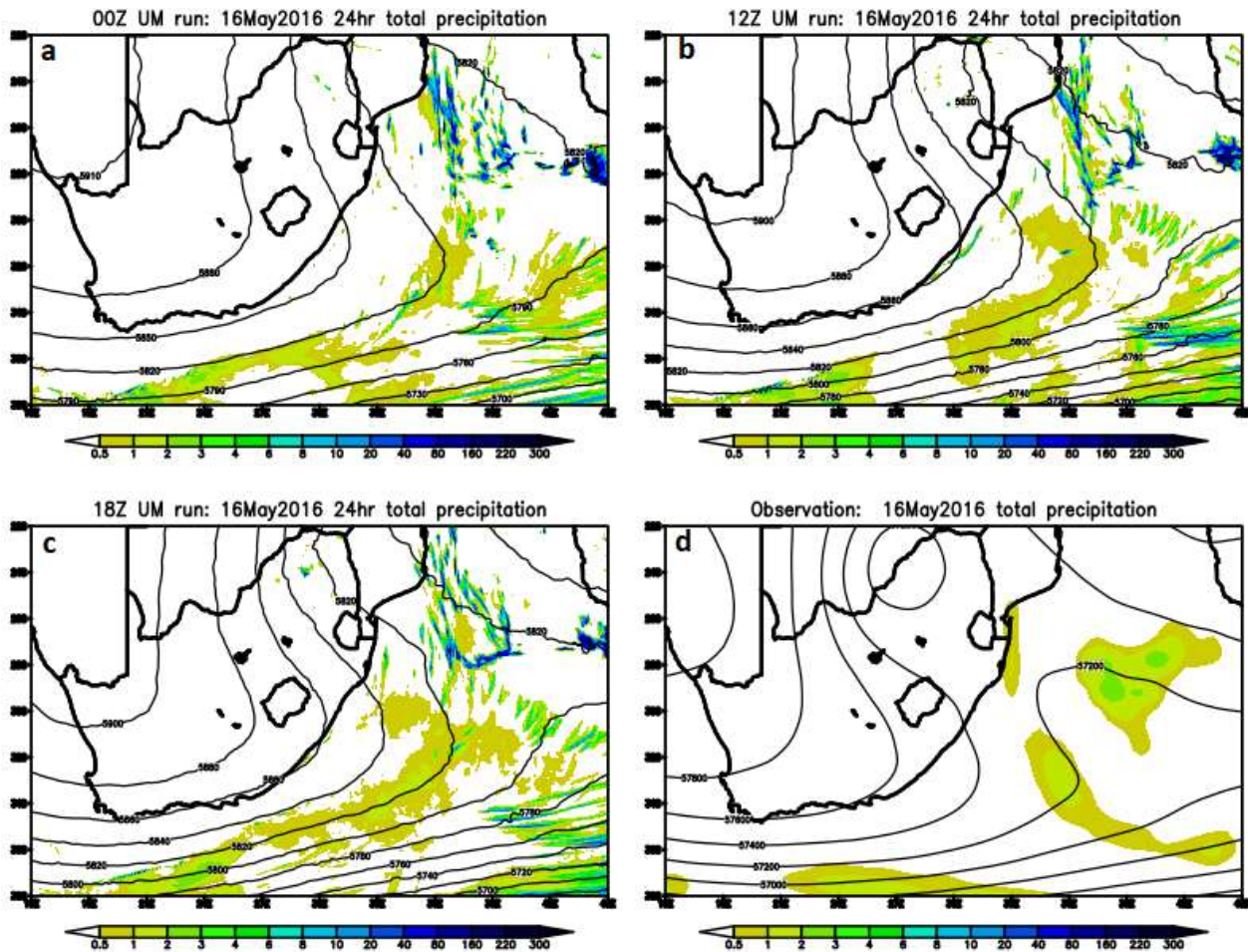


Figure 5. 4: 24hr. Total precipitation at (a) 00Z, (b) 12Z and (c)18Z runs of the 4.4 km Unified Model (UM) vs (d) observation on **16 May 2016**.

### 5.2.2 Event of 26-27 July 2016

On 26<sup>th</sup> July 2016, the centre of COL was located over the Northern Cape Province. The three simulations with the different lead times, placed the centre of the system more South compared to the observations. The 18Z simulation which has the shortest lead time, placed the centre of the system South, the furthest from observations. Model simulation at 00z,12z and 18z indicated the rainfall of between 8 mm to 120 mm over the eastern and southern parts of the country (Fig. 5.5 a, b and c). Similarly, the observation showed most of rainfall activities over the eastern and southern parts with high figures over the parts of North West, Free State and Eastern Cape provinces as well as in Lesotho (Fig. 5.5 d). The model was accurate in simulating the area which was associated with heavy rainfall during this event. However, the model also simulated rainfall over a large part of the Northern Cape Province that was not observed and this result is found in

all the three simulations. The simulations for the simulations do not show much rainfall along the south coast, while observations do indicate some rainfall in this area. The simulated rainfall is shifted more to the south than what is observed. This is a feature that may be associated with the centre of the COL system as already indicated which is simulated to be located south of where the system is observed in all the simulations (Fig. 5.5 d). Figure 5.6 shows the timing of the simulated versus observed rainfall over an area which was linked with heavy precipitation during the event. All the model runs tend to overestimate rainfall when compared with the observation.

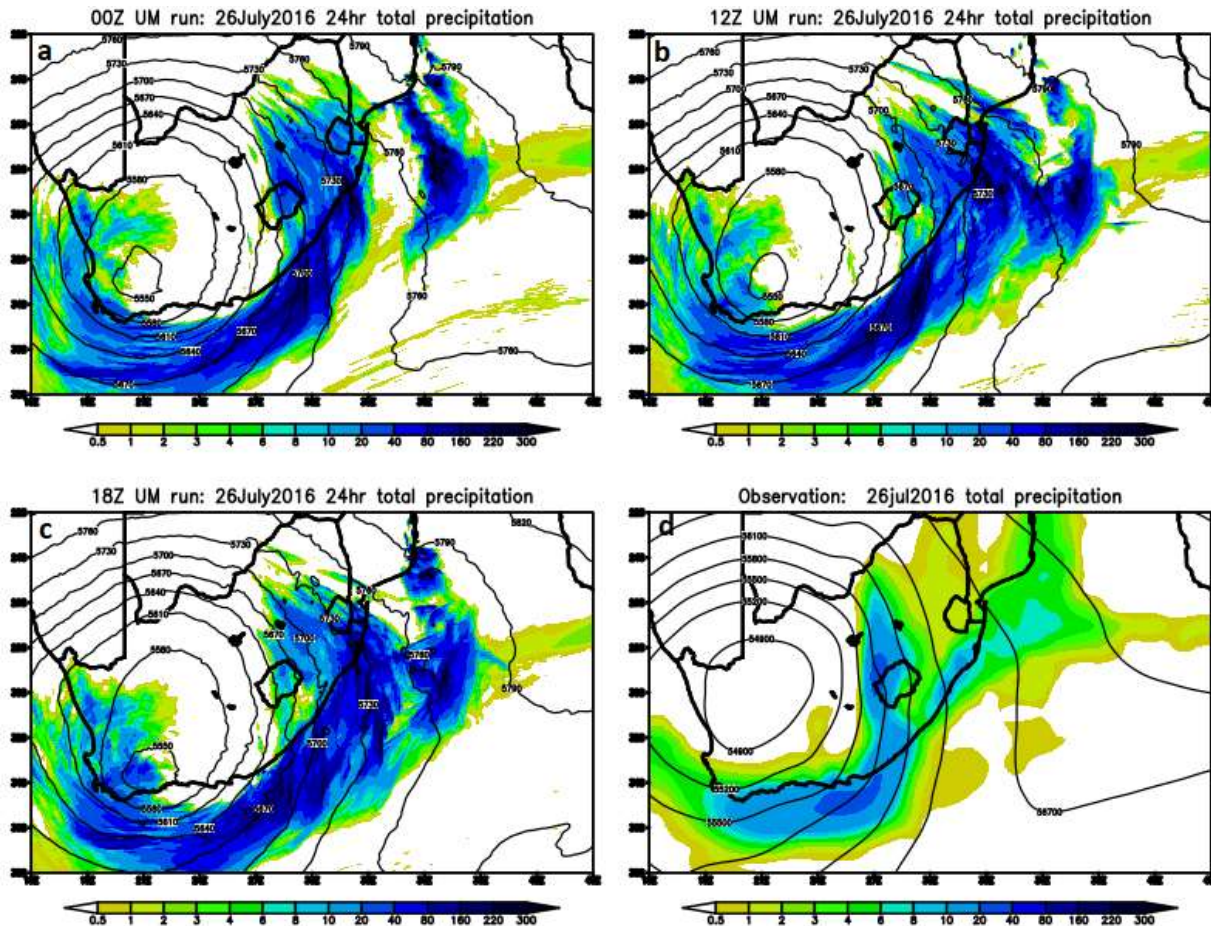


Figure 5. 5: 24hr. Total precipitation at (a) 00Z, (b) 12Z and (c)18Z runs of the 4.4 km Unified Model (UM) vs (d) observation on **25 July 2016**.

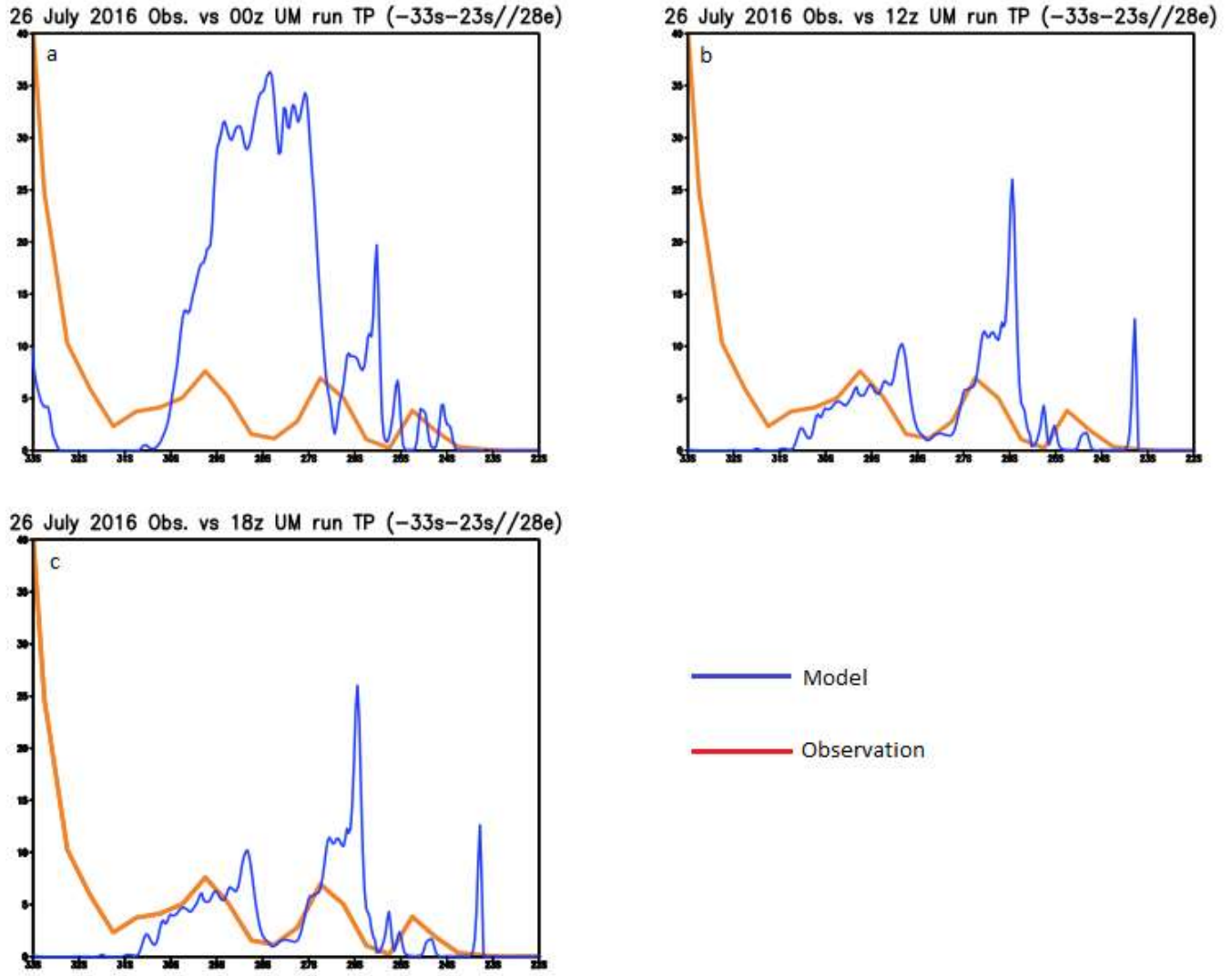


Figure 5. 6: 4.4 km Unified Model run simulations vs observation 24 hours total precipitation at -33°S to 23°S//28°E on **26 July 2016**.

On 27<sup>th</sup> July 2016, the center of the system was located over the Western Cape Province as indicated in the observed plot (Figure 5.7 d). All the simulation places the centre of the system more towards the east into the Eastern Cape Province. All simulations showed the rainfall amount of between 4 mm to 120 mm over the parts Free State, Western and Northern Cape Provinces (Fig. 5.7 a, b and c). Observation showed rainfall activity shifted over the Northern Cape and Mpumalanga provinces as well as over the coastal areas of the KwaZulu-Natal Province (Fig. 5.7 b). The simulated rainfall extends further east compared to the observations. Further, rainfall was also observed over the eastern parts of the country, that was not captured by any of the model

configurations which placed all the rainfall over the Indian ocean. This shows the likely effect on the types of warnings forecasters issue where sometimes warnings are issued for the wrong provinces or not issued at all because of the wrong placement of systems and rainfall in the model simulations.

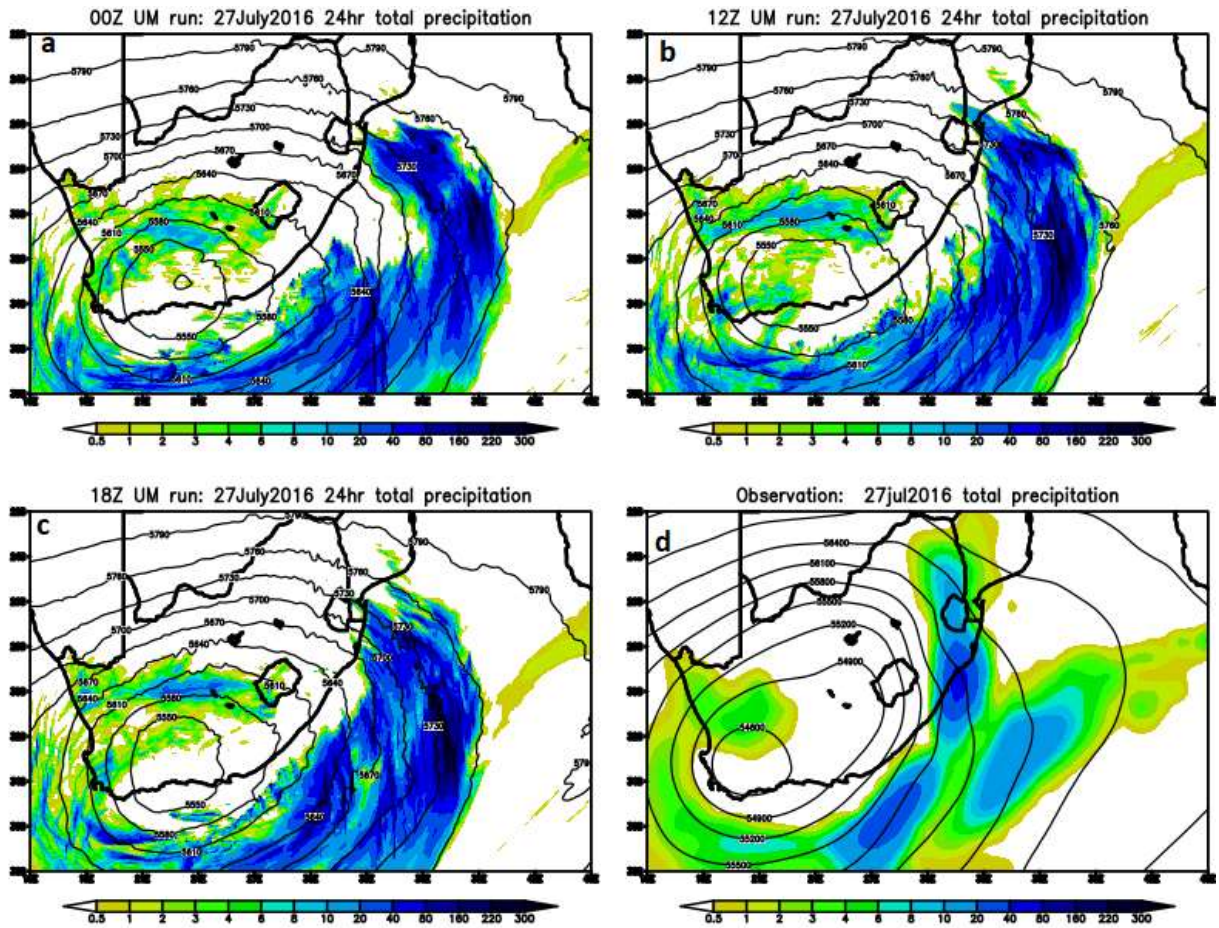


Figure 5. 7: 24hr. Total precipitation at (a) 00Z, (b) 12Z and (c)18Z runs of the 4.4 km Unified Model (UM) vs (d) observation on **27 July 2016**.

### 5.2.3 Event of 10-11 October 2017

On 10<sup>th</sup> October 2017, all simulations indicated the COL over the parts of Free State and KwaZulu-Natal provinces. All the model runs simulated a rainfall of about 120 mm spreading from parts of the Kwazulu-Natal Province and Lesotho to the Indian Ocean. With a clearly visible low, observation indicated rainfall over the KwaZulu-Natal Province spreading to the South Indian Ocean. Little rainfall was also observed spreading from the eastern parts of Limpopo Province through Mozambique to the South Indian Ocean (Fig. 5.8 d). Figure 5.9 indicates the amount of rainfall simulated and observed over the south-eastern part of the country at 23<sup>o</sup>-35<sup>o</sup>S along 30<sup>o</sup>E

during the event. 00Z run simulated rainfall later than the observed initial time of precipitation. 12Z and 18Z managed to simulate exact initial time of rainfall with observation.

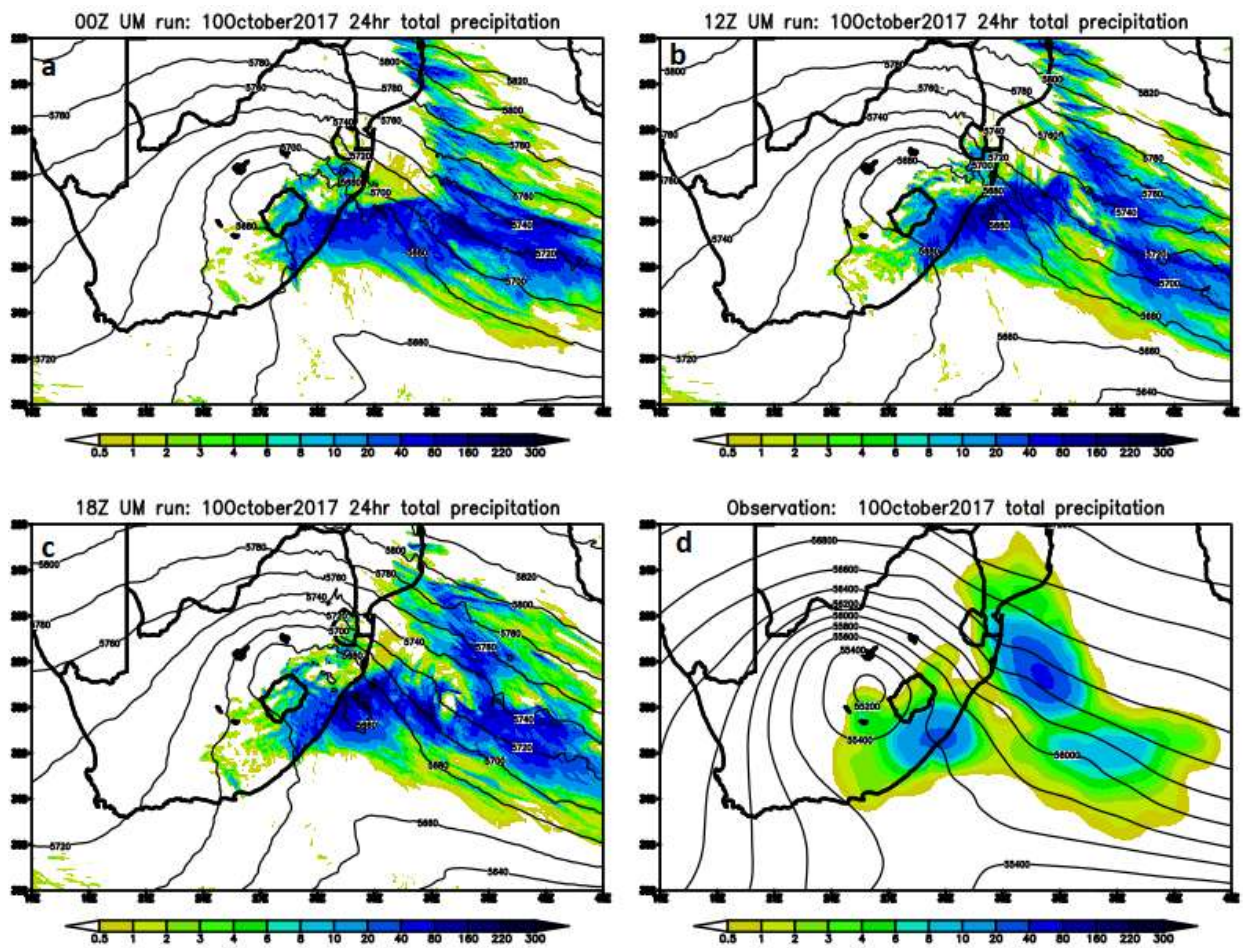
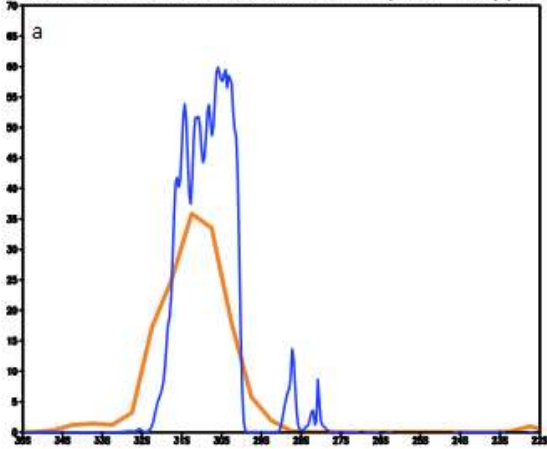
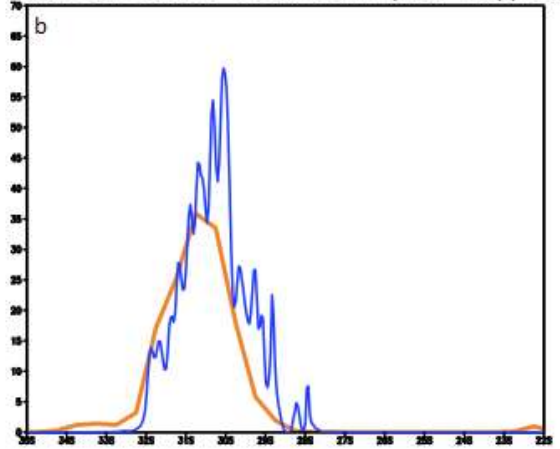


Figure 5. 8: 24hr. Total precipitation at (a) 00Z, (b) 12Z and (c)18Z runs of the 4.4 km Unified Model (UM) vs (d) observation on **10 October 2017**.

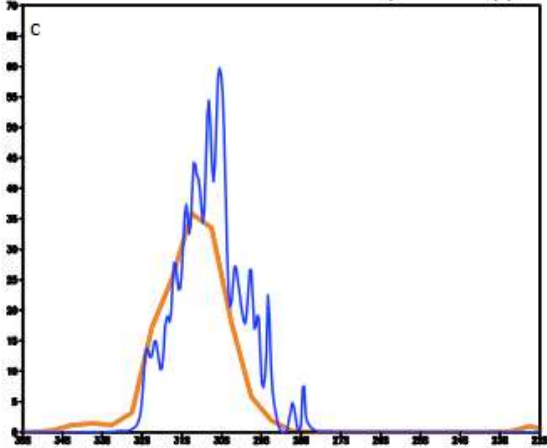
10 Oct. 2017 Obs. vs 00z UM run TP (-35s-23s//30e)



10 Oct. 2017 Obs. vs 12z UM run TP (-35s-23s//30e)



10 Oct. 2017 Obs. vs 18z UM run TP (-35s-23s//30e)



— Model  
— Observation

Figure 5. 9: 4.4 km Unified Model run simulations vs observation 24 hours total precipitation at -35°S to 23°S//30°E on **10 October 2017**.

On 11 October, the model simulated the system located over the South Indian Ocean, with close geopotential height on 00Z and 18Z simulations (Fig. 5.10 a and c). At this stage, all simulations indicated rainfall over the southern and eastern parts of the system (Fig.5.10 a, b and c). Higher than simulated rainfall was observed over the Indian Ocean with a strong closed geopotential height (Fig. 5.10 d).

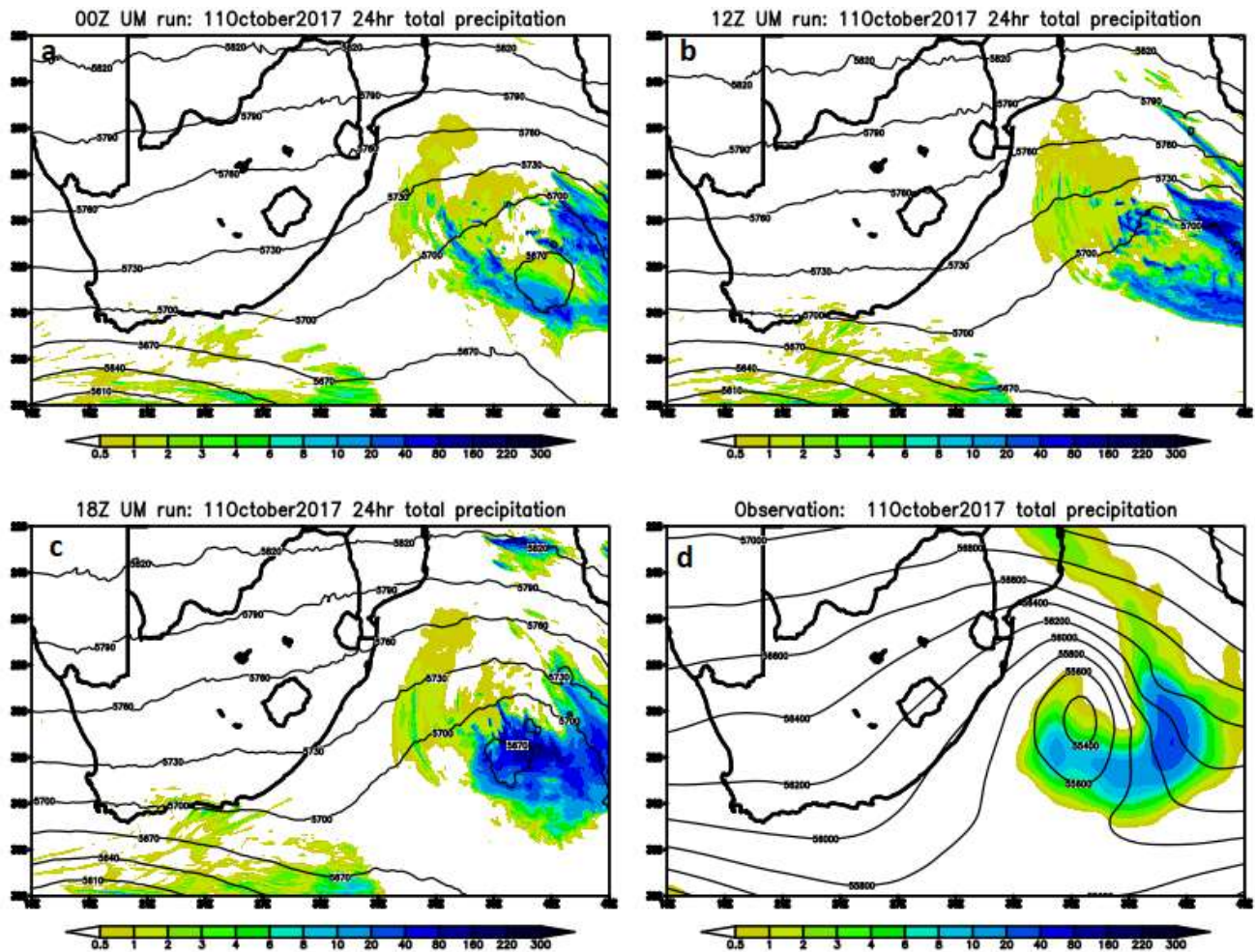


Figure 5. 10: 24 hours Total precipitation at (a) 00Z, (b) 12Z and (c)18Z runs of the 4.4 km Unified Model (UM) vs (d) observation on **11 October 2017**.

#### 5.2.4 Event of 15-17 November 2017

On 15 November 2017, the model runs simulated a closed geopotential height over the central, northern and western parts of the country. The center of the system was simulated covering parts of North West, Free State, Northern, Eastern and Western Cape provinces (Fig. 5.11 a, b and c). All model runs simulated rainfall of between 80 mm to 180 mm over the most eastern parts of the country. At this stage, a deep trough was observed over the western parts of the country, covering Northern and Western Cape provinces with high rainfall activity covering parts of Eastern and Western cape provinces (Fig. 5.11 d). When analyzing rainfall over the location (18°S-40S°//31°E) of deep convection, the model simulations were able to indicate areas which were indicated with deep convection (Fig. 5.12).

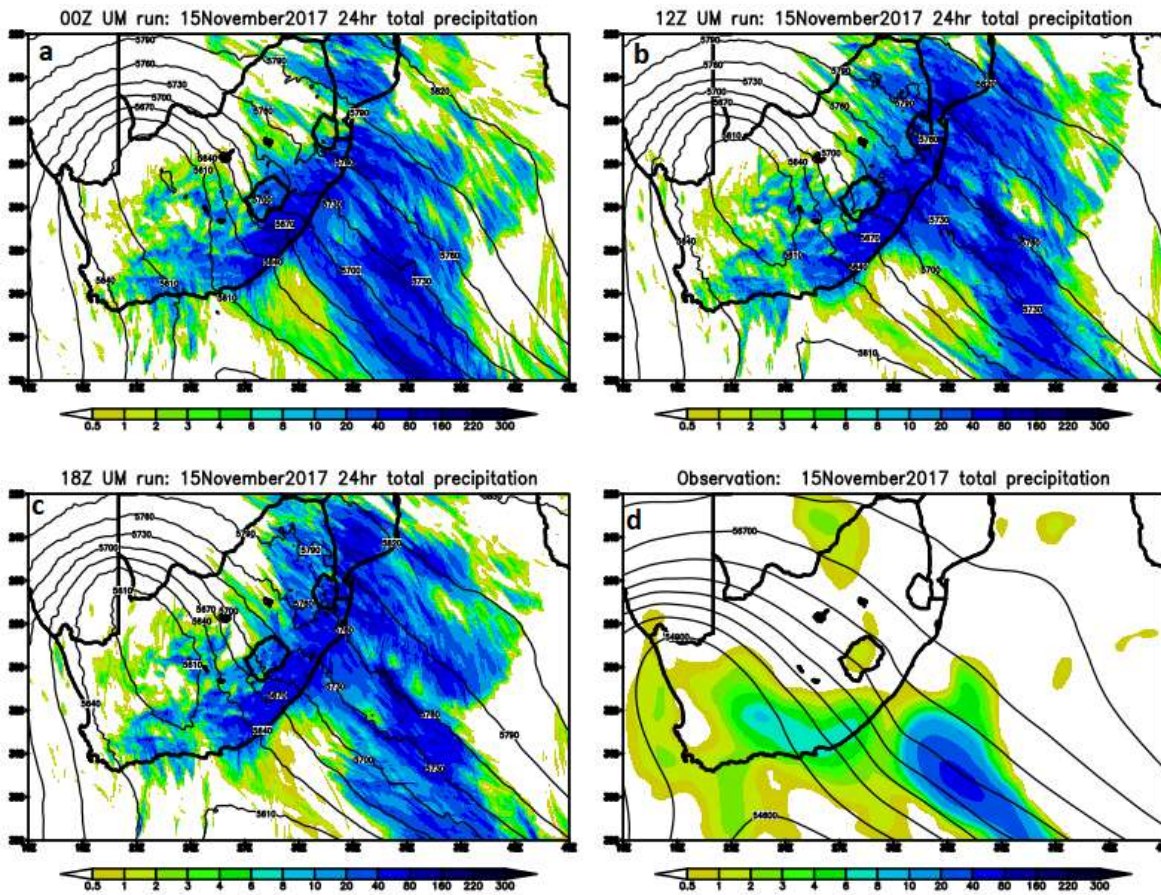
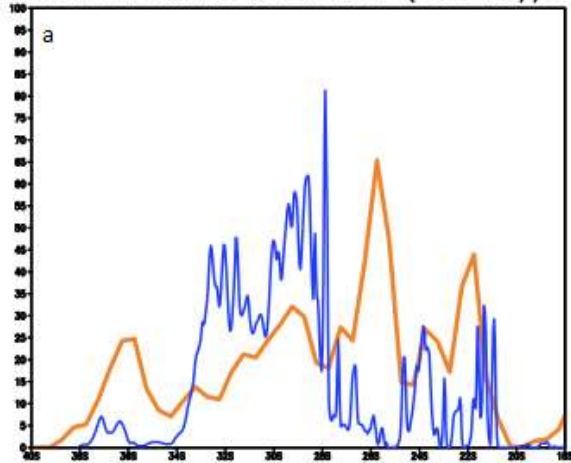
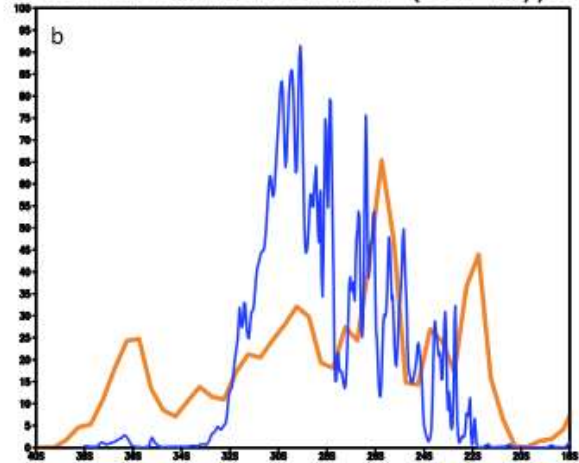


Figure 5. 11: 24hr. Total precipitation at (a) 00Z, (b) 12Z and (c)18Z runs of the 4.4 km Unified Model (UM) vs (d) observation on 15 November 2017.

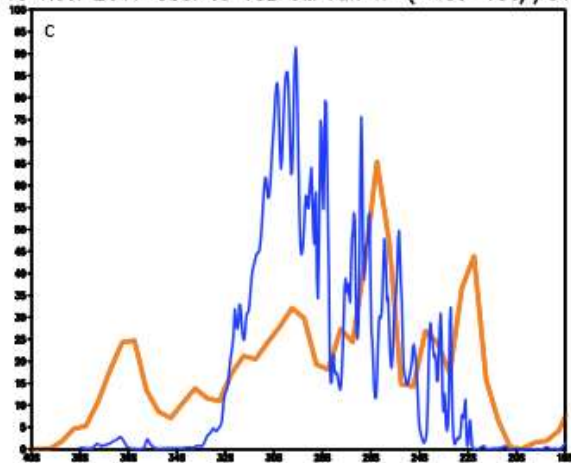
15 Nov. 2017 Obs. vs 00z UM run TP (-40s-18s//31e)



15 Nov. 2017 Obs. vs 12z UM run TP (-40s-18s//31e)



15 Nov. 2017 Obs. vs 18z UM run TP (-40s-18s//31e)



— Model  
— Observation

Figure 5. 12: 4.4 km Unified Model run simulations vs observation 24 hours total precipitation at -40°S to -18°S//30°E on **15 November 2017**.

On 16<sup>th</sup> November 2017, the 00z and 12z runs (Fig. 5.13 a and b) simulated the center of the system located over the center of the country, covering several parts of Gauteng, North-West, Free State, KwaZulu-Natal and Eastern Cape provinces when comparing with the model (Fig. 5.13 d). Rainfall of between 80 mm to 180 mm was simulated over the eastern coastal parts of the KwaZulu-Natal Province with high amount over the South Indian Ocean in all model runs (Fig. 5.13 a, b and c). Observation also showed the system located over the central parts of the country with rainfall activity over Lesotho and the eastern parts of Free State, Eastern Cape and Limpopo provinces. High values of rainfall of above 80 mm were observed over the Indian Ocean and Mozambique Channel (Fig. 5.13 d).

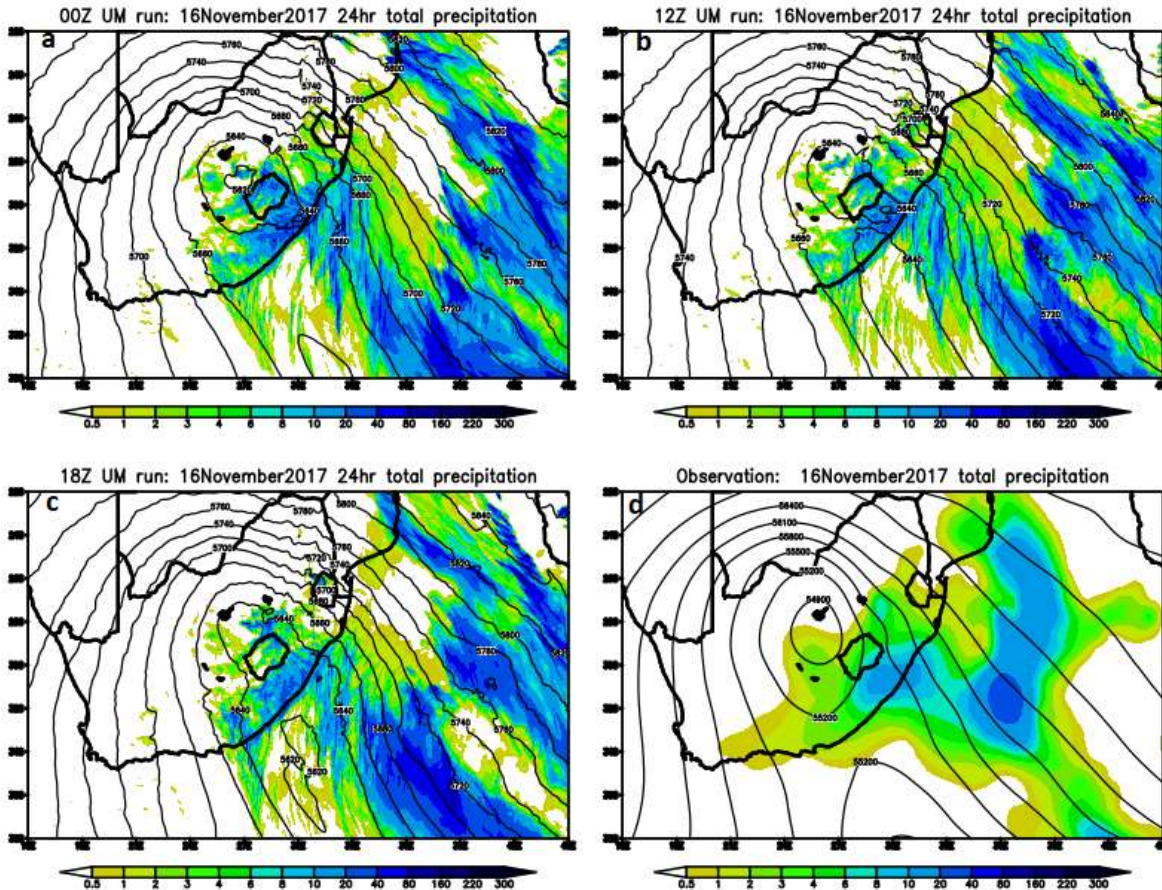


Figure 5. 13: 24hr. Total precipitation at (a) 00Z, (b) 12Z and (c)18Z runs of the 4 km Unified Model (UM) vs (d) observation on **16 November 2017**.

On 17<sup>th</sup> November 2017, the center of the system was simulated over the south western Indian Ocean. At this stage, all runs simulated amounts of 10 mm to 80 mm rainfall over the center of the system as well as near the western side of Madagascar (Fig. 5.14 a, b and c). The observation identified the system closer to the south eastern coastal areas of the country. This led to the rainfall of between 10 mm to 60 mm observed over the coastal areas. High rainfall of more than 80 mm was observed over the south eastern side of the system over the Indian Ocean (Fig. 5.10 d).

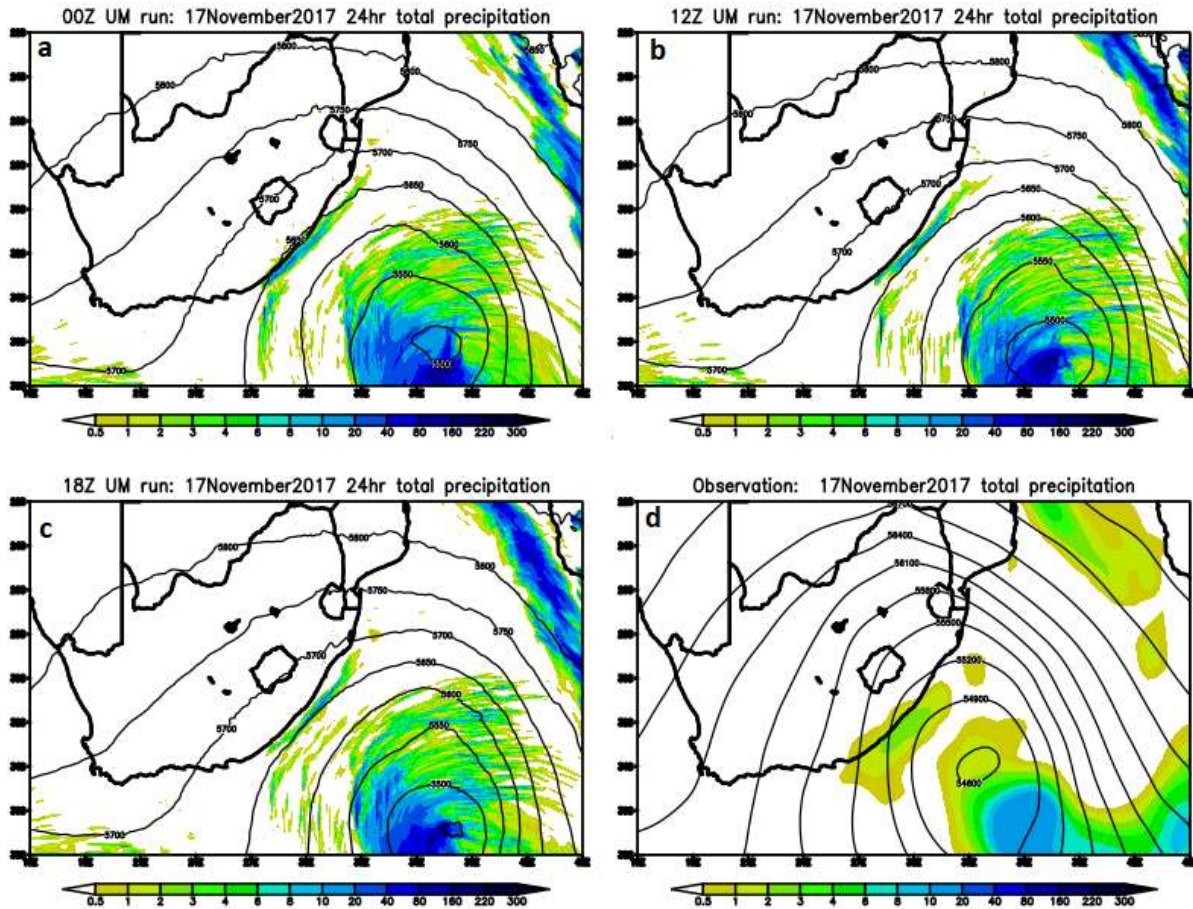


Figure 5. 14. 15: 24hr. Total precipitation at (a) 00Z, (b) 12Z and (c)18Z runs of the 4.4 km Unified Model (UM) vs (d) observation on **17 November 2017**.

### 5.3 Summary

In this chapter, the accuracy of the Unified Model in simulating the location of the COL weather systems with their associated areas of deep moist convection is tested. The three model runs, namely, 00Z, 12Z and 18Z, were checked against the observation. Using the visual inspection method, the model is able to simulated the location of the systems as well as the areas associated with deep moist convection and heavy rainfalls. However, the model tends to simulate the events differently depending on their near surface pressure systems observed in chapter 4. When simulating the events which are associated with high near the surface, the model poorly simulates the closed geopotential height at 500 hPa when compared with the observation. The model simulations tend to accurately simulate the center and areas of heavy rainfall when simulating events which are coupled with both low- and high-pressure systems near the surface.

Furthermore, the model runs tend to simulate areas of high rainfall better while underestimating areas with low amount of rainfall.

## Chapter 6

### Conclusions and future work

#### 6.1 Introduction

The study focused on the characteristics of the severe cut-off low (COL) systems and their predictability using, 4.4 km horizontal resolution Unified Model (UM) over South Africa. COLs are one of the anticipated weather systems associated with extreme weather conditions over the country. The study analyzed the recent COL events which have been associated with heavy rainfalls from 2011 to 2017. The skill of the 4.4 km UM was tested in simulating areas associated with the deep moist convection during the occurrence of the identified COL events.

This chapter provides a discussion and synthesis of the key findings of the current study, as well as their contribution to the existing knowledge. The comparison of the results of this study and other studies about the COL systems in South Africa is also provided. Recommendations and implications in relation to the characteristics of the severe COL events and their predictability by 4.4 km UM are also discussed.

#### 6.2 Discussion and synthesis of key findings

##### 6.2.1 Recent Cut-off Lows in South Africa: seasonality and structure

COL systems are identified on the 500 hPa pressure level by a closed geopotential height contour lasting for then 24 hours. During the early stages of the systems, COLs are characterized by a deep trough with a zonal flow of air over the west of the country. The troughs are characterized by a linear shaped pool of negative potential vorticity at the early stage. A cyclonic pool of negative potential vorticity becomes clearly visible, with a fully developed cold core at 500 hPa. The intensified stages of recent COL systems (2011-2017) are characterized by pools of cyclonic negative potential vorticity and cold air over their center. Furthermore, mature stages of COLs are characterized by negative values of vertical velocity, inverted comma shaped cumulus and cumulonimbus clouds as well as severe precipitation along their east and polar sides.

Near the surface, COL systems can either coupled with a high-pressure circulation or with a high- and low-pressure circulation. COL systems which are associated with both low- and high-pressure circulation are associated with the occurrence of the cold fronts. More precisely, due to the instability promoted by the presence of the cold pool, there is an enhancement of the comma shaped cumulus and cumulonimbus development on the east side (e.g. Caruso and Businger

2006; Buckley *et al.* 2007). Taljaard (1995) also found that precipitation is often located along the east and polar side of the general COL systems. During the occurrence of COLs, coastal and mountain regions are often subjected to high accumulative precipitation (Muller *et al.* 2008).

The distribution of COLs frequency varies from season to season. When compared with previous studies on the characteristics of COL events, the findings of this study are slightly different on the seasonal distribution of COL systems over South Africa. Over region A of the study area, more COL events were observed during June-July-August (JJA) followed by September-October-November (SON) and low events during March-April-May (MAM) with no system observed during December-January-February (DJF). Over region B of the study area, more COL events were observed during JJA followed by SON with no system observed during both DJF and MAM seasons of the study period. High number of COL events which occurs during JJA lasts for more than 4 days. Several previous studies on the characteristics of COL events such as Molekwa (2013), Tyson and Preston-White (2000), Taljaard (1985) and Singleton and Reason (2007) found high seasonal distribution of COL systems during MAM.

COL systems may develop over the South Atlantic Ocean and transit over the south-west coast, or might proceed in a north-westerly direction across the country to the South Indian Ocean. In this study we found a high occurrence of COL systems over region A ( $-22^{\circ}\text{S}$  to  $-32^{\circ}\text{S}$ ) of the study area. This different to the preferred location ( $32^{\circ}\text{S}$ - $45^{\circ}\text{S}$ ) of the COL systems indicated by previous studies (e.g. Engelbrecht *et al.* 2015; Favre *et al.* 2012).

The study findings correlate with the findings of Singleton and Reason (2007a) who also found a shift on the preferred seasons and location of the COL systems over South Africa.

### 6.2.2 Simulating rainfall in Cut-off Lows using the 4.4 km Unified Model

The 4.4 km Unified Model is able to simulate the location of the COL systems over South Africa when using geopotential height at 500 hPa. However, the location of the centre of the system does not always match that which is observed, with biases of the system seen in all directions. This was found to be the case for all lead times (i.e. 24 hours, 12 hours and 6 hours) that were considered. When the location of the centre of the system matches the observations, the simulated rainfall also matches the observations. When the centre of the system is further east, the rainfall is also simulated to be further east, and the same applies for displacements in other directions. For all the cases that were considered the model was found to overestimate rainfall. Overall the results indicate that the UM is a useful tool for the forecasters, and can help with the

provision of early warnings, despite some shortcomings of underestimate areas of low precipitation whilst overestimating precipitation areas of deep convection.

### 6.3 Implications and future work

Climate change have negative impacts on the different economic activities, as well as the life of people southern Africa. More climate models are projecting changes in the weather characteristics over the region particularly in regard to temperature and rainfall distribution over the region. A better understanding about the characteristics of weather systems which play a significant role on the distribution of rainfall over South Africa is very important. This will improve the forecast of the characteristics of severe weather condition which are associated with occurrence of COL weather systems.

Even though the characteristics of COL events, which are coupled with different surface pressure circulation were analyzed, the influence of surface and stratospheric processes on deep convection during COL systems were not considered and need further investigation. Following key findings about the significant shift on the location and seasonal distribution of COL events over South Africa (Singleton and Reason, 2007b), the cause of the shifting still needs to be studied. While characteristics associated with the occurrence of COL systems have been analyzed, the intrusion of stratospheric ozone during the development of COL events still requires further research.

Furthermore, the study examined the skill of the 4.4 km Unified Model which is currently being used to simulate areas of deep moist convection and heavy rainfall during regional convective weather events over South Africa. The South African Weather Service (SAWS) can use the findings of this study to improve the forecast the amount of rainfall associated with the severe convective weather systems. The skill of NWP models can only be as good as the accuracy and completeness of the observations used to initialize them. There is need for installation of more automatic weather stations particularly in regions of complex terrain. Upper air observations would also help with the thermodynamic structure of the atmosphere which is currently mostly derived from the reanalysis.

### 6.4 Conclusion

The study identified COL weather systems, by closed geopotential height at 500 hPa from 2011 to 2017. Identified COL systems were associated with pools of cyclonic potential vorticity and cold air in the center. By analyzing the surface circulation patterns associated with the identified

systems, some events were coupled with cold fronts. During their mature stages COL systems were observed with comma shaped clouds and precipitation over their eastern flanks. The study also found a significant shift on the location and seasonal distribution of COL events. High occurrence of COL events was found transiting over the north-east with high number of occurrences during austral winter season. The 4.4 km UM can simulate areas and amount of rainfall with slightly more figures during the occurrence of COL events across the country. Following these findings, forecasters can be aware about the accuracy of the model in simulating rainfall which will assist to provide more relevant weather alerts during the occurrence of convective weather systems to the public.

## References

- Aceituno, P., 1992. El Niño, the Southern Oscillation, and ENSO: Confusing names for a complex ocean–atmosphere interaction. *Bull. am. meteor. soc.*, 73, 483–485
- Acker, J., Soebiyanto, R., Kiang, *et al.*, 2014. Use of the NASA Giovanni data system for geospatial public health research: example of weather-influenza connection. *ISPRS Int. J. Geo-Inf.*, 3, 1372-1386
- Anthens, R. A., 1977. A cumulus parameterization scheme utilizing a one- dimensional cloud model. *Mon. Wea. Rev.*, 105, 3, 270-286
- Arakawa, A. and Schubert. W.H., 1974. Interaction of cumulus cloud ensemble with large-scale environment. Part I. *J. Atmos. Sci*, 31,671-701
- Barsby, I. and Diab R.D., 1995. Total ozone and synoptic weather relationships over southern Africa and surrounding oceans. *J. Geophys. Res*, 100, 3023–3033
- Bengtsson, L., Hagemann, S. and Hodges, K.I., 2004. Can climate trends be calculated from reanalysis data?. *J. Geophys. Res. Atmospheres*, 109.
- Berggren, R., Bolin B. and Rossby C.G., 1949. An aerological study of zonal motion, its perturbations and break-down. *Tellus*, 1, 14–37
- Blamey, R.C. and Reason, C.J.C., 2013. The role of mesoscale convective complexes in southern Africa summer rainfall. *Journal of climate*, 26,1654-1668.
- Botai, C.M., Botai, J.O. and Adeola, A.M., 2018. Spatial distribution of temporal precipitation contrasts in South Africa. *S. Afr. J. Sci.*, 114, 70-78
- Bryan, G. H. and Rotunno, R., 2005. Statistical convergence in simulated moist absolutely unstable layers. Preprints, 11<sup>th</sup> Conf. on Mesoscale Processes, Albuquerque, NM, *Amer. Meteor. Soc.*, 1M.6
- Buckley, B.W., Leslie, L.M, Sullivan, W., *et al.*, 2007. A rare East Indian Ocean autumn season tropical cut-off low: impacts and a high-resolution modelling study. *Meteorol. Atmos. Phys.*, 96, 61–84
- Bureau of Meteorology, 2012: Record-breaking La Niña events: An analysis of the La Niña life cycle and the impacts and significance of the 2010–11 and 2011–12 La Niña events in Australia. <http://www.bom.gov.au/climate/enso/history/ln-2010-12/SAM-what.shtml> Accessed online on 15 April 2017

- Campetella, C.M. and Possia N.E., 2006. Upper-level cut-off lows in southern South America. *Meteorol. Atmos. Phys.*, 96, 181–191
- Caruso, S.J. and Businger S., 2006. Subtropical cyclogenesis over the central North Pacific. *Wea. Forecast.*, 193–205
- Cassola, F., Ferrari, F. and Mazzino, A., 2015. Numerical simulations of Mediterranean heavy precipitation events with the WRF model: A verification exercise using different approaches. *Atmos. Res.*, 164, 210-225
- Chikoore, H. and Jury, M. R., 2010. Intraseasonal variability of satellite derived rainfall and vegetation over southern Africa. *Earth Interact.*, 14, doi:10.1175/2010EI267.1
- Chin, S. M., Franzese, O., Green, D. L. and Hwang, H. L., 2002. Temporary Losses of Highway Capacity and Impacts on Performance. Report ORNL/TM-2002/3
- Crimp, S. J., Lutjeharms, J. R. E. and Mason, S. J., 1998. Sensitivity of a tropical-temperate trough to sea-surface temperature anomalies in the Agulhas retroflexion region. *Water SA*, 24, 93–101
- Dando P., 2004. Unified Model Documentation Paper version 3.0, *Met Office Fitzroy Road Exeter, Devon EX1 3PB, United Kingdom*, 460
- Davies, T., Cullen, M. J. P., Malcolm, A. J., *et al.*, 2005. A new dynamical core for the Met Office's global and regional modelling of the atmosphere, *Q. J. Roy. Meteorol. Soc.*, 131, 1759–1782, doi:10.1256/qj.04.101
- Davolio, A., Miglietta, M.M., Diomede. T., *et al.*, 2008: A meteo-hydrological prediction system based on a multi-model approach for precipitation forecasting. *Nat. Hazards Earth Syst. Sci.*, 8, 143–149
- Done, J., C. A. Davis, and M. Weisman, 2004: The next generation of NWP: Explicit forecasts of convection using the weather research and forecasting (WRF) model. *Atmos. Sci. Lett.*, 5, 110–117
- Doswell, C. A.III., Brooks, H. E. and Maddox, R. A., 1996. Flash flood forecasting: An ingredients-based methodology. *Wea. Forecast.*, 11, 560–581
- Doty, B., 1995. The grid analysis and display system. *GRADS Manual*, 10, 148
- Du Plessis, J.A. and Schloms, B., 2017. An investigation into the evidence of seasonal rainfall pattern shifts in the Western Cape, South Africa. *JS Afr. Inst. Civ Eng.*, 59, pp.47-55

- Dyson, L.L. and Van Heerden, J. 2001. The heavy rainfall and floods over the north-eastern interior of South Africa during February 2000. *S. Afr. J. Sci.*, 97, 80-86
- Dyson, L.L. and Van Heerden, J., 2002. A model for the identification of tropical weather systems over South Africa. *Water SA*, 28, 249-258
- Dyson, L.L., 2009. Heavy daily-rainfall characteristics over the Gauteng Province. *Water SA*, 35
- ENCA, 2015. Cut-off Lows' a common occurrence in SA weather, <https://www.enca.com/weather/cut-lows-common-occurrence-sa-weather> Accessed on 17/08/2018
- Engelbrecht, F.A., Landman W.A., Engelbrecht C.J. *et al.*, 2011. Multi-scale climate modelling over Southern Africa using a variable-resolution global model. *Water SA*, 37, 637–658. <https://www.ajol.info/index.php/wsa/article/view/72827> Accessed on 12/10/2018
- Engelbrecht, C.J. and Landman, W.A., 2015. Seasonal forecasting of synoptic type variability: potential intraseasonal predictability relevant to the Cape south coast of South Africa, University of Pretoria, South Africa
- Engelbrecht, C.J., 2016. Dynamics of climate variability over the all-year rainfall region of South Africa. Doctoral dissertation, University of Pretoria
- EUMETSAT, 2011. Winter lightning associated with cut-off low over South Africa [https://www.eumetsat.int/website/home/Images/ImageLibrary/DAT\\_2351448.html](https://www.eumetsat.int/website/home/Images/ImageLibrary/DAT_2351448.html) Accessed online on 17/08/2018
- EUMETSAT, 2012. intense surface and cut-off low over South Africa. [https://www.eumetsat.int/website/home/Images/ImageLibrary/DAT\\_2398021.html](https://www.eumetsat.int/website/home/Images/ImageLibrary/DAT_2398021.html) Accessed online on 20/10/2018
- EUMETSAT, 2016. Precipitation tracks over Botswana and South Africa. [https://www.eumetsat.int/website/home/Images/ImageLibrary/DAT\\_3201877.html](https://www.eumetsat.int/website/home/Images/ImageLibrary/DAT_3201877.html) Accessed online on 17/09/2018
- EUMETSAT, 2019. Operating satellites. <https://www.eumetsat.int/website/home/AboutUs/WhatWeDo/OperatingSatellites/index.html> Accessed online on 17/08/2018

- Favre, A., Hewitson, B., Lennard, C., Cerezo-Mota, R. and Tadross, M., 2012. Cut-off Lows in the South Africa region and their contribution to precipitation. *Clim. Dyn.*, 41, 2331–2351, doi 10.1007/s00382-012-1579-6
- Favre, A., Hewitson, B., Tadross, M., Lennard, C. and Cerezo-Mota, R., 2011. Relationships between Cut-off Lows and the semiannual and southern oscillations. *Clim. Dyn.*, 38, 1473–1487
- Fuenzalida, H.A., Sanchez, R. and Garreaud, R.D., 2005. A climatology of cutoff lows in the southern hemisphere. *J. Geophys. Res.*, 110, doi: 10.1029/2005JD005934
- Fauchereau, N., Pohl, B., Reason, C.J.C., Rouault, M. and Richard, Y., 2009. Recurrent daily OLR patterns in the Southern Africa/Southwest Indian Ocean region, implications for South African rainfall and teleconnections. *Climate Dynamics*, 32(4), pp.575-591.
- Fauchereau, N., Trzaska, S., Rouault, M. and Richard, Y., 2003. Rainfall variability and changes in southern Africa during the 20th century in the global warming context. *Natural Hazards*, 29, 139-154
- Gibson, J. K., Källberg P., Uppala S., Hernandez A., Nomura A. and Serrano E., 1999. ERA-15 description (version 2—January 1999). ECMWF Re-Analysis Project Report Series 1, ECMWF. 84 pp [http://www.ecmwf.int/research/era/ERA-15/Report\\_Series/index.html](http://www.ecmwf.int/research/era/ERA-15/Report_Series/index.html) Accessed online on 17/11/2018
- Gimeno, L., Trigo, R.M., Ribera, P. and Garcia, J.A., 2007. Special issue on cut-off low systems. *Meteorol. Atmos. Phys*, 96, 1-2
- Gornall, I.J., Betts, R., Burke, E., *et al.*, 2010. Implications of climate change for agricultural productivity in the early twenty-first century. *Philos. Trans. Royal Soc. B.*, 365, 2973-2989
- Gregory, D., Inness, P. and Julie M., 1999. Unified Model documentation paper 27 Convection Scheme Climate Research Meteorological Office, United Kingdom
- Gruber, A., and Krueger A. F., 1984. The status of the NOAA outgoing longwave radiation data set, *Bull. Amer. Meteor. Soc.*, 65,958-962
- HAMNET Emergency Communications., 2016. A division of the South African Radio League. <http://hamnet.co.za/2016/07/> Accessed online on 17/08/2018
- Harrison, M.S.J., 1984. A generalized classification of South African summer rain-bearing synoptic systems. *Int. J. Climatol.*, 4, 547-560

- Hart, N.C.G., Reason, C.J.C. and Fauchereau, N., 2010. Tropical-Extratropical Interactions over southern Africa: Three Cases of Heavy Summer Season Rainfall. *Mon. Weather Rev.*, 138, 2608-2623
- Hart, N.C.G., Reason, C.J.C. and Fauchereau, N. 2012. Cloud bands over Southern Africa: seasonality, contribution to rainfall variability and modulation by the MJO. *Clim. Dyn.*, doi: 10.1007/s00382-012-1589-4
- Hoerling, M. and Kumar, A., 2003. The perfect ocean for drought. *Science*, 299, 691-694
- Holloway, C. E., Woolnough, S. J., and Lister, G. M. S., 2012. Precipitation distributions for explicit versus parametrized convection in a large-domain high-resolution tropical case study, *Q. J. R. Meteorol. Soc.*, 138, 1692–1708
- Hoskins, B. J., McIntyre M. E., and Robertson A. W., 1985. On the use and significance of isentropic potential vorticity maps. *Q. J. R. Meteorol. Soc.*, 111, 877–946
- Houze, R. A., Jr., 2004. Mesoscale convective systems. *Rev. Geophys.*, 42, 1–43, <https://doi.org/10.1029/2004RG000150>
- Hu, K., Lu, R. and Wang, D., 2010. Seasonal climatology of cut-off lows and associated precipitation patterns over Northeast China. *Meteorol. Atmos. Phys.*, 106, 37-48
- Illari, L., 1984. A diagnostic study of the potential vorticity in a warm blocking anticyclone. *J. Atmos. Sci.*, 41, 3518–3526.
- Independent Online (IOL News), Gauteng hail horror., 2012. <https://www.iol.co.za/news/south-africa/gauteng/gauteng-hail-horror-1407784> Accessed online on 17/08/2018
- Independent Online (IOL News), Weather wreaks havoc around SA.,2011. <https://www.iol.co.za/news/south-africa/weather-wreaks-havoc-around-sa-1080771> Accessed online on 20/08/2018
- Jayakumar, A., Sethunadh, J., Rakhi, R., *et al.*, 2017. Behavior of predicted convective clouds and precipitation in the high-resolution Unified Model over the Indian summer monsoon region. *Earth and Space Sci.*, 4, 303-313
- Jeong, J.H., Walther A., Nikulin G., Jones C. *et al.*, 2011. Diurnal cycle of precipitation amount and frequency in Sweden: observation versus model simulation. *Tellus A*, 63, <https://www.tandfonline.com/doi/abs/10.1111/j.1600-0870.2011.00517.x>

- Johnson, W.B. and Viezee, W., 1981. Stratospheric ozone in the lower stratosphere – I. Presentation and interpretation of aircraft measurements. *Atmos. Environ.*, 15, 1309–1323
- Jolliffe, I.T. and Stephenson, D.B., 2012. Forecast verification: a practitioner's guide in atmospheric science, Chichester, U.K. Wiley.
- Jury M.R, and Pathack B., 1991. A study of climate and weather variability over the tropical southwest Indian Ocean. *Meteorol. Atmos Phys.*, 47, 37–48. doi: 10.1007/BF01025825
- Jury, M.R., and Levey K., 1993. The climatology and characteristics of drought in the Eastern Cape of South Africa. *Int. J. Climatol.*, 13, 629-641
- Kalnay E., 2003. Atmospheric Modeling, Data Assimilation and Predictability. Cambridge University Press, UK
- Kalnay, E., Kanamitsu, M., Kistler, R., *et al.*, 1996. The NCEP/NCAR 40-year reanalysis project. *Bull. Amer. Meteor. Soc.*, 77,437-472
- Kanamitsu, M., Ebisuzaki, W., Woollen, J., *et al.*, 2002. The NCEP Climate Forecast System Reanalysis. *Bull. Meteor. Soc.*, 83, 1631-1643
- Kettlewell, P. S., Sothern, R. B. and Koukkari, W. L., 1999. UK wheat quality and economic value are dependent on the North Atlantic oscillation, *J. Cereal Sci.*, 29, 205-209
- Katsanos, D., Retalis, A., Michaelides, S., 2016. Validation of a high-resolution precipitation database (CHIRPS) over Cyprus for a 30-year period. *Atmos. Res.* 169 (Part B), 459–464.
- Kiladis, G. and Diaz, H., 1989. Global climatic anomalies associated with extremes in the southern oscillation. *J. Climatol.*, 2, 1069–1090
- Kohonen, T., 1988. Self-Organization and Associative Memory, Springer-Verlag, ISBN 0-387-18314-0, New York, Berlin, Heidelberg
- KUO, H. L., 1965. On the formation and intensification of tropical cyclones through latent heat release by cumulus convection. *J. Atmos. Sci.*, 22, 40-63
- Landman, W.A. and Beraki A., 2010. Multi-model forecast skill for mid-summer rainfall over southern Africa. *Int. J. Climatol.*, 32, 303-314. <http://dx.doi.org/10.1002/joc.2273>
- Landman, W.A. and Goddard L., 2005. Predicting southern African summer rainfall using a combination of MOS and perfect prognosis. *Geophys. Res. Lett.*, 32, L15809, doi: 10.1029/2005GLO22910

- Lean, H.W., *et al.*, 2008. Characteristics of high-resolution versions of the Met Office Unified Model for forecasting convection over the United Kingdom. *Mon. Weather Rev.*, 136, 3408-3424
- Lee, H.T., Gruber A., Ellingson R. G. *et al.*, 2007: Development of the HIRS Outgoing Longwave Radiation climate data set. *J. Atmos. Ocean. Tech.*, 24, 2029–2047
- Liang, X.Z., Li L., Dai A. and Kunkel K.E., 2004. Regional climate model simulation of summer precipitation diurnal cycle over the United States. *Geophys. Res. Lett.*, 31 <http://dx.doi.org/10.1029/2004GL021054>
- Lindesay, J.A. and Jury, M.R. 1991. Atmospheric circulation controls and characteristics of a flood event in central South Africa, *Int. J. Climatol.*, 11, 609–627
- Liu, Y., Weisberg, R.H., 2011. A review of self-organizing map applications in meteorology and oceanography. In: Mwasiagi, J.I. (Ed.), *Self-Organizing Map Applications and Novel Algorithm Design*. InTech, Rijeka, Croatia.
- Lloyd, S., Acker, J.G., Prados, A.I., *et al.*, 2008. Using NASA's Giovanni Web Portal to access and Visualize satellite-based earth science data in the classroom. Teaching with the New Geoscience Tools: Visualizations, Models and Online Data. [http://irina.eas.gatech.edu/EAS6145\\_Spring2011/Giovanni-tutorial.pdf](http://irina.eas.gatech.edu/EAS6145_Spring2011/Giovanni-tutorial.pdf) Accessed on 10/12/2018
- Luo, D. H. and Ji L. R., 1991. Observational study of dipole blocking in the atmosphere (in Chinese). *Sci. Atmos. Sinica*, 15, 52–57
- Luo, D. H. and Ji, L.R., 2005. A barotropic envelope Rossby soliton model for block—eddy interaction. Part IV: Block activity and its linkage with a sheared environment. *J. Atmos. Sci.*, 62, 3860–3884
- Mackellar, N., New, M. and Jack, C., 2014. Observed and modelled trends in rainfall and temperature for South Africa: 1960-2010. *S. Afr. J. Sci.*, 110, 1-13
- Macron, C., Pohl, B., Richard, Y. and Bessafi, M., 2014. How do tropical temperate troughs form and develop over southern Africa? *J. Climate*, 27, 1633-1647
- Mahlobo, D.D., 2013. The Verification of different model configurations of the Unified Atmospheric Model over South Africa. Doctoral dissertation, University of Pretoria
- Malguzzi, P. and Malanotte-Rizzoli, P., 1984. Nonlinear stationary Rossby waves on nonuniform zonal winds and atmospheric blocking. Part I: The analytical theory. *J. Atmos. Sci.*, 41, 2620–2628

- Malherbe, J., Englebrecht, F.A., Landman, W.A. and Englebrecht C.J., 2012. Tropical systems from the southwest Indian Ocean making landfall over the Limpopo River Basin, southern Africa: a historical perspective. *Int. J. Climatol.*, 32, 1018-1032. doi: 10.1002/joc.2320
- Malherbe, J., Landman, W.A. and Engelbrecht, F.A., 2014. The bi-decadal rainfall cycle, Southern Annular Mode and tropical cyclones over the Limpopo River Basin, southern Africa. *Clim Dyn.*, 42, 3121-3138. doi: 10.1007/s00382-013-2027-y
- Mason, S.J. and Jury, M.R., 1997. Climatic variability and change over southern Africa: a reflection on underlying processes. *Prog. Phys. Geogr.*, 21, 23-50
- McWilliams, J. C., 1980. An application of equivalent modons to atmospheric blocking. *Dyn. Atmos. Oceans*, 5, 43–66
- Meque, A.O., 2015. Investigating the link between southern African droughts and global atmospheric teleconnections using regional climate models. Doctoral dissertation, University of Cape Town
- Met Office, 2019. Unified Model <https://www.metoffice.gov.uk/research/modelling-systems/unified-model> Accessed on 02/03/2019
- Meukaleuni, C., Lenouo, A. and Monkam, D., 2016. Climatology of convective available potential energy (CAPE) in ERA-Interim reanalysis over West Africa. *Atmos. Sci. Lett.*, 17, 65-70
- Molekwa, S., 2013. Cut-off lows over South Africa and their contribution to the total rainfall of the Eastern Cape Province. Doctoral dissertation, University of Pretoria
- Muller, A., Reason, C.J.C. and Fauchereau, N., 2008. Extreme rainfall in the Namib Desert during late summer 2006 and influences of regional ocean variability. *Int. J. Climatol.*, 28, 1061–1070  
<http://dx.doi.org/10.1175/JCLI-D-11-00375.1>
- Narita, M. and Ohmori S., 2007 Improving precipitation forecasts by the operational nonhydrostatic mesoscale model with the Kain–Fritsch convective parameterization and cloud microphysics. Preprints, 12th Conf. on Mesoscale Processes, Waterville Valley, NH, *Amer. Meteor. Soc.*, 3.7
- Ndarana, T. and Waugh, D.W., 2010. The link between cut-off lows and Rossby wave breaking in the Southern Hemisphere. *Q. J. R. Meteorol. Soc.*, 136, 869–885
- Ndarana, T., Bopape, M.M., Waugh, D. *et al.*, 2018. The Influence of the Lower Stratosphere on Ridging Atlantic Ocean Anticyclones over South Africa. *Clim. Dyn.*, 3, 6175-6187

- Neiman, P. J., Persson P. O. G., Ralph F. M., Jorgensen, D. S. P., White. A. B. and Kingsmill, D. E., 2004. Modification of fronts and precipitation by coastal blocking during an intense landfalling winter storm in southern California: Observations during CALJET. *Mon. Wea. Rev.*, 132, 242–273
- Nelson, G. G. and Persaud, R., 2002. Weather, A Research Agenda for Surface Transportation Operations. *Public Roads*, 65, 24-29
- Nhemachena, C., Mano, R., Muwanigwa, V. and Mudombi, S., 2014. Perceptions on climate change and its impact on livelihoods in Hwange district, Zimbabwe. *Jàmbá: Journal of Disaster Risk Studies*, 6, 1-6
- Variability over Southern Africa and the Question of ENSO's Influence on Southern Africa. *J. Climate.*, 16, 555-562
- Nieto, R., Sprenger, M., Wernli, H., Trigo, R.M. and Gimeno, L., 2008. Identification and Climatology of Cut-off Lows near the Tropopause. *Ann. N. Y. Acad. Sci.*, 1146, 256-290
- Nikulin, G., Giorgi, F., Asrar, G., *et al.*, 2012. Precipitation climatology in an ensemble of CORDEX-Africa regional climate simulations. *J. Climate.*, 25, 6057–6078
- Palmén, E.H. and Newton, C.W., 1969. Atmospheric circulation systems: their structure and physical interpretation, 13. Academic press
- Palmer, E., 1949. Origin and structure of high-level cyclones south of the maximum westerlies. *Tellus*, 1, 22-31
- Pelly, J.L., The predictability of atmospheric blocking, Doctoral dissertation, The University of Reading, England
- Petch, J.C., 2006. Sensitivity studies of developing convection in a cloud-resolving model. *Quart. J. Roy. Meteor. Soc.*, 132, 345–358
- Phakula, S., 2017. Modelling intra-seasonal rainfall characteristics over South Africa. Masters dissertation, University of Pretoria
- Philippon, N., Rouault, M., Richard, Y. and Favre, A., 2012. The influence of ENSO on winter rainfall in South Africa. *Int. J. Climatol.*, 32, 2333-2347. doi: 10.1002/joc.3403
- Pohl, B., Fauchereau N., Richard Y., Rouault M. and Reason, C.J.C., 2009. Interactions between synoptic, intraseasonal, and interannual convective variability over southern Africa. *J. Climate*, 33, 1033–1050

- Pook, M.J., 1994. Atmospheric blocking in the Australasian region in the Southern Hemisphere winter. Doctoral dissertation, University of Tasmania
- Porcu, F., Carrassi A., Medaglia C.M., Prodi, F. and Mugnai, A., 2007. A study on cut-off low vertical structure and precipitation in the Mediterranean region. *Meteorol. Atmos. Phys.*, 96, 121–140
- Preston-Whyte, R. A. and Tyson, P. D. 1988. The Atmosphere and Weather of southern Africa. Oxford University Press, Cape Town, 207-249
- Prein, A. F., and Coauthors, 2015. A review on regional convection-permitting climate modeling: Demonstrations, prospects, and challenges. *Rev. Geophys.*, 53, 323–361, <https://doi.org/10.1002/2014RG000475>
- Price, J.D., and Vaughan, G., 1992. Statistical studies of cut-off-low systems. *Annal. Geophys.*, 10,96-102
- Qi, L., Wang, Y. and Leslie, L. M., 2000. Numerical simulation of a cut-off low over southern Australia. *Meteorol. Atmos. Phys.*, 74, 103-115
- Ramaswamy, V., Schwarzkopf M.D. and Shine K.P., 1992. Radiative forcing of climate from halocarbon induced global stratospheric ozone loss. *Nature*. 355, 810–812
- Raymond, D. J., Raga, G. B., Bretherton, C. S., *et al.*, 2003. Convective forcing in the intertropical convergence zone of the east Pacific. *J. Atmos. Sci.*, 60, 2064–2082
- Reason, C.J.C. and Mulenga, H., 1999. Relationships between South African rainfall and SST anomalies in the southwest Indian Ocean. *International Journal of Climatology: A Journal of the Royal Meteorological Society*, 19(15), pp.1651-1673
- Reason C.J.C., and Keibel, A., 2004. Tropical Cyclone Eline and its unusual penetration over the Southern African mainland. *Wea. Forecasting*. 19, 789–805. doi: 10.1175/1520-0434 0192.0.CO
- Reason C.J.C., Landman, W. and Tennant, W., 2006. Seasonal to decadal prediction of southern African climate and its links with variability of the Atlantic Ocean. *Bull. Am. Meteorol. Soc.* 87941-955
- Reason, C. J. C. and Rouault, M., 2005. Links between the Antarctic Oscillation and winter rainfall over western South Africa. *Geophys. Res. Lett.*, 32, L07705, doi: 10.1029/2005GL022419
- Reason, C.J.C., 2007. Tropical cyclone Dera, the unusual 2000/01 tropical cyclone season in the South West Indian Ocean and associated rainfall anomalies over Southern Africa. *Meteorol. Atmos. Phys.*, 97, 181-188

- Reboita, M.S., Nieto, R., Gimeno, L., *et al.*, 2010. Climatological features of cutoff low systems in the Southern Hemisphere. *J. Geophys. Res.*, 115, D17104. doi: 10.1029/2009JD013251
- Renwick, J. and Thompson, D., 2006. The southern annular mode and New Zealand climate. *Water Atmos.*, 14, 24-25
- Rex, D. F., 1950a. Blocking action in the middle troposphere and its effects upon regional climate: I. An aerological study of blocking action. *Tellus*, 2, 196–211
- Rex, D.F., 1950b. Blocking action in the middle troposphere and its effects upon regional climate: II. The climatology of blocking action. *Tellus*, 2, 275–301
- Riemann-Campe K., Fraedrich K., and Lunkeit F., 2009. Global climatology of convective available potential energy (CAPE) and convective inhibition (CIN) in ERA-40 reanalysis. *Atmos. Res.*, 93, 534–545
- Risbey, J.S., Pook, M.J., McIntosh, P.C., *et al.*, 2009. Characteristics and variability of synoptic features associated with cool season rainfall in southeastern Australia. *Int. J. Climatol.*, 29, 1595–1613
- Romero, R., Doswell C. A. III. and Ramis C., 2000. Mesoscale numerical study of two cases of long-lived quasi-stationary convective systems over eastern Spain. *Mon. Wea. Rev.*, 128, 3731–3751
- Ropelewsky, C. F. and Halpert M.S. 1996. Quantifying southern oscillation – precipitation relationships. *J. Climate.*, 9, 1043-1059
- Sabo, P., 1992. Application of the Thermal Front Parameter to Baroclinic Zones around Cut-off Lows. *Meteorol. Atmos. phys.* 47, 107-115
- Schreck, C., Lee, H.T. and Knapp, K., 2018. HIRS Outgoing Longwave Radiation—Daily Climate Data Record: Application toward Identifying Tropical Subseasonal Variability. *Rem. S.*, 10, 1325
- Schulze, R.E., 2005. Section A agriculture and climate change in South Africa: setting the scene chapter A3 adaptation to climate change in South Africa's agriculture sector. *Agriculture and Climate Change in South Africa: On Vulnerability, Adaptation and Climate Smart Agriculture*, 39
- Shutts, G. J., 1983. The propagation of eddies in diffluent jet-streams: Eddy vorticity forcing of blocking flow fields. *Quart. J. Roy. Meteor. Soc.*, 109, 737–761
- Singleton, A.T. and Reason, C.J., 2006a. A numerical model study of an intense cutoff low-pressure system over South Africa. *Mon. Wea. Rev.*, 135, 1128–1150

- Singleton, A.T. and Reason, C.J., 2006b. Numerical simulations of a severe rainfall event over the Eastern Cape coast of South Africa: sensitivity to sea surface temperature and topography. *Tellus*, 58, 355–367
- Singleton, A.T. and Reason, C.J.C., 2007. Variability in the characteristics of cut-off low pressure systems over subtropical southern Africa: sensitive to sea surface temperature and topography. *Tellus*, 58, 355-367
- Song, Y., Lü, D., Li, Q., Bian, J., Wu, X. and Li, D., 2016. The impact of cut-off lows on ozone in the upper troposphere and lower stratosphere over Changchun from ozonesonde observations. *Adv. Atmos. Sci.*, 33, 135-150
- South African Weather Bureau., 1972. District rainfall for South Africa and the annual march of rainfall over southern Africa. South African Weather Bureau, WB35, Pretoria
- South African Weather Service, 2012. Climate Summary of South Africa. South African Weather Service, Pretoria, South Africa
- South African Weather Service, 2012. Daily Weather Bulletin South African Weather Service, Pretoria, South Africa
- South African Weather Service, 2017. <http://www.weathersa.co.za/learning/educational-questions/62-what-is-climate-variables-are-reordered-by-south-african-weather-service-stations> Accessed on 17/08/2017
- South African Weather Service, 2015. Severe Weather Report: 01 June – 04 June <https://www.overstrand.gov.za/en/documents/strategic-documents/severe-weather/1852-severe-weather-event-01-june-04-june-2015/file> Accessed online on 17/08/2018
- Steppeler, J., Doms, G.U. Schattler, H.W. *et al.*, 2003. Meso-gamma scale forecasts using the nonhydrostatic model LM. *Meteor. Atmos. Phys.*, 82, 75–96
- Sud, Y., and Molod, A., 1988. The roles of dry convection, cloud radiation feedback processes, and the influence of recent improvements in the parameterization of convection in the GLA GCM. *Mon. Wea. Rev.*, 116, 2366-2387
- Taljaard, J.J., 1959. South Africa airmasses: their properties, movement and associated weather. Ph.D. Thesis, University of the Witwatersrand

- Taljaard, J.J., 1985. Cut-off lows in the South African region. *South African Weather Bureau Technical Paper 14*, 153
- Taljaard, J.J., 1986. Change of rainfall distribution and circulation patterns over southern Africa summer. *Int. J. Climatol.*, 27, 295-310
- Taljaard, J.J., 1994. Atmospheric Circulation Systems, Synoptic Climatology and Weather Phenomena of South Africa, Part 1: Controls of the weather and climate of South Africa. SA Weather Bureau, Department of Transport, Pretoria. Technical Paper no. 27
- Taljaard, J.J., 1995. Atmospheric circulation systems, synoptic climatology and weather phenomena of South Africa. Part 2: atmospheric circulation systems in the South African region. South African Weather Bureau, Technical Paper 28
- Taljaard, J.J., 1996. Atmospheric Circulation Systems, Synoptic Climatology and Weather Phenomena of South Africa, Part 6: Rainfall in South Africa., Department of Environmental Affairs and Tourism, Pretoria. South African Weather Bureau, Technical Paper no. 32
- Tang, X. and Lou S.L., 2006. Evolution of Dipole-Type Blocking Life Cycles: Analytical Diagnoses and Observations. Shanghai Jiao Tong University, Shanghai, and Ningbo University, Ningbo, China
- Tennant, W. J., Toth, Z. and Rae, K.J., 2007. Application of the NCEP Ensemble Prediction System to Medium-Range Forecasting in South Africa: New Products, Benefits, and Challenges. *Weather Forecast.*, 22, 18-35
- Tibaldi, S. and Molteni, F., 1990 On the operational predictability of blocking. *Tellus*, 42A, 343-365.
- Traveller24 News Alerts, SA set for week of disruptive, stormy weather <http://www.traveller24.com/News/Alerts/sa-set-for-week-of-disruptive-stormy-weather-20160725#commentsSection> Accessed online on 05/10/2017
- Triegaardt, D.O., Terreblanche, D.E., van Heerden, J. *et al.*, 1988. The Natal floods of September 1987. *South African Weather Bureau Technical Paper*, 19, 62
- Trouet, V. and Van Oldenborgh, G.J., 2013. KNMI Climate Explorer: a web-based research tool for high-resolution paleoclimatology. *Tree Ring Res.*, 69, 3-13
- Tyson, P. D. and Preston-White, R.A., 2000. The Weather and Climate of Southern Africa. Second Edition, Oxford University Press, Cape Town, 396

- Twitchett, A.F., 2012. Predictability and dynamics of potential vorticity streamers and connections to high impact weather. University of Leeds
- Unified Model - Met Office <https://www.metoffice.gov.uk/research/modelling-systems/unified-model>  
Accessed online on 06/11/2018
- Urbain, M., Clerbaux, N., Ipe, A., *et al.*, 2017. The CM SAF TOA radiation data record using MVIRI and SEVIRI. *Rem. S.*, 9, 466.
- Wallace, J. and Hobbs, P., 2006. Atmospheric science: an introductory survey, 2nd edn. Academic Press
- Washington, R. and Todd, M., 1999. Tropical-Temperate Links in southern African and Southwest Indian Ocean Satellite-Derived Daily Rainfall. *Int. J. Climatol.*, 19, 1601-1616
- Washington, R., and Preston, A., 2006. Extreme wet years over southern African: Role of Indian Ocean sea surface temperatures. *J. Geophys. Res.*, 24, 555-568
- Weldon, D. and Reason, C.J.C., 2013. Variability of rainfall characteristics over the South Coast region of South Africa. *Theor. Appl. Climatol.*, 113: 287-295. doi: 10.1007/s00704-013-0882-4
- Weldon, D. and Reason, C.J.C., 2014. Variability of rainfall characteristics over South Coast region of South Africa. *Theor. Appl. Climatol.*, 115, 177-185. doi: 10.1007/s00704-013-0882-4
- Wood, N., Staniforth, A., White, A., *et al.*, 2014. An inherently mass-conserving semi-implicit semi-Lagrangian discretization of the deep-atmosphere global nonhydrostatic equations, *Q. J. Roy. Meteorol. Soc.*, 140, 1505–520, doi:10.1002/qj.2235,
- Williams E. and Renno N. 1993. An analysis of the conditional instability of the tropical atmosphere. *Mon. Wea. Rev.*, 121, 21–36
- Van Heerden, J. and Taljaard, J.J., 1998. Africa and surrounding waters. Meteorology of the Southern Hemisphere. *Meteorol. Monogr.*, 27,141–174
- Vigaud, N., Pohl, B. and Cretat, J. 2012. Tropical-temperate interactions over southern Africa simulated by a regional climate model. *Clim. Dyn.*, 39, 2895–2916, doi:10.1007/s00382-012-1314-3
- Yeh, S.W., Kug, J.S., Dewitte, B., *et al.*, 2009. El Niño in a changing climate. *Nature*, 461, 511
- Yu, C.-K. and Smull B. F., 2000. Airborne Doppler observations of a land-falling cold front upstream of steep coastal orography. *Mon. Wea. Rev.*, 128, 1577–1603

Zerroukat, M., 2010. A simple mass conserving semi-Lagrangian scheme for transport problems. *J. Comput. Phys.*, 229, 9011–9019, <https://doi.org/10.1016/j.jcp.2010.08.017>.

Zhao, S., and Sun, J., 2007. Study on cut-off low-pressure systems with floods over northeast Asia. *Meteorol. Atmos. Phys.*, 96, 159-180